Plant Physiology Preview. Published on November 3, 2015, as DOI:10.1104/pp.15.01076

1 **PLANT PHYSIOLOGY – RESEARCH ARTICLE**

2

3 **RUNNING HEAD**

4 Transcriptome of induced CAM in *Talinum*

5

6

7 Corresponding author:

8 Andreas P.M. Weber

9 Tel.: +49 211 81 12347; fax: +49 211 81 13706

10 E-mail address: andreas.weber@hhu.de

11

12 Research Area:

13 Biochemistry and Metabolism

14

15 **TITLE**

16 Reversible Burst of Transcriptional Changes During Induction of Crassulacean Acid
17 Metabolism (CAM) in *Talinum triangulare*

18

19 **Dominik Brilhaus[1], Andrea Bräutigam, Tabea Mettler-Altmann, Klaus Winter, Andreas P.**
20 **M. Weber***

21

22 Institute of Plant Biochemistry, Cluster of Excellence on Plant Sciences (CEPLAS), Heinrich-Heine-University,
23 Universitätsstraße 1, D-40225 Düsseldorf, Germany (D.B., A.B., T. M.-A., A. P. M. W.); Smithsonian Tropical
24 Research Institute, PO Box 0843-03092, Balboa, Ancón, Republic of Panama (K. W.)

25

26 One-sentence summary:

27 Rapid, reversible induction of Crassulacean acid metabolism (CAM) in conjunction with
28 pronounced reconfiguration of carbon metabolism enables *T. triangulare* to survive cycles of
29 severe drought.

30

[1]This work was supported by the International Graduate Program for Plant Science (iGRAD-Plant; to D. B.) and grants from Deutsche Forschungsgemeinschaft (DFG) (EXC 1028; IRTG 1525 to A. P. M. W.). K.W. was supported by the Smithsonian Tropical Research Institute.

*Address correspondence to andreas.weber@hhu.de

ABSTRACT

Drought tolerance is a key factor for agriculture in the 21st century as it is a major determinant of plant survival in natural ecosystems as well as crop productivity. Plants have evolved a range of mechanisms to cope with drought, including a specialized type of photosynthesis termed Crassulacean acid metabolism (CAM). CAM is associated with stomatal closure during the day as atmospheric CO_2 is assimilated primarily during the night, thus reducing transpirational water loss. The tropical herbaceous perennial species *Talinum triangulare* is capable of transitioning, in a facultative, reversible manner, from C_3 photosynthesis to weakly expressed CAM in response to drought stress. The transcriptional regulation of this transition has been studied.

Combining mRNA-Seq with targeted metabolite measurements, we found highly elevated levels of CAM-cycle enzyme transcripts and their metabolic products in *T. triangulare* leaves upon water deprivation. The carbohydrate metabolism is rewired to reduce the use of reserves for growth, support the CAM-cycle and the synthesis of compatible solutes. This large-scale expression dataset of drought-induced CAM demonstrates transcriptional regulation of the C_3 – CAM transition. We identified candidate transcription factors to mediate this photosynthetic plasticity, which may contribute in the future to the design of more drought-tolerant crops via engineered CAM.

INTRODUCTION

Drought is a major determinant of both plant survival in natural ecosystems and plant productivity in agriculture (Lobell and Gourdji, 2012). Plants have evolved a range of physiological and non-physiological traits to cope with water deficit stress (Bartels and Sunkar, 2005). Drought adaptation includes leaf shedding in perennials or completing the life cycle while enough water is present in annuals. Few species (i.e., so-called resurrection plants) tolerate extreme dehydration (Ingram and Bartels, 1996) and resume life upon water resupply. Other plants have evolved strategies to cope with drought such as specialized biochemical pathways, cells, tissues, and organs to survive water scarcity by mitigating the reduction in tissue water loss (Chaves et al., 2003).

Water limitation sensed in the roots or leaves triggers stress signals, which include but are not limited to abscisic acid (ABA) (Bray, 1997; Zhu, 2002; Chaves et al., 2003; Bartels and Sunkar, 2005). The immediate consequence of an ABA signal is stomatal closure (Kollist et al., 2014). This can lead to short-term carbon dioxide (CO_2) limitation of photosynthesis potentially causing oxidative stress, which is mitigated by protective systems (Bartels and Sunkar, 2005; Flexas et al., 2006). The accumulation of compatible solutes is induced to protect the cellular machinery from consequences of leaf water loss and to lower the water potential of the leaf (Hare et al., 1998). These molecules include sugars such as raffinose, trehalose and sucrose, sugar alcohols like mannitol and inositol, and amino acids and their derivatives such as proline or glycine betaine (Hare et al., 1998; Elbein et al., 2003). The signaling cascade has been largely elucidated. ABA is bound by the PYRABACTIN RESISTANCE1 AND PYR1-LIKE REGULATORY COMPONENTS OF ABA RECEPTOR family proteins, which upon binding inhibit the TYPE 2C AND TYPE 2A PROTEIN PHOSPHATASES (PP2C) (Cutler et al., 2010). This inhibition, in turn, relieves the inhibition of the protein kinase OPEN STOMATA 1 and other kinases, which phosphorylate their targets including the ABA RESPONSIVE ELEMENT BINDING FACTORS. They finally trigger ABA-responsive gene expression (Park et al., 2009). The capability to reduce leaf water loss is variable between species and leaf water loss exceeding a threshold irreversibly damages a leaf (Lawlor and Cornic, 2002).

The tropical herbaceous dicot *Talinum triangulare* (Jacq). Willd. [according to The Plant List Kew

now considered a synonym of the accepted name *Talinum fruticosum* (L.) Juss, but referred to within this work as *T. triangulare* to relate to extensive ecophysiological work on "*T. triangulare*" by Herrera et al. (1991), Taisma and Herrera (1998), Herrera (1999), Taisma and Herrera (2003) and Herrera et al. (2015)], in the family *Talinaceae* (formerly *Portulacaceae*) responds to intermittent drought (Harris and Martin, 1991; Herrera et al., 1991) in two ways. Leaves change from a horizontal to a vertical orientation and exhibit leaf-rolling (Herrera et al., 1991; Taisma and Herrera, 1998; Herrera, 1999). Leaves induce Crassulacean acid metabolism (CAM) in a reversible, facultative manner (Taisma and Herrera, 1998; Herrera, 2009; Winter and Holtum, 2014; Herrera et al., 2015).

CAM is a carbon concentrating mechanism allowing stomatal closure during the day as atmospheric CO_2 is primarily assimilated during the night by PHOSPHO*ENOL*PYRUVATE CARBOXYLASE (PEPC) (Osmond, 1978). The produced organic acids (mainly malic acid) are decarboxylated during the following day to provide CO_2 for the secondary, light-driven carboxylation via RUBISCO. The magnitude of CAM varies between and within plant species (Borland et al., 2011). While constitutive CAM plants are ontogenetically determined to engage in this photosynthetic mode at some point in their life cycle, in facultative CAM plants a transition to CAM occurs in response to water-deficit stress (Winter et al., 2008; Winter and Holtum, 2014). The ability to experimentally control the timing of CAM induction and CAM-to-C_3 reversal makes facultative CAM plants excellent systems to identify key components of CAM.

Extensive physiological, molecular, and mutant-based studies of facultative CAM were focused on but not restricted to the halophyte *Mesembryanthemum crystallinum* and aided to understand central concepts of the CAM-cycle (Winter and Willert, 1972; Holtum and Winter, 1982; Cushman et al., 2008a). These included a microarray-based large scale gene expression data set (Cushman et al., 2008b), which described major changes in mRNA steady state levels during the salinity-induced transition from C_3 to CAM. Reversibility of CAM back to C_3 photosynthesis after irrigation was re-initiated has been documented for several species including *T. triangulare* (reviewed in Winter and Holtum, 2014). To date it is not fully understood, how this metabolic plasticity is transcriptionally accomplished (Yang et al., 2015). We studied the *T. triangulare* transition from well-watered to water-limited and back to well-watered conditions (i) to test how CAM induction and its reversion are controlled at the level of mRNA abundance and (ii) to

evaluate CAM- and drought-specific changes in metabolite levels.

120

RESULTS

Nocturnal Acidification

Following germination, *T. triangulare* was grown well-watered for 28 days. Subsequently, water was withheld for 12 days before re-watering. Fresh weight to dry weight ratio after 4, 9, and 12 days of water deprivation showed slight, continuous (1.1%, 4.8%, 15.0%, respectively) decreases compared to day 0, which were significant on day 12 (Fig. 1A). Measurements of titratable acidity were used as an indicator of the presence or absence of CAM activity in leaves (Fig. 1B). In well-watered plants, acidity levels were low (10 μmol H^+ g^{-1} FW) and did not change in the course of the night. Withholding water for four days did not significantly alter titratable acidity compared to well-watered plants. Significant nocturnal acidification, indicative of CAM, was observed in plants from which water was withheld for 9 and 12 days, consistent with previous findings of Herrera et al. (1991) and Winter and Holtum (2014). Drought stress also resulted in pronounced leaf rolling (Fig. 1C). Following re-watering for two days, plants returned to a full C_3 photosynthetic pattern without nocturnal increases in tissue acidity and unrolled leaves (Fig. 1B and 1C). However, fresh weight to dry weight ratio was significantly lower (22.7%) compared to day 0 (Fig. 1A).

Changes in Transcript and Metabolite Levels

Samples for mRNA-Seq were taken at midday and midnight prior to the drought-treatment (day 0, well-watered), on day 4, day 9, and day 12 of drought, and again 2 days after re-watering (Fig. 2A and 2B). Biological triplicates yielded on average 40.7 million reads over the time course (Supplemental Table S1). Of those, an average of 52% could be mapped for quantification to the reference genome of *Arabidopsis thaliana* (Supplemental Table S1 and Material and Methods). The mapped reads matched 16,766 *A. thaliana* genes with at least one read per gene. This is comparable to the yield of cross species mapping with equidistant species for both number of genes matched and percentage of mapped reads (Gowik et al., 2011). Within species mapping on the assembled contigs resulted in 81% mapped reads, but indicated that the assembly suffers from the known limitations of transcriptome assembly such as contig fragmentation (Franssen et al., 2011) (Supplemental Dataset S2).

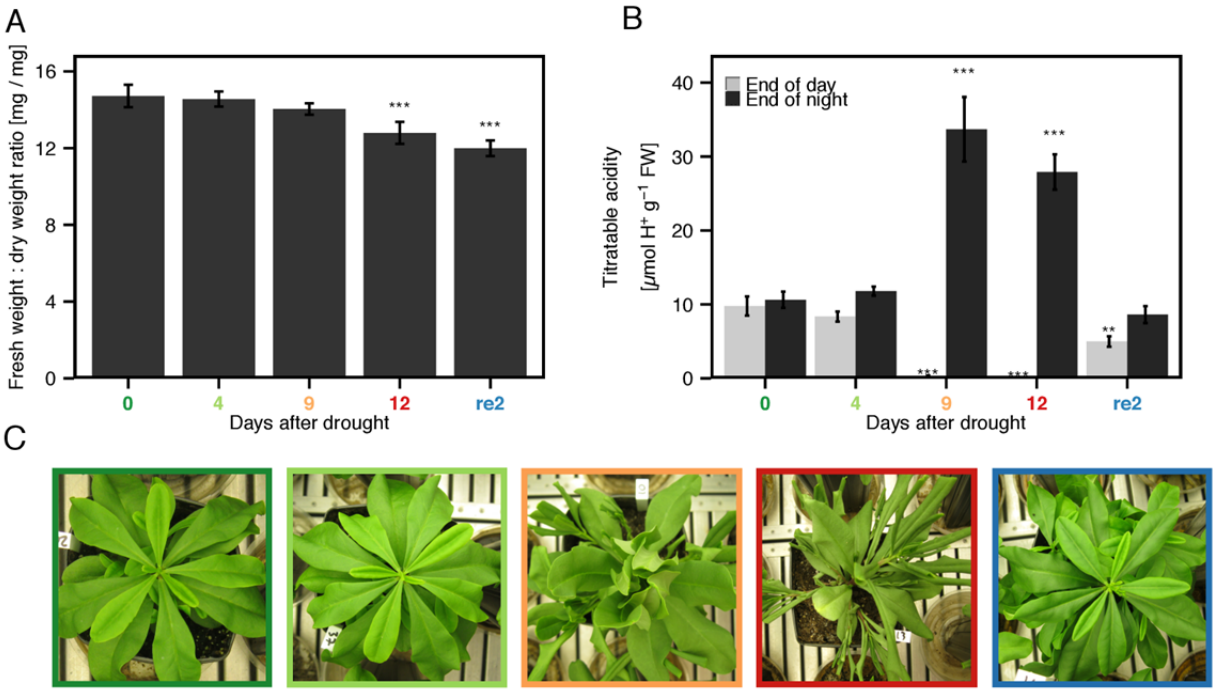

Figure 1. Time course in response to 0 (darkgreen), 4 (light green), 9 (orange) and 12 (red) days of drought and 2 days after re-watering (re2, blue) in *Talinum triangulare*. A, Fresh weight to dry weight ratio (Mean ± SE of leaves harvested at the middle of the day and the middle of the night, n = 14-16). B, Levels of titratable acidity of leaves (Mean ± SE, n = 8-16). C, Representative pictures of plants during the course of the experiment. Asterisks indicate Student's *t* test significance in comparison to day 0 at $***P < 0.001$, $**P < 0.01$, $*P < 0.05$.

Statistical evaluation including multiple hypothesis testing correction (by DESeq2, for details see Materials and Methods) identified significantly differential gene expression for 4,628 genes (28% of the whole transcriptome) at midday and 5,191 genes (31% of the transcriptome) at midnight on day 9 as well as 6,143 genes (37% of the transcriptome) at midday and 6,565 genes (39% of the transcriptome) at midnight on day 12 compared to well-watered plants (day 0), i.e. during the two days during which pronounced CAM activity was observed (Fig. 2B).

On day 9, 2,117 (12.6%) and 2,213 (13.2%) genes were upregulated, while 2,511 (15%) and 2,978 genes (17.8%) were downregulated at midday and midnight, respectively. On day 12, 2,713 (16.2%) and 2,897 (17.3%) genes were upregulated, while 3,430 (20.5%) and 3,668 genes (21.9%) were downregulated at midday and midnight, respectively. A Venn analysis indicated that 1,634 genes and 2,180 genes were shared among the genes up- and downregulated at midday, respectively (Fig. 2B), while at midnight 1545 upregulated and 1865 downregulated genes were shared (Supplemental Figure S1.). A small percentage (1.9% and 2.1% of upregulated and 1.2%

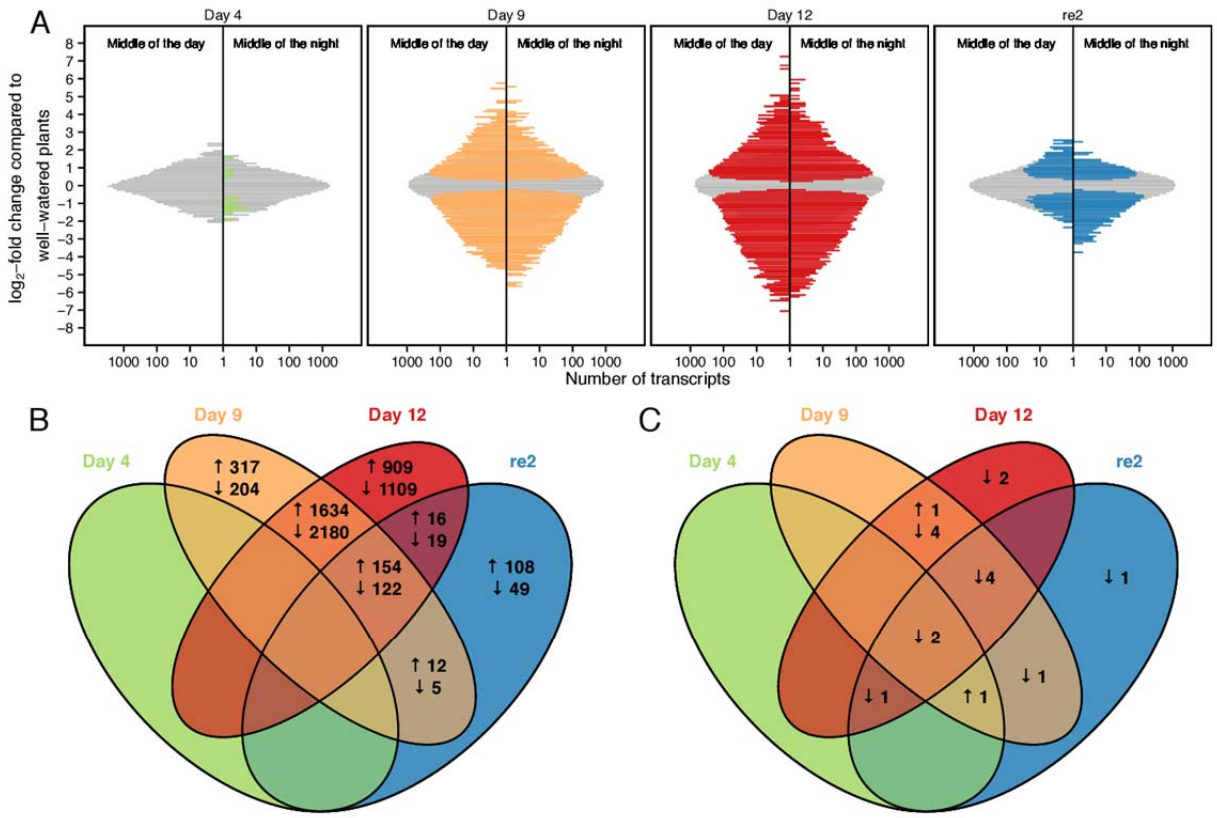

Figure 2. Changes in leaf transcriptomes and metabolomes under varying levels of water availability. A, Histograms of $\log_2$-fold changes in gene expression compared to day 0 ($\log_{10}$-scaled). Colored bars indicate significant changes (DESeq2, $q < 0.01$). B, C, Venn diagrams representing overlapping changes (↑: increased, ↓: depleted) in gene expression (B, DESeq2 $q < 0.01$, n = 3, 16,766 genes analyzed in total), or metabolite levels (C, Student's *t* test, $p < 0.05$, n = 3-4, 39 metabolites measured in total) at the middle of the day between water-limited stages compared to day 0. See supplemental Figure S1. for analogous Venn diagrams of changes at the middle of the night.

and 1.9% of downregulated genes at midday and midnight, respectively) was exclusively differentially regulated on day 9. On day 4 of water-deprivation, no differentially expressed genes (DEGs) were detectable compared to well-watered conditions at midday, while at midnight 16 genes were up- and 35 were downregulated (Supplemental Fig. S1). Upon re-watering the number of significantly DEGs was reduced to 485 at midday (3% of the transcriptome) and 1,632 (10% of the transcriptome) at midnight. To compare the changes of steady state levels of mRNA and metabolites, 39 metabolites were quantified at midday and midnight on days 0, 4, 9, 12 and after

re-watering for 2 days (Fig. 2C, Supplemental Fig. S1 and Supplemental Table S2). On day 4, nine metabolites were significantly different from well-watered plants at either midday or midnight. In leaves harvested at day 9 and 12, 13 and 14 of the 39 metabolites differed significantly at midday, while 6 and 11 metabolites differed significantly at midnight, respectively. The highest total number of significant changes was observed in re-watered plants, 10 at midday and 16 at midnight compared to day 0. Both the transcriptome analysis and the targeted metabolite profiling showed that transcriptome and metabolome were markedly altered in *T. triangulare* plants, which experience drought. While changes in mRNA abundance were largely reversed upon re-watering (Fig. 2A), the metabolic state remained altered.

CAM-Related Transcriptional Changes

Transcript abundance of known enzymes of the CAM-cycle *sensu stricto* (*s.s.;* i.e. carboxylation and decarboxylation) and *sensu lato* (*s.l.*; i.e. encoding auxiliary steps such as starch turnover and glycolysis for phospho*enol*pyruvate (PEP) generation) were analyzed during C_3-CAM-C_3 transitions. Transcripts encoding four CAM-cycle enzymes *s.s.*, namely PEPC, NADP-MALIC ENZYME (NADP-ME), NAD-ME and PYRUVATE, *ORTHO*PHOSPHATE DIKINASE (PPDK) had higher steady state levels at both midnight and midday on day 9 and/or day 12 of water-limitation (Fig. 3 and Supplemental Dataset S3).

CARBONIC ANHYDRASE (CA) catalyzes the hydration of CO_2 to HCO_3^- at physiological pH and thereby is thought to support providing PEPC with its substrate in CAM plants (Tsuzuki et al., 1982). The gene encoding cytosolic BETA-CARBONIC ANHYDRASE3 (BCA3) was unchanged in expression upon drought but already highly expressed in C_3 conditions (2,498 rpm on day 0). This is in agreement with an earlier study finding no differences in CA activity in *M. crystallinum* in C_3 and CAM mode (Tsuzuki et al., 1982). Two lowly expressed genes encoding CA isoforms (alpha CA3 between 2.7 and 10 rpm and BCA5 between 23.7 and 80.7 rpm) were upregulated at midday on both days. Upregulation of major carbonic anhydrase isoforms as it was found for *M. crystallinum* (Cushman et al., 2008b), could not be detected in *T. triangulare*.

The gene *PPC* encodes PEPC, which catalyzes the CO_2 carboxylation at night. *PPC* was upregulated 25-fold at midnight (to 15,510 rpm, expression rank 4 on day 12) on day 9 and 12,

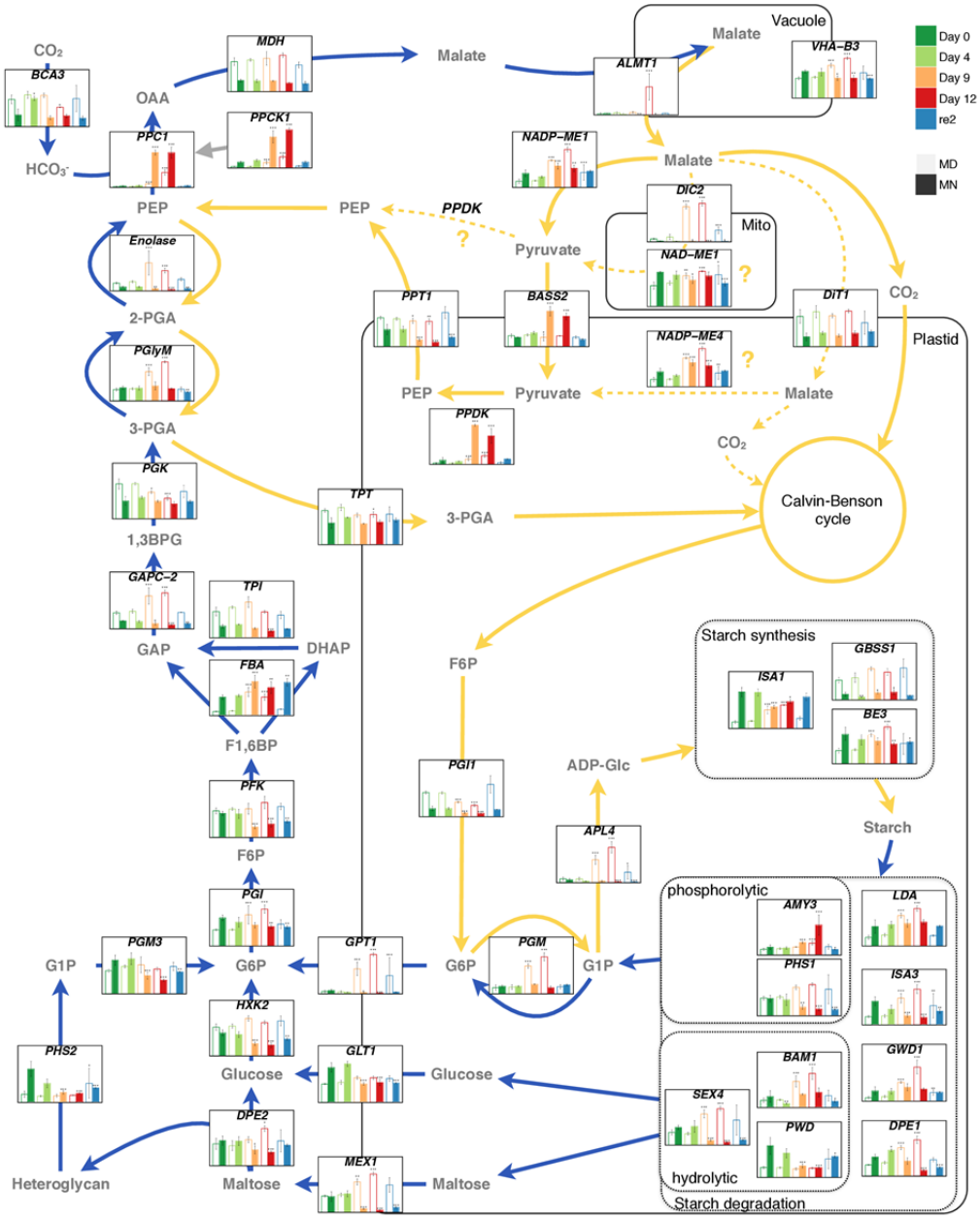

Figure 3. Abundances of CAM genes *sensu stricto* and *sensu lato*. Scheme of carbon assimilation via CAM and gene expression of central enzymes and transporters. Metabolites are represented in grey. Transcript levels were measured at the middle of the day and the middle of the night in leaves of *T. triangulare* plants under five different stages of water availability. Scaled to largest expression by gene; Mean ± SD, n = 3. Asterisks indicate differential gene expression in comparison to day 0 as determined by DESeq2, * q < 0.05:, ** q < 0.01:, *** q < 0.001. Abbreviations are explained in the text and in Supplemental Dataset S3. Blue and yellow arrows represent reactions occurring at night and day, respectively. Grey arrow indicates phosphorolytic actication of PPC via PPCK. Question mark and dotted arrows indicate putative activity of plastidial NADP-ME, mitochondrial NAD-ME and cytosolic PPDK as discussed in the text. Separation into phosphorolytic and hydrolytic starch degradation is based on the models presented by Weise et al. (2011) and Streb and Zeeman (2012). 1,3-BPG, 1,3-Bisphosphoglycerate; 2-PGA, 2-Phosphoglycerate; 3-PGA, 3-Phosphoglycerate; ADP-Glc, ADP-glucose; DHAP, Dihydroxyacetone phosphate; F1,6BP, Fructose 1,6-bisphosphate; F6P, Fructose 6-phosphate; G1P, Glucose 1-phosphate; G6P, Glucose 6-phosphate; GAP, Glyceraldehyde 3-phosphate; Mito, Mitochondrion; OAA, Oxaloacetate; PEP, Phospho*enol*pyruvate, re2, 2 days after re-watering

198 respectively. The coding sequences of *PPC* vary between C_3, C_4 and CAM plants (Bläsing et al.,
199 2000; Paulus et al., 2013). The coding sequences of the four *T. triangulare PPC* contigs with on
200 average at least 100 reads mapped were extracted from the assembly, translated and aligned with

PEPC sequences from various C_3, C_4 and CAM plants (http://www.uniprot.org, Supplemental Fig. S2 and Supplemental Table S3). The *T. triangulare* contigs encoding for PEPC showed characteristics of both C_3 and C_4 PEPCs. PEP saturation kinetics is known to be determined by the amino acid at position 780 (counting based on *Zea mays* sequence CAA33317), which in C_4 plants is typically serine and in C_3 plants alanine (Bläsing et al., 2000). Sensitivity to malate inhibition is determined by the amino acid at position 890, glycine in C_4 plants and arginine in C_3 plants (Paulus et al., 2013). While at position 890 all contigs encoded for the C_3-typical arginine in *T. triangulare*, at position 780 contig Tt63271 (7,638 rpm at midnight on day 9) and Tt9871_8 (1,198 rpm at midnight on day 12) encoded for the C_3 typical alanine, Tt9871_4 (1,409 rpm at midnight on day 9) and Tt9871_6 (399 rpm at midnight on day 12) encoded for the C_4-typical serine (Supplemental Fig. S2). Read mapping on the contig level identified all isoforms as upregulated during CAM (Supplemental Table S3), however, it cannot be determined, whether Tt63271 and Tt9871_8, Tt9871_4 and Tt9871_6 are alleles or recent duplicates.

Oxaloacetate (OAA) resulting from PEP carboxylation is reduced to malate by MALATE DEHYDROGENASE (MDH). The cytosolic *MDH* was unchanged but constitutively highly expressed in C_3 conditions (941 rpm at midday on day 0) and during CAM (1141 rpm, expression rank 110 at midday on day 12). Malate is stored as malic acid in the vacuole during the night (Cheffings et al., 1997). Genes encoding two malate channels of the ALUMINUM-ACTIVATED MALATE TRANSPORTER (ALMT) family were upregulated sixfold and 28-fold at midnight, but reached only 4 and 19 rpm after upregulation, respectively. While below 1 rpm in abundance at any other day, transcripts encoding the TONOPLAST DICARBOXYLATE TRANSPORTER are detectable on day 12 (MD: 5 rpm, MN: 11 rpm). *VHA-B3,* encoding the subunit B3 of the vacuolar ATPase (V-ATPase), which sustains the electrochemical gradient during import of malic acid (White and Smith, 1989), is the major expressed subunit, being significantly upregulated twofold on day 12. Of the 11 other genes encoding for V-ATPase subunits, two were unaltered and eight genes were slightly but significantly downregulated during CAM (Supplemental Table S4). *TYPE I PROTON-TRANSLOCATING PYROPHOSPHATASE* is downregulated two-fold and three-fold at midday of days 9 and 12.

During the day, malic acid is released from the vacuole and, depending on the species, is believed to be decarboxylated by NADP-ME, NAD-ME, and/or PEP CARBOXYKINASE

(PEPCK) (Dittrich, 1976). In *T. triangulare*, the plastidial *NADP-ME4* was upregulated fivefold at midday to 780 rpm and the apparent cytosolic *NADP-ME1* was upregulated sixfold to 579 rpm, while *NAD-ME1* was twofold upregulated to 173 rpm and *PEPCK* was not significantly upregulated. The *T. triangulare* contigs of NADP-ME extracted from the assembly with high read mappings possess a target peptide and cluster with the plastidial AtNADP-ME4 with high bootstrap support (Supplemental Fig. S3 and Supplemental Table S5). In contrast to the downregulation of one isoform of *NADP-ME* at midnight in *M. crystallinum* (Cushman et al., 2008b), both genes encoding NADP-ME isoforms were upregulated at both midday and midnight on both CAM days. Transcript amounts of the plastidial DICARBOXYLATE TRANSPORTERS were unaltered (DiT1, expression between 256 and 381 rpm at midday, DiT2 between 48 and 105 rpm), while all three mitochondrial DICARBOXYLATE CARRIERS were upregulated at midday on both CAM days (DIC1 15-fold to 787 rpm, DIC2 12-fold to 899 rpm, DIC3 14-fold to 310 rpm on day 12). The plastidial pyruvate importer BILE-ACID SODIUM SYMPORTER 2 (BASS2) was upregulated at night on both CAM days (4-fold to 411 rpm on day 9). Pyruvate, produced by malate decarboxylation, is phosphorylated to PEP by PPDK encoded by a single gene (9-fold upregulated to 18,371 rpm at midnight on day 9) and fed back to gluconeogenic starch synthesis (Kluge and Osmond, 1971). Extraction, alignment and quantification of two different contigs encoding for PPDK (Supplemental Table S6) revealed markedly increased transcript amounts during CAM exclusively for one contig, Tt26901, which encodes for a protein with a 77 amino acid shorter N-terminus. At midnight on day 12 transcript amounts for Tt26901 were 59-fold higher than for the longer PPDK encoding contig Tt24575 (Supplemental Table S6). Transcript amounts of the PEP/PHOSPHATE TRANSLOCATOR (PPT), catalyzing the export of PEP to the cytosol, were downregulated during CAM (4-fold to 23 rpm at midnight on day 12).

Another important aspect of CAM photosynthesis is starch turnover and its connection to the carboxylation/decarboxylation cycle. During the night, starch is degraded, likely both via the phosphorolytic and hydrolytic pathways, to provide PEP for PEPC via glycolysis (Weise et al., 2011). Four genes encoding enzymes, required both for phosphorolytic and hydrolytic starch degradation according to Weise et al. (2011) and Streb and Zeeman (2012), LIMIT DEXTRINASE (LDA), ISOAMYLASE3 (ISA3), GLUCAN WATER DIKINASE (GWD1) and DISPROPORTIONATING ENZYME 1 (DPE1), were upregulated at midday on both CAM days (e.g. on day 12: 4-fold to 178 rpm, 4-fold to 195 rpm, 10-fold to 995 rpm and 3-fold to 197 rpm,

respectively). *ISA3* is downregulated threefold at midnight on both CAM days and *DPE1* is downregulated at midnight of day 12. Genes encoding enzymes specific for hydrolytic starch degradation, PHOSPHOGLUCAN PHOSPHATASE (abbreviated SEX4 for STARCH EXCESS 4) and BETA-AMYLASE1 (BAM1) were upregulated at midday (5-fold to 863 rpm and 3-fold to 150 rpm, respectively) as well, while the gene encoding PHOSPHOGLUCAN, WATER DIKINASE (PWD) was downregulated at midnight on both CAM days. Of the two exporters, MALTOSE EXPORTER1 (MEX1) and PLASTIDIC GLUCOSE TRANSLOCATOR1 (GLT1) exporting the hydrolytic breakdown products maltose and glucose (Weber et al., 2000; Niittylä et al., 2004), only the gene encoding MEX1 was significantly upregulated twofold on both CAM days at midday. MEX1 and GLT1 were both downregulated at midnight on both CAM days. The cytosolic enzymes catalyzing the conversion of glucose and maltose to glucose-phosphates (HEXOKINASE2 (HXK2), DPE2, STARCH PHOSPHORYLASE2 (PHS2) and PHOSPHOGLUCOMUTASE3 (PGM3)) were all downregulated at midnight upon drought (e.g. on day 12: 2-fold to 78 rpm, 2-fold to 110 rpm and 3-fold to 111 rpm, respectively). Of the enzymes specific for phosphorolytic starch degradation, the gene encoding ALPHA-AMYLASE3 (AMY3) was upregulated (4-fold on day 12 to 702 rpm), while the plastidial PHS1 gene was downregulated (3-fold on day 12 to 252 rpm) at midnight on both CAM days. The glucose-6-phosphate (G6P) exporter (*GPT*) expression was highly induced at midday upon CAM induction (17-fold; 1,095 rpm on day 12) and downregulated at midnight on day 12 (5-fold to 20 rpm).

The genes encoding cytosolic glycolytic enzymes PHOSPHOGLUCOSE ISOMERASE (PGI, upregulated twofold to 171 rpm at midday), PHOSPHOFRUCTOKINASE (PFK, constitutive level at midday ranging from 275 to 361 rpm), FRUCTOSE-BISPHOPHATE ALDOLASE (FBA, upregulated 5-fold at midday on day 12 to 1247 rpm), TRIOSEPHOSPHATE ISOMERASE (TPI, constitutive level at midday ranging from 980 to 1,541 rpm), SUBUNIT C2 OF GLYCERALDEHYDE-3-PHOSPHATE DEHYDROGENASE (GAPC-2, upregulated 2-fold at midday to 2,649 rpm), PHOSPHOGLYCERATE MUTASE (PGlyM, upregulated at midday 4-fold to 675 rpm) and ENOLASE (upregulated 3-fold to 2,273 rpm) were of high abundance or more abundant in CAM at midday. The gene encoding PHOSPHOGLYCERATE MUTASE (PGK) is of lower abundance (2-fold at midday to 1,167 rpm on day 12). The glycolytic enzymes, whose transcripts were more abundant, produce 3-phosphoglycerate (3-PGA), which may enter

293 the chloroplast via TRIOSE PHOSPHATE/PHOSPHATE TRANSLOCATOR (TPT, constitutive
294 level ranging from 1,632 to 2,905 rpm). Triose-phosphates (3-PGA and GAP) resulting from
295 RUBISCO based carbon fixation and from recycling the pyruvate out of the decarboxylation
296 reaction can be stored as starch. The genes encoding starch precursor biosynthetic enzymes,
297 PHOSPHOGLUCOMUTASE (PGM) and the LARGE SUBUNIT 4 OF ADP-GLUCOSE
298 PYROPHOSPHORYLASE (APL4), were more abundant (6-fold to 1063 rpm and 9-fold to 3790
299 rpm at midday on day 12, respectively) and transcript levels of the GRANULE-BOUND
300 STARCH SYNTHASES (GBSS) were unchanged while those of ISA1 and STARCH
301 BRANCHING ENZYME3 (BE3) were significantly less abundant (4-fold to 66 rpm and 3-fold to
302 296 rpm at midday, respectively). The transcript levels of more abundant genes involved in
303 carboxylation, decarboxylation, glycolysis, and gluconeogenesis were reduced to the levels of
304 well-watered plants upon re-watering, except for *GWD* (3-fold upregulated at midday), *GPT1*
305 (4-fold upregulated at midday) and *NADP-ME1* (3-fold upregulated at midday), which remained
306 highly abundant on day 2 after re-watering.

307

308

309 **Malate, Citrate, Soluble Sugars and Starch**

310 In C_3 performing plants, malate levels were somewhat higher at midday than at midnight (Fig.4,
311 day 0, 4, and 2 days after re-watering). By contrast, in plants exhibiting CAM (Fig.4, day 9 and 12;
312 and Supplemental Table S2), malate levels were up to eightfold higher at midnight as compared to
313 midday and up to fourfold higher as compared to midnight during C_3. The increased malate levels
314 at midnight are consistent with the increased acidification measured at the end of the night (Fig.
315 1B) but did not reflect the full diurnal amplitude during the light/dark cycle. As midnight levels are
316 higher than midday levels, malate decarboxylation may occur quite rapidly during the first 6 hours
317 of the light period (Fig. 4). Citrate showed a similar pattern to malate, as observed in other CAM
318 species (Winter and Smith, 1996; Lüttge, 2002), with increased amounts during the night in CAM
319 plants compared to C_3 plants albeit with a lower amplitude than malate. In agreement with the C_3
320 plant *A. thaliana* (Smith et al., 2004), *T. triangulare* leaves performing C_3 photosynthesis showed
321 high glucose, fructose and sucrose pool sizes at the middle of the day reflecting high

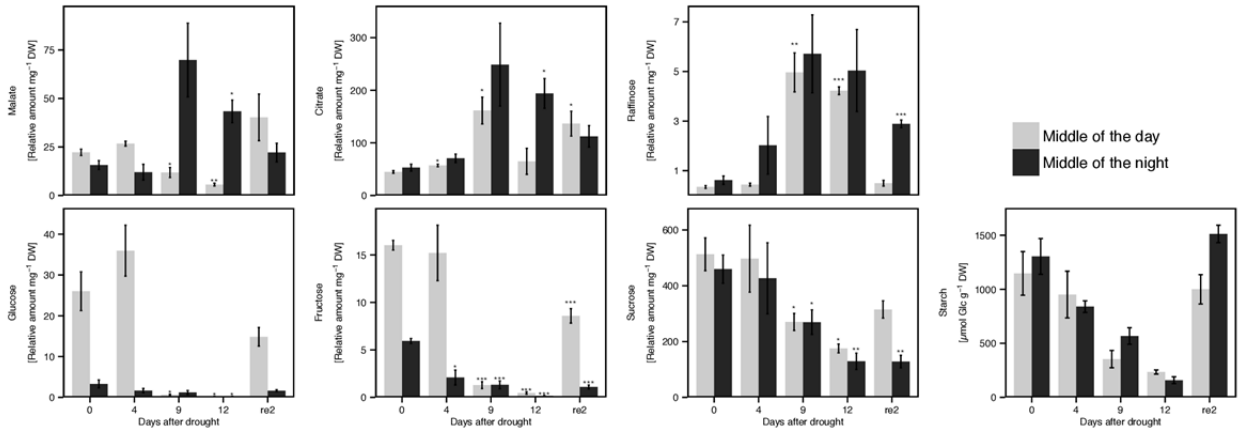

Figure 4. Levels of organic acids, soluble sugars and starch in *T. triangulare* in response to varying levels of water availability. Except for starch, all metabolites were measured by GC-MS and normalized to dry weight (DW) and internal ribitol standard (Mean ± SE, n = 3-4, asterisks indicate Student's *t* test significance in comparison to day 0 at $***P < 0.001$, $**P < 0.01$, $*P < 0.05$). Starch was normalized to DW (Mean ± SE, n = 2-4). re2, 2 days after re-watering.

photosynthetic activity (Fig. 4). While glucose and fructose levels dropped at night, sucrose levels in the middle of the night were high, probably due to sucrose synthesis from starch during the night as reported previously (Chia et al., 2004; Smith et al., 2004). The amounts of glucose, fructose, and sucrose during the day and night dropped in CAM conditions (day 9 and 12) and were accompanied by reduced amounts of starch. The total amount of starch showed a continuous decrease from day 4, 9 to 12. Two days after re-watering, starch levels were increased to the amounts before drought, while glucose, fructose and sucrose pools were not fully restored.

The photorespiratory metabolites glycerate and glycolate were significantly reduced in CAM conditions (Supplemental Fig. S4). During the day, glycerate was depleted 40.2-fold and 238.9-fold on days 9 and 12, and during the night 3.6-fold and 16.7-fold. Glycolate was depleted during the day on day 9 and 12 (2.2-fold and 3.1-fold).

The contents of the putative compatible solute raffinose increased significantly during day (14.4-fold and 12.3-fold) and night (9.2-fold and 4.7 fold) on day 9 and 12 compared to day 0 and the increased amounts at night were not fully reverted two days after re-watering (Fig. 4). Well-known compatible solutes in C_3 plants (Bohnert, 1995; Hare et al., 1998), proline and the sugar alcohol mannitol, were only enriched in individual plants of the biological replicates (Supplemental Fig. S5).

Mapman and *K*-means Clustering Indicate Multiple Layers of Response and Regulation

In order to understand alterations of mRNA amounts beyond the changes in the

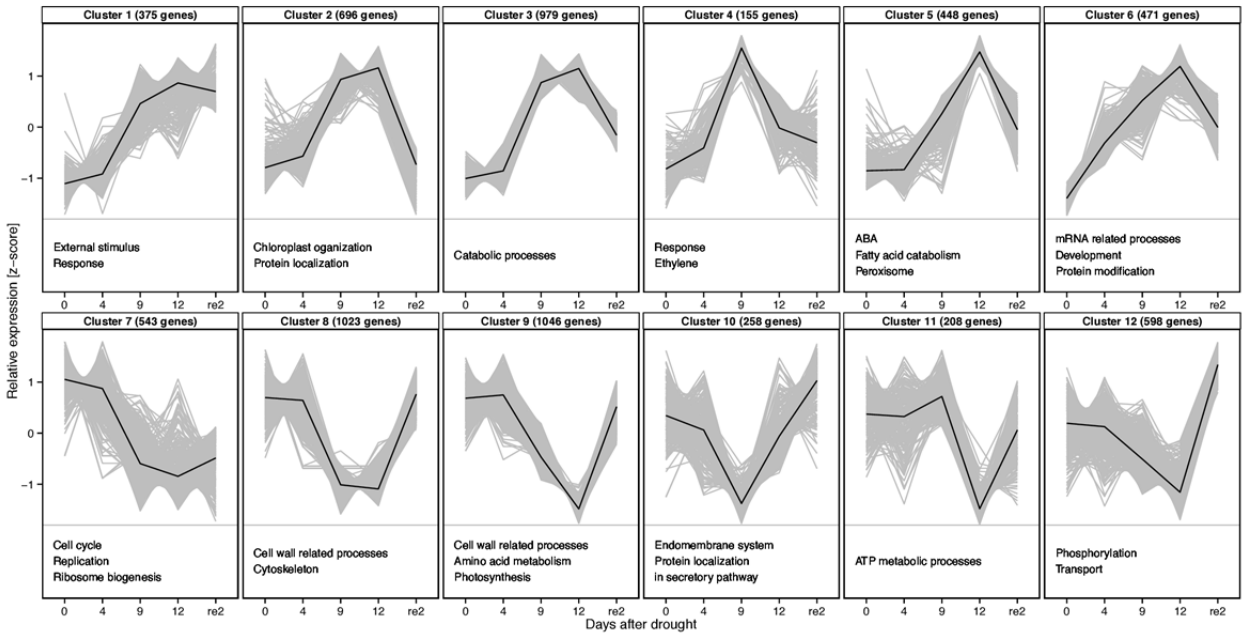

Figure 5. *K*-means clustering of relative gene expression and selected enriched gene ontology (GO) terms. Genes that were found to be differentially expressed in the middle of the day between one of the water-limited stages and day 0 (DESeq2, q < 0.01) were used for the *k*-means approach (6800 genes in total). For the full list of enriched GO Terms see Supplemental Dataset S4. Grey line, expression of single genes; black line, average of all genes in cluster; re2, two days after re-watering.

CAM-related genes described earlier (Fig. 3), three independent analyses were used to test general changes at the metabolic pathway and single gene level: (i) Mapman-based analysis using all values followed by Wilcoxon Rank Sum test (see Materials and Methods) for enrichment (Thimm et al., 2004) (Supplemental Fig. S6), (ii) *k*-means clustering of the significantly changed genes followed by gene ontology (GO) term enrichment analysis (Fig. 5), and (iii) manual inspection of the 50 genes with the highest fold changes on day 12 (Table 1 and Table 2). In Mapman (Supplemental Fig. S6), the metabolism overview again indicated little to no gene expression changes on day 4 of drought and re-watered plants compared to well-watered samples and massive changes during days 9 and 12 of water-limitation (Supplemental Fig. S6). The changes included downregulation of genes involved in cell wall metabolism (Supplemental Dataset S4). Genes of cell wall proteins of all classes were markedly downregulated ($q < 10^{-6}$ at midday), as were the biosynthesis genes for cell wall polymers (cellulose: $q < 10^{-08}$, modifiers: $q < 10^{-10}$ at midday , pectin esterases: $q < 10^{-11}$, pectate lyase: $q < 10^{-11}$, precursor synthesis: $q < 10^{-7}$, hemicellulose: $q < 10^{-6}$ at midnight). Downregulation of photosynthetic genes of the light reactions was visible on day 9 but more pronounced on day 12 of drought ($q < 10^{-5}$). Consistent with the previous analysis (Fig. 3), starch turnover genes ($q < 10^{-4}$) and genes of glycolysis ($q < 10^{-3}$ on day 12) were strongly upregulated. Additional strong upregulation was limited to the genes in the raffinose synthesis

pathway ($q < 10^{-2}$), the committed step of proline biosynthesis, and to the myo-inositol oxidases (Tables 1 and 2).

K-means clustering grouped 6,800 significantly DEGs at midday compared to day 0 by transcriptional pattern into twelve clusters (Fig. 5). Six clusters contained 3,124 genes ascending (clusters 1 – 6, Fig. 5) and six clusters contained 3,676 genes descending with pronounced water-limitation (clusters 7 -12, Fig. 5). The clusters with ascending genes included one cluster with gradual increase up to day 12 and only little recovery after 2 days of re-watering (cluster 1). This cluster was enriched in GO terms related to external stimulus, and response. Clusters 2 and 3 show mostly stable expression between days 9 and 12 and the expression was fully (cluster 2) and partially (cluster 3) recovered upon two days of re-watering. The list of genes with fully restored abundance of cluster 2 is enriched in GO terms related to chloroplast organization, protein localization, and starch. The genes in cluster 3 recovered only partially to well-watered levels after re-watering and this cluster showed significant enrichment of terms related to catabolic processes. Cluster 4 was only transiently upregulated on day 9 of water withholding but dropped back to background levels on day 12. It was enriched with GO terms relating to responses to signals, which include ethylene and mechanical stimulus. The expression of genes in clusters 5 and 6 peaked on day 12. Genes of cluster 5 only responded after 9 d of drought, increased sharply towards day 12 and mostly recovered after 2 days of re-watering and were enriched in GO terms related to ABA, fatty acid catabolism, and peroxisomes. The expression of genes in cluster 6 responded already after 4 days of drought, was only partially reverted and was enriched for mRNA related processes, development and protein modification.

Similar to cluster 1, where genes were upregulated and stayed mostly up despite re-watering, cluster 7 contained genes that dropped in expression during day 9 and 12 of drought and barely recovered. Cluster 7 was enriched in genes related to growth, i.e. in GO terms referring to DNA replication, cell cycle, and ribosome genesis. Genes of cluster 8 were similarly downregulated during CAM conditions but fully recovered upon re-watering. This cluster is enriched in GO terms related to cell wall processes, and cytoskeleton. Genes in cluster 9 only responded on day 9, further increased on day 12 of drought and fully recovered after re-watering. This cluster was enriched in GO terms related to cell wall related processes, amino acid metabolism, and photosynthesis. Cluster 10 was the mirror cluster of cluster 4, which peaked on

388 day 9, and included genes with peak downregulation on day 9. It was enriched in genes related to
389 protein localization in the secretory pathway and the endomembrane system, including the protein
390 population of the plasma membrane. Downregulation of genes in clusters 11 and 12 peaked on day
391 12. Genes in cluster 11 responded only after 12 d of drought and fully recovered after re-watering.
392 This cluster was enriched in processes related to nucleotide metabolic processes. Expression of
393 genes in cluster 12 began decreasing on day 4, continued to decrease until day 12, and after
394 re-watering were increased above well-watered levels. This overshoot cluster was enriched in
395 genes related to posttranslational modification in particular phosphorylation and transport.
396 Analogous *k*-means clustering of 7,563 significant DEGs at midnight revealed large overlap of
397 major changes in comparison to day 0 at midday (Supplemental Figure S7, Supplemental Dataset
398 5). Taken together, the clusters with elevated expression during drought mostly contained genes
399 enriched in GO terms related to catabolism, RNA metabolism and also related to signaling. The
400 clusters with reduced gene expression contained genes related to growth from photosynthesis over
401 amino acid synthesis and cell wall processes to DNA replication and cell cycle.

402 To highlight the results of the analysis at the pathway level, the top 50 of significantly
403 induced (Tab. 1) and repressed (Tab. 2) genes on day 12 of water limitation were analyzed. Of the
404 fifty genes with the highest upregulation on day 12 in *T. triangulare*, 22 were upregulated by ABA
405 in *A. thaliana* (Tab. 1). The CAM gene *PPC* was among the top fifty upregulated genes. Six genes
406 were related to production of compatible solutes or their precursors including raffinose,
407 beta-alanine, and sugar alcohols. One gene encoding a LATE EMBRYOGENESIS ABUNDANT
408 (LEA) protein was among the top 50 induced genes as well as a heat inducible chaperone and the
409 oxidative stress responsive OXIDATIVE STRESS3 (OXS3). Light protection was seemingly
410 strengthened as evidenced by EARLY LIGHT INDUCIBLE1 (ELIP1), FTSH PROTEASE6
411 (FTSH6) and two dyneins, which may be involved in organelle repositioning (Heddad and
412 Adamska, 2000; Hutin et al., 2003; Zelisko et al., 2005). Proteins encoded by eleven of the fifty
413 most induced genes were involved in regulation: the SNF1 RELATED KINASE REGULATORY
414 SUBUNIT GAMMA1 (KING1), the F-box protein EID1-LIKE 3 (EDL3), RHO
415 GUANYL-NUCLEOTIDE EXCHANGE FACTOR11, and four transcription factors including
416 SOMNUS and a PLATZ transcription factor. There were also three transport proteins affected.

417 The fifty genes most reduced in expression on day 12 included 21 genes involved in cell

418 wall synthesis, nine genes related to lipid metabolism and the vacuolar aquaporin TONOPLAST
419 INTRINSIC PROTEIN2;2 (Tab. 2). Downregulation of DNA replication via downregulation of
420 the genes (*MINICHROMOSOME MAINTENANCE 2-3 and 5-7*) encoding five of six subunits of
421 the helicase and downregulation of the gene encoding DNA-directed DNA polymerase
422 INCURVATA2 was also evident among the fifty most downregulated genes, indicating cell-cycle
423 arrest.

424 **Mediators of the Transcriptional Changes**

425 *K*-means clustering identified a multi-layer response with genes only transiently regulated
426 on day 9 of drought and with genes with sustained change on both day 9 and day 12 of drought. To
427 identify the candidate transcriptional regulators mediating the responses, genes encoding for
428 putative transcription factors were extracted from PlnTFDB (Pérez-Rodríguez et al., 2010) and
429 tested for differential expression on either day 9 or day 12 of water limitation relative to the
430 well-watered state (day 0) and for cluster membership. Of 1,449 identified transcription factor
431 genes, 582 (40%) were differentially regulated on either day 9 or day 12 or both compared to
432 well-watered plants (Supplemental Dataset S6). Of the 582, a subset of 19 transcription factor
433 genes belonged to cluster 4, the genes, which were only transiently upregulated on day 9 of
434 drought (Tab. 3). These included eight TFs of the APETALA2 AND ETHYLENE-RESPONSIVE
435 ELEMENT BINDING PROTEINS (AP2-EREBP) class including C-REPEAT/DRE BINDING
436 FACTORS (CBF2 and CBF3), which are known to be stress induced (Zou et al., 2011), REDOX
437 RESPONSIVE TRANSCRIPTION FACTOR1 (RRTF1) and ETHYLENE RESPONSE
438 FACTOR8 (ERF8). Both CBFs were shown to bind the drought responsive element DNA
439 sequence (Liu et al., 1998). Two zinc finger transcription factors, SALT TOLERANCE ZINC
440 FINGER (STZ) and SALT-INDUCIBLE ZINC FINGER2 (SFZ2) belonged to cluster 4. STZ was
441 shown to function as a transcriptional repressor in response to drought and ABA (Sakamoto et al.,
442 2000; Sakamoto et al., 2004), while SFZ2 is induced by salt stress (Sun et al., 2007). In addition,
443 three genes encoding NO APICAL MERISTEM (NAC) domain proteins, one GRAS, one bZIP
444 and three MYB-domain proteins made up the transcriptional part of cluster 4. The known
445 functions of transcription factors in the transient group indicated that *T. triangulare* underwent a
446 transient general stress response commonly observed in plants mediated primarily by the drought
447 responsive element binding transcription factors.

448 Of the remaining 563 genes encoding transcription factor candidates, the top 25
449 upregulated were analyzed for known functions (Tab. 4). The ABA-responsive proliferation
450 inhibitor SOMNUS (SOM) was the most highly upregulated transcription factor on day 12. The
451 top 25 also included four genes encoding transcription factors known to be involved in ABA
452 signaling, NUCLEAR FACTOR Y, SUBUNIT A1 (NF-YA1), NF-YA9 and HOMEOBOX7
453 (HB7) and one NAC-like transcription factor, NAC-LIKE, ACTIVATED BY AP3/PI (NAP),
454 which acts upstream of ABA biosynthesis and promotes chlorophyll degradation (Yang et al.,
455 2014). In addition, two transcription factors of the Orphans family, ETHYLENE RESPONSE 2
456 (ETR2) and ETHYLENE INSENSITIVE 4 (EIN4), which were shown to antagonistically control
457 seed germination under salt stress (Wilson et al., 2014) as well as three heat shock factor family
458 proteins were amongst the 25 most upregulated transcription factors. The sustained response of
459 *T. triangulare* included ABA responsive transcription factors and growth associated regulators,
460 while the transient response included the DRE responsive TFs of the CBF family.

461 To test if phytohormones other than ABA are also involved in the drought response, the
462 overlap between genes significantly changed on day 12 at midday and genes specifically altered by
463 the application of different hormones in *A. thaliana* (Goda et al., 2008) was determined and
464 statistically evaluated. Among the genes shown to be upregulated during hormone treatment of *A.*
465 *thaliana* with ABA, auxin, brassinosteroids, cytokinine and ethylene, only the ABA-upregulated
466 genes were enriched amongst the *T. triangulare* drought-inducible genes (Supplemental Fig. S8).
467 434 ABA-regulated genes of *A. thaliana* were drought-induced genes in *T. triangulare* and
468 accordingly, 541 ABA-regulated genes of *A. thaliana* were repressed by drought in *T. triangulare.*
469 The ABA-, auxin-, brassinosteroids and ethylene-downregulated genes were enriched amongst the
470 *T. triangulare* drought-repressed genes. However, only few genes were shown to be repressed by
471 auxin, brassinosteroids, and ethylene (90, 11, and 23, respectively). Thus, among the
472 phytohormones, ABA made the major contribution to the control of drought-controlled genes and
473 likely controls at least one-fifth of the genes differentially regulated under drought conditions in *T.*
474 *triangulare*.

475 To visualize the ABA contribution to changes in general metabolism, the Mapman map of
476 ABA induced changes in *A. thaliana* was compared with those occurring in *T. triangulare*
477 (Supplemental Fig. S9). The map of ABA responsive genes replicates the induction of raffinose

478 synthesis genes, and a mild reduction of photosynthesis genes but failed to result in the major
479 changes in cell wall synthesis and changed photorespiration, sulfur metabolism and secondary
480 metabolism. The ABA signal detected in *A. thaliana* at the level of metabolic gene expression is
481 not fully congruent with the signals detected in *T. triangulare* indicating additional layers of
482 regulation in *T. triangulare*.

483

484

DISCUSSION

Facultative CAM

During CAM induction in *T. triangulare*, several key components of the CAM-cycle *s.s.* were transcriptionally upregulated such as genes encoding PEPC, NADP-ME, NAD-ME, and PPDK (Fig. 3). Other components, including transcripts of MDH and BCA3, remained unchanged but were constitutively highly expressed already prior to CAM induction. This is consistent with enzyme activity data for MDH (Holtum and Winter, 1982) and CA (Tsuzuki et al., 1982) in *M. crystallinum* operating in the C_3 and CAM modes, that were already very high in the C_3 state. Nonetheless, Cushman et al. (2008) found additional upregulation of these enzymes during salt-induced CAM in *M. crystallinum*. In C_4 photosynthesis, activities of the corresponding carboxylation and decarboxylation enzymes required for CAM are not temporally but spatially separated into different cell types (Sage, 2003). In C_4 species of the genera *Flaveria* and *Cleome*, NAD-MDH is also not transcriptionally elevated relative to C_3 sister species (Bräutigam et al., 2011; Gowik et al., 2011) and CA only in some but not in all cases (Bräutigam et al., 2014).

In contrast to the canonical scheme of the CAM-cycle with NADP-ME localized in the cytosol (Holtum et al. (2005) and references therein), we found two isoforms of NADP-ME to be upregulated at both midday and midnight during CAM in the cross species mapping (Fig. 3 and Supplemental Dataset S3). The contig analysis indicates that indeed two contigs are highly expressed, however both possess a target peptide (Emanuelsson et al., 2000) and cluster with the plastidial AtNADP-ME4 with high bootstrap support. (Supplemental Fig. S3). The putative plastidic malate importers of the DiT family are not upregulated (Supplemental Dataset S3). NAD-ME was also upregulated albeit at lower absolute levels, but concomitant with the required malate importer DIC (Supplemental Dataset S3). Taken together the data suggest that multiple routes for decarboxylation are possible. Unlike in the transcriptomic analyses of C_4 species (Bräutigam et al., 2011; Gowik et al., 2011), the transcriptomic evidence favors neither pathway in *T. triangulare*. It cannot be excluded that the low levels of CAM photosynthesis detected in *T. triangulare* (Winter et al., 2014) are supported by multiple decarboxylation routes. Ideally our findings on the transcript levels of NAD(P)-ME would be confirmed by enzyme activity data, but so far all biochemical assays to measure activity in leaf material failed due to a suppression

514 effect derived from an unknown constitute of the *T. triangulare* plant extract (Supplemental Fig.
515 S10). Experimental differentiation of the biochemical pathway of malate decarboxylation in the
516 light during CAM in *T. triangulare* will be part of future work.

517 PPDK was strongly upregulated during CAM-induction in *T. triangulare* (Fig. 3). In *M.*
518 *crystallinum*, the plastidic location of PPDK was demonstrated by measurements of enzyme
519 acvitity combined with studies of pyruvate metabolism of intact isolated chloroplasts (Winter et
520 al., 1982; Holtum et al., 2005). However, immunogold labeling of PPDK in the CAM species
521 *Kalanchoë blossfeldiana* (Kondo et al., 2001) also raises the possibility of cytosolic PEP
522 regeneration. In support of this hypothesis, the contig Tt26901, which encodes PPDK with a
523 truncated N-terminus, showed markedly higher transcript amounts on days 9 and 12 compared to
524 day 0 and compared to the longer contig, which encodes for a putative target peptide. The contigs
525 possibly represent splicing variants of the same gene and encode for PPDKs dually targeted to the
526 cytosol (Tt26901, truncated N-terminus) or the chloroplast (Tt24575) as found in *A. thaliana*
527 (Parsley and Hibberd, 2006). In C_4 species (NADP-ME and NAD-ME type), where the
528 regeneration of PEP is invariably localized in the plastids, the transporters for pyruvate import (i.e.
529 BASS2 and NHD1) and PEP export (i.e. PPT) are increased in expression compared to C_3 sister
530 plants (Bräutigam et al., 2008; Furumoto et al., 2011; Bräutigam et al., 2014). Interestingly, while
531 BASS2 was upregulated but lowly expressed at midnight, transcripts encoding transporters of the
532 PPT family were found to be downregulated during the C_3-CAM switch in *T. triangulare*
533 (Supplemental Dataset S3). This contrasts with *M. crystallinum* where transcriptional induction of
534 PPT was detected (Kore-eda et al., 2005). Transcripts matching the NHD1 gene were not detected.
535 The absence of a target peptide in the major contig encoding for PPDK suggests that concomitant
536 with the missing NHD1 and downregulated PPT, *T. triangulare* employs cytosolic PPDK. In
537 addition to PPDK, both isoforms of PPDK regulatory protein, which promote circadian regulation
538 of PPDK activity by dark-phased phosphorolytic inactivation (Dever et al., 2015), were slightly
539 but significantly induced during CAM in *T. triangulare* (Supplemental Dataset S3).

540 During the evolution of C_4, the change of a single amino acid residue in the N-terminal
541 region of PEPC, namely from alanine to serine, was shown to increase the enzyme's kinetic
542 efficiency compared to C_3 sister plants (Svensson et al., 1997; Bläsing et al., 2000; Svensson et al.,
543 2003; Gowik et al., 2006). It was recently shown that in C_4 and CAM species within the

Caryophyllales, to which the *Talinaceae* belong, the isogenes of a recurrently recruited gene lineage encoding PEPC1, namely *ppc1-E1c,* almost exclusively encodes the C_4-like Ser780 (Christin et al., 2014). In the same study, in response to reduced irrigation the expression of *ppc1-E1c* was upregulated at night in *Portulaca oleracea*, a C_4 species with facultative CAM (Christin et al., 2014). The two *PPC* contigs, Tt9871_4 and Tt9871_6, that exhibit the C_4-like Ser780 (Supplemental Fig. S2A and Supplemental Table S3) indeed cluster together with *ppc1-E1c* isoforms of *Talinaceae and P. oleracea* (Supplemental Fig. S2B). However, highest transcript levels and the most drastic elevation in abundance during CAM induction was found for contig Tt63271, which encodes for the C_3-like Ala780 and clusters in the *ppc1-E1b* clade. Low level CAM photosynthesis apparently employs different PEPC genes compared to C_4 photosynthesis or fully expressed CAM photosynthesis. At night, PEPC is activated through phosphorylation via PEPC kinase (Carter et al., 1991), the activity of which is regulated transcriptionally through a circadian oscillator (Hartwell et al., 1996; Borland et al., 1999; Hartwell et al., 1999; Taybi et al., 2000). Phosphorylated PEPC is less sensitive to feedback inhibition by malate (Hartwell et al., 1996; Taybi et al., 2000; Taybi et al., 2004). Consistent with the circadian regulation and strong upregulation of PEPC kinase at night during CAM induction in *M. crystallinum* (Hartwell et al., 1999; Cushman et al., 2008b; Dever et al., 2015), PEPC kinase was most markedly upregulated at midnight during CAM in *T. triangulare* (expression rank 300 on day 12, Supplemental Dataset S3) enabling increased PEPC activity at night. In contrast to C_4 plants, PEPC of CAM plants needs to be efficiently switched off during the light through feedback inhibition by malate exported from the vacuole to prevent futile cycling of CO_2 (Borland et al., 1999). All of the PEPC isoforms identified as upregulated in *Talinum* carry an arginine residue at position 890 (Supplemental Fig. S2 and Supplemental Table S3) (Paulus et al., 2013) and are thus likely feedback inhibited both by malate export during the day and once vacuolar storage capacity is exceeded during the night.

The upregulation of CAM-cycle genes was accompanied by elevated malate and citrate levels during the night and reduced malate levels during the day (Fig. 4) in agreement with increase in nocturnal acidity (Fig. 1). Photorespiration is not inactivated during the decarboxylation phase of CAM (Niewiadomska and Borland, 2007; Lüttge, 2011), and we observed a mostly stable expression of photorespiratory genes during the C_3-CAM transition (Supplemental Table S7). Reduced steady-state metabolite pools of glycerate and glycolate

(Supplemental Fig. S4), as well as the reduced sugar levels, were likely a consequence of reduced overall photosynthetic rate. Nocturnal carbon assimilation rates during CAM were estimated to be reduced to approx. 5% of CO_2 fixation in the light in the C_3 mode (Winter and Holtum, 2014). Hence, the associated metabolite fluxes during CAM are expected to be low.

The carboxylation reaction during the night depends on degrading starch for PEP production. The degradation can be either phosphorolytically or hydrolytically (Häusler et al., 2000; Weise et al., 2011). Some but not all transcripts encoding these two alternate starch breakdown pathways were upregulated (Fig. 3). Phosphorolytic starch breakdown preserves some of the energy released during breakage of the glycosidic bonds in starch and therefore consumes less ATP for activation of the released glucose residues. ATP, ADP and/or free phosphate may balance hydrolytic and phosphorolytic starch breakdown depending on the ATP demand of the cytosol. Using starch and malate contents at the end of the night and the end of the day, the amount of starch turnover was calculated as sufficient to support the level of photosynthesis during CAM (Supplemental Table S8). Efficient starch turnover apparently required elevated expression of both, starch synthesis and starch degradation genes, as well as sufficient branching of the starch to allow rapid degradation (Fig. 3). Based on strong upregulation of *GPT*, which was among the top 50 upregulated genes at midday, and the upregulation of *MEX1* (Fig. 3), glycolysis likely operated in the cytosol, which was confirmed by the transcriptional upregulation of all but one of the cytosolic glycolytic enzymes (Fig. 3). Taken together, inducible CAM required upregulation of key CAM-cycle genes, elevation of starch turnover by changes in selected genes and increased expression of cytosolic glycolytic genes. While starch turnover capacity is increased (Fig. 3), the amount of starch is reduced (Fig. 4), which may be explained by lowered photosynthetic capacity during CAM (Winter et al., 2014). In contrast to *T. triangulare*, CAM can substantially contribute to carbon gain in *M. crystallinum* (Winter and Holtum, 2007), and following salinity-induced CAM starch accumulation is increased and directly correlates with acidification (Haider et al., 2012).

The rapid induction of CAM-related gene expression and the co-expression of ABA- related signaling networks upon drought stress points to a direct connection to the ABA signaling network as shown for *Kalanchoë blossfeldiana* (Taybi et al., 1995) and *M. crystallinum* (Taybi and Cushman, 2002). Control of CAM induction may be exerted either directly by ABA–mediated

phosphorylation and activation of transcription factors or by downstream effectors (Table 4).

Drought Response and Carbon Resource Utilization

Beyond CAM photosynthesis, additional processes contribute to the adaptation of *T. triangulare* to drought, such as a classical drought response and management of carbon resources. Water limitation leads to stomatal closure during the day (Herrera et al., 1991; Winter and Holtum, 2014), which reduces the photosynthetic carbon assimilation and hence pool sizes of soluble sugars such as sucrose, glucose, and fructose during the day and the night (Fig. 4). Under severe drought stress, part of these remaining soluble sugars may act as compatible solutes, retain water in the cells and protect cellular structures against damage. In contrast to the overall loss of these sugars, substantial accumulation of raffinose was observed (Fig. 4) likely triggered by transcriptional upregulation of raffinose biosynthesis (Supplemental Fig. S6 and Tab. 1). During cold acclimation in *A. thaliana* (Nägele and Heyer, 2013) and *Ajuga reptans* (Findling et al., 2014), non-aqueous fractionations localized raffinose to variable extents within the vacuole, cytosol and chloroplast stroma. At this point we do not know, whether raffinose accumulating in drought-stressed *T. triangulare* functions as a compatible solute in the cytosol, supports osmotic pressure maintenance in the vacuole or has protective functions for membranes and/or proteins within the plastid or cytosol (Nishizawa et al., 2008). Although the gene encoding PYRROLINE-5-CARBOXYLATE SYNTHASE (P5CS), which catalyzes the committed step for proline synthesis, was upregulated during CAM (expression rank 57 on day 12 at midday, Supplemental Dataset S1), proline accumulated only in some but not all plants tested (Supplemental Fig. S5). Similarly, levels of the sugar alcohols glycerol, mannitol, myoinositol and sorbitol, which could potentially act as compatible solutes, were not significantly altered during drought, although mannitol accumulated in individual plants (Supplemental Fig. S5 and S11). The discrepancy between transcript and metabolite measurements is likely based on the fact that the transcriptome precedes the metabolome. Although genes were upregulated in all replicates (Supplemental Dataset S1), the metabolic status may be delayed.

Stomatal closure reduces the consumption of absorbed light energy in photosynthesis, potentially leading to short-term redox stress. Among the top 50 upregulated genes, four were involved in light stress, e.g. the gene of ELIP1 (Hutin et al., 2003), which is ABA induced in *A.*

634 *thaliana* (Tab. 1). Genes encoding components of light stress-induced oxidation of fatty acids in
635 the peroxisomes were enriched in cluster 3, representing induced genes that do not quite reach
636 well-watered levels after re-watering (Fig. 5). Thus, despite leaf-angle changes and leaf rolling
637 (Taisma and Herrera (2003) and Fig. 1) that reduce light exposure, a transcriptional upregulation
638 of light protection mechanisms is seemingly required to aid leaf functioning. Additionally, the
639 increase of raffinose, shown to act as a scavenger of hydroxyl radicals in *A. thaliana* (Nishizawa et
640 al., 2008), might play a role in supporting leaf functioning.

641 Under drought, increased use of resources such as fatty acids and proteins was induced
642 (Fig. 5), which might explain the slight increase in free amino acids (Noctor and Foyer, 2000)
643 (Supplemental Fig. S11). Catabolism of fatty acids through peroxisomal processes was induced by
644 day 9 already, maintained on day 12 and only partially reversed upon re-watering. Genes involved
645 in processes related to mRNA turnover were also increased during drought (Fig. 5, cluster 6).
646 These induced catabolic processes were however not associated with permanent damage as the
647 transcriptome returned to pre-stress status upon re-watering (Fig. 2). Most genes encoding
648 anabolic processes such as photosynthesis and amino acid biosynthesis and transport were
649 transcriptionally downregulated (Fig. 5 and Supplemental Fig. S6), but returned to pre-stress
650 levels after re-watering. For example, cell wall biosynthesis was downregulated and completely
651 reversed upon re-watering (Fig. 5, clusters 8 and 9 and Supplemental Fig. S6). Finally, genes
652 involved in replication and the cell cycle were among the most downregulated genes overall on
653 day 12 (Tab. 2) and processes related to replication and ribosome biogenesis were among those,
654 which were downregulated upon drought but did not return to well-watered levels after
655 re-watering (Fig. 5, cluster 7). Apparently, after two days, the expression levels of genes involved
656 in primary production are increased however transcript levels of growth-related genes (e.g. genes
657 involved in replication, translation and cell division) have not yet completely recovered. This
658 might be due to the fact that the full resource availability has not been restored within two days
659 reflected by the still altered starch and metabolite pools (Fig. 2).

660 **Regulation of the Coordinated Drought Response**

661 Clustering differential gene expression indicated that the response of *T. triangulare* is
662 multi-layered since clusters respond and recover at different time-points to different degrees (Fig.

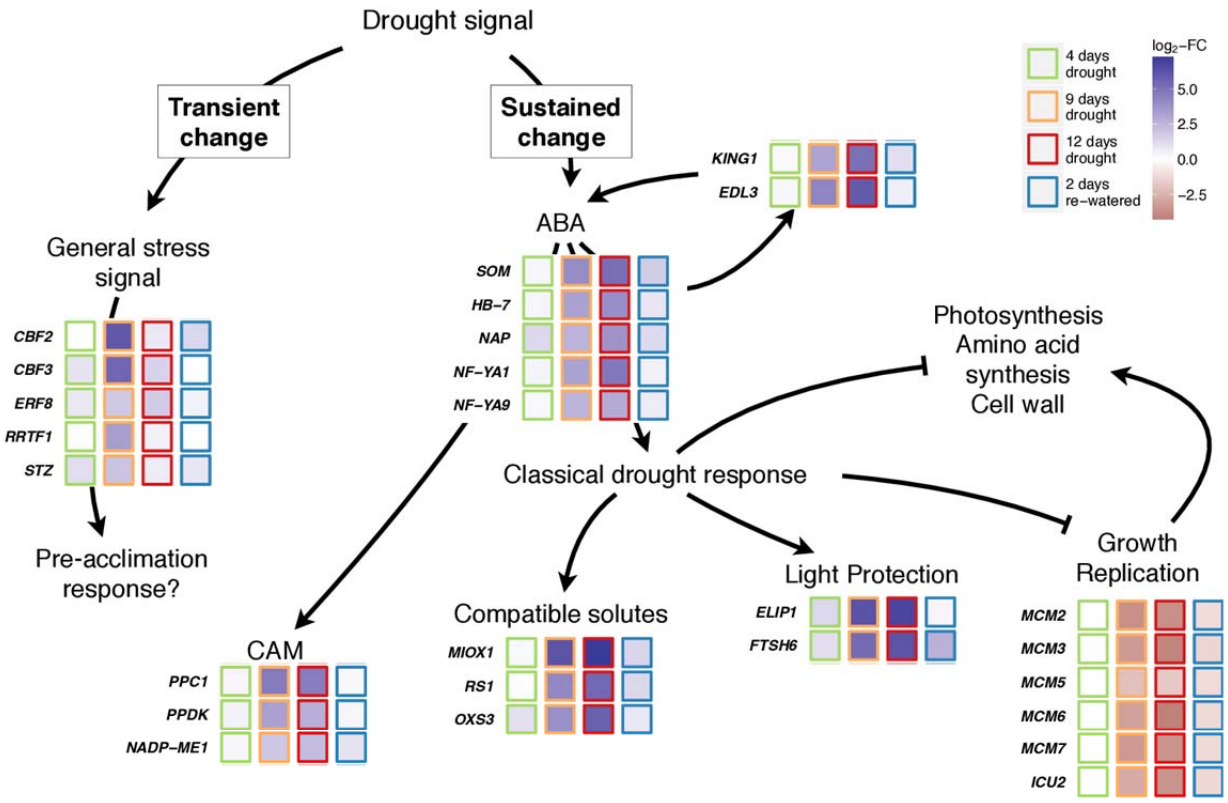

Figure 6. Proposed regulation of the coordinated drought response in *T. triangulare*. Shown are genes discussed in the text. A general stress signal was mediated by transcription factors, which were transiently upregulated on day 9 (*CBF2, C-repeat/DRE binding factor 2; CBF3, C-repeat/DRE binding factor 3; ERF8, ethylene response factor 8; RRTF1, redox responsive transcription factor 1; STZ, salt tolerance zinc finger*) and triggered a yet unclear response. The sustained response to persistent drought was primarily mediated via ABA, the activity of which was maintained through a feed-forward loop (*KING1, SNF1-related protein kinase regulatory subunit gamma 1; EDL3, EID1-like 3*), through ABA-responsive transcription factors (*SOM, SOMNUS*; *HB-7, homeobox 7; NAP, NAC-like, activated by AP3/PI; NF-YA1, nuclear factor Y, subunit A1 and NF-YA9*) and besides the induction of CAM (see Fig. 3 for details: *PPC1, phosphoenolpyruvate carboxylase 1; PPDK, Pyruvate phosphate dikinase, PEP/pyruvate binding domain; NADP-ME1, NADP-malic enzyme 1*) included a classical drought response, i.e. synthesis of compatible solutes (*RS1, Raffinose synthase 1; MIOX1, myo-inositol oxygenase 1; OXS3, oxidative stress 3*) and light protection (*ELIP1, early light inducible protein 1; FTSH6, FTSH protease 6*). At the same time, growth was repressed through downregulation of the replication cassette (*MCMs, minichromosome maintenance; ICU2, incurvata 2*)) and processes related to photosynthesis, amino acid synthesis and cell wall synthesis (see Fig. 5 and Supplemental Fig. S4) allowing *T. triangulare* to engage in a state of quiescence during drought. Log_2-FC, absolute maximum log_2-fold changes in gene expression compared to day 0 at midday or midnight.

3). Initially, drought stress induced a general stress response (clusters 4 and 9, Fig. 5) and a specific ABA mediated response (cluster 5, Fig. 5 and Supplemental Fig. S8). A conceptual model integrating the transcriptomic data is depicted in Fig. 6. The general stress response included the CBFs, which are known to bind the drought responsive element (Zhu, 2002). However, their

upregulation was transient and no longer detectable on day 12 of water limitation (Supplemental Dataset S6). During this initial stress response, our data indicate changes of the endomembrane system (cluster 9, Fig. 5). In contrast, the ABA mediated response was further increased on day 12 (cluster 5, Fig. 5). The transcriptomic response also indicated a feed-forward loop with higher expression of KING1, which activates ABA signaling, and EDL3, which mediates ABA signaling (Tab. 1). At the same time, the expression of a PP2C was increased (expression rank 424 on day 12 at midnight, Supplemental Dataset S1), which is required to attenuate the signaling pathway once the stress signal is removed (Umezawa et al., 2009). Hence, *T. triangulare* plants are transcriptionally enabled to both sustain the ABA signal to the transcriptome and also to switch it off once the stress is removed upon re-watering. The ABA signal is likely overlaid with a carbon starvation signal. This additional signal may explain why several clusters did not recover to well-watered expression levels although soil moisture was restored. Catabolism-related processes only recovered partially (Fig. 5, clusters 3 and 5) and replication and ribosome biogenesis related genes recovered only marginally (Fig. 5, cluster 7).

The candidate transcription factors downstream of the initial signal, which is probably at least in part ABA-mediated, are those, which are significantly upregulated with a large magnitude. They include highly induced ABA-dependent transcription factors, such as HB7, NF-YA1 and 9 or NAP (Tab. 4) as well as the phosphorylation-controlled ABA dependent transcription factors not detectable in the transcriptome analysis. Stalled growth, which is part of the response, may also at least in part be dependent on ABA as SOMNUS is highly induced upon drought (Tab. 1, (Lim et al., 2013). SOMNUS is required to control germination cessation in seeds downstream of the signal perception cascade (Kim et al., 2008) and thus likely controls effector genes required for growth. The trehalose-phosphate and SnRK1 mediated signaling (Baena-Gonzalez et al., 2007) does not significantly overlap with the signals observed in *T. triangulare.*

692 # CONCLUSION

693 This study showed that the response of *T. triangulare* to drought stress was associated with
694 profound and reversible changes in the transcriptome. Known key enzymes of the CAM-cycle and
695 some of those connected to carbohydrate metabolism were upregulated, as were genes encoding
696 functions associated with a classical drought response, including light protection and the synthesis
697 of compatible solutes. Genes related to growth, photosynthesis, the synthesis of cell walls, and
698 amino acids were downregulated in response to drought while catabolic processes were
699 upregulated. A set of transcription factors likely to be involved in mediating these responses was
700 identified. *T. triangulare* is easy to grow, flowers and produces seeds within few weeks after
701 germination, and rapidly induces CAM in response to drought stress, thereby exhibiting important
702 attributes of a potential model system to study key components of a drought response which
703 includes CAM and its signaling components under stress. Research on *T. triangulare* may in the
704 future contribute to engineering drought coping strategies such as CAM via synthetic biology into
705 C_3 crop plants with the goal to improve their performance in water-limited environments (Yang et
706 al., 2015).

707

MATERIALS AND METHODS

Plant Material and Growth Conditions

Talinum triangulare plants were grown in Miracle-Gro Potting Mix (Miracle Gro, Marysville, OH) in "Short-One" treepots, 1.6 l (Stuewe and Sons, Tangent, OR). The experiment was initiated with 28 day old plants in a controlled environment chamber (EGC, Chagrin Falls, OH) maintained under 12 h light (30 °C, 37% relative humidity) / 12 h dark (22 °C) cycles. Photon flux density at leaf level was 425 μmol m^{-2} s^{-1}. Irrigation was withheld on day 1 and recommenced on day 14. Leaves were harvested when plants were well-watered as well as after 4, 9 and 12 days of water-deprivation and watered for two days following the drought period.

Titratable Acidity

Mature leaves of the same plants used for RNASeq and metabolite profiling were harvested at the end of the light and dark periods, respectively, and frozen in liquid nitrogen after measurement of fresh weight. Organic acids were extracted by sequentially boiling leaves in 50% methanol and water. Titratable acidity was determined by measuring the volume of 5 mM KOH required to neutralize the aqueous extract to pH 6.5.

Metabolite Profiling

Lyophilized leaf material was extracted for metabolite analysis by gas chromatography-mass spectrometry (GC-MS) according to (Fiehn et al., 2000) using a 7200 GC-QTOF (Agilent). Data analysis was conducted with the Mass Hunter Software (Agilent). For relative quantification, all metabolite peak areas were normalized to the peak area of the internal standard ribitol added prior to extraction.

RNA Extraction, Preparation and Sequencing of Illumina Libraries

The topmost mature un-shaded leaves (of approximately 3 - 4.5 cm length) of *T. triangulare* were harvested in the middle of the light or the middle of the dark period and immediately frozen in liquid nitrogen. RNA was isolated from ground tissue using the GeneMatrix Universal RNA Purification Kit (EURx Ltd.). Residues of DNA were removed with DNase (New England

734 Biolabs). RNA integrity, sequencing library and fragment size were analyzed on a 2100
735 Bioanalyzer (Agilent). Libraries were prepared using the TruSeq RNA Sample Prep Kit v2
736 (Illumina), and quantified with a Qubit 2.0 (Invitrogen). Samples were multiplexed with 12
737 libraries per lane and sequenced in single-end mode (Rapid Run, 150 bp read length) on an
738 Illumina HiSeq 2000 platform, yielding ~14 million reads per library.

739 **Contig Assembly and Sequence Alignment**

740 In order to substantiate cross-species mapping against the sequenced reference genome of *A.*
741 *thaliana*, Illumina libraries from representative samples (day 0, day 9 and 2 days after re-watering)
742 were pooled and paired-end sequenced (Rapid Run, 100 bp read length) on an Illumina HiSeq
743 2000 platform for assembly of contigs. Trinity assembly of the reads using Trinity (Grabherr et al.,
744 2011) in default mode yielded 105,520 contigs, which were collapsed to 39,781 putative open
745 reading frames using Transdecoder (transdecoder.github.io) and manual removal of duplicated
746 contigs (Suppl. File 2). Remapping placed 81% of the original 150bp reads on the ORFs. Contigs
747 were annotated via BlastX implemented in BLAST+ (Camacho et al., 2009) against peptide
748 sequences of the *Beta vulgaris* reference genome RefBeet-1.1 (Dohm et al., 2013) and peptide
749 sequences of a minimal set of the TAIR10 release of the *A. thaliana genome*
750 (http://www.arabidopsis.org/). Protein sequences were aligned using Clustal Omega at
751 www.ebi.ac.uk (Sievers et al., 2011). Phylogenetic analyses were performed with the PhyML tool
752 (Guindon et al., 2010) implemented in SeaView 4 (Gouy et al., 2010) in default mode after
753 Gblocks creation with least stringent parameters.

754

755 **Read Mapping and Gene Expression Profiling**

756 Illumina reads were aligned to a minimal set of coding sequences of the TAIR 10 release of the *A.*
757 *thaliana* genome (http://www.arabidopsis.org/) using BLAT (Kent, 2002) in protein space. The
758 minimal transcriptome was obtained as described in Gowik et al. (2011) and contains 21,869
759 nuclear encoded protein-coding genes. The best BLAT hit for each read was determined by (i)
760 lowest e-value and (ii) highest bit score. Raw read counts were transformed to reads per million
761 (rpm) to normalize for the number of reads available at each sampling stage. Cross-species

mapping takes advantage of the completeness and annotation of the *A. thaliana* genome and overcomes the limitations of transcriptome assembly (Franssen et al., 2011; Schliesky et al., 2012). To quantify abundance of contigs, the 150 bp single-end reads were mapped onto the assembled contigs using the RNA-Seq analysis tool implemented in the CLC genomics workbench version 8.5 (www.clcbio.com) in default mode.

Data Analysis

Data analysis was performed using R statistics software (R version 3.2.1 provided by the CRAN project, http://www.R-project.org). Differential gene expression was analyzed with the DESeq2 package (Love et al., 2014) in default mode. Automatic independent filtering retained 16,766 genes with nonzero total read count. A significance threshold of 0.01 was applied after p-value adjustment with false discovery rate via Benjamini-Hochberg correction (Benjamini and Hochberg, 1995). Log_2 expression ratios calculated by DESeq2 were used for downstream analysis. For *k*-means clustering, transcript levels were log_2-transformed and scaled via calculation of z-scores by gene. One *k*-means clustering was performed for each daytime of sampling (MD and MN) by R statistics software with 6,800 (MD) and 7,563 (MN) genes that were determined as differentially expressed genes (DEG) compared to well-watered (day 0), respectively. Enrichment for gene ontology (GO) terms of biological processes within *k*-means clusters was performed via Fisher's Exact Test implemented in the R-package topGO (Alexa et al., 2006) (including DEG as the background set, significance level of $\alpha = 0.01$). All log_2-fold changes of water-limited days compared to day 0 were used for pathway analysis in Mapman (Thimm et al., 2004). Wilcoxon Rank Sum test implemented in Mapman was used to test for enrichment and corrected for multiple hypothesis testing via Benjamini-Hochberg correction (Benjamini and Hochberg, 1995). *Arabidopsis* response to treatments with the phytohormones ABA (abscisic acid), ACC (1-Aminocyclopropane-1-carboxylic acid, a precursor of ethylene), BL (brassinolid, a brassinosteroid), IAA (indole-3-acetic acid, i.e. auxin) and zeatin (a cytokinine) were extracted from AtGenExpress and are based on microarrays by Goda et al. (2008). Response to hormone treatment ($n = 3$) compared to mock treatment ($n = 3$) was called significant at $q < 0.01$ (corrected after Benjamini and Hochberg, 1995). Overlap of *T. triangulare* reponse to drought with *Arabidopsis* response to hormone treatments was calculated using Fisher's Exact Test ($p < 0.001$). All log_2-fold changes (treatment vs. mock) of *Arabidopsis* response to ABA treatment (Goda et al.,

2008) were used for pathway analysis in Mapman. Data was annotated with publicly available information for *A. thaliana* (TAIR10, http://www.arabidopsis.org/). Full quantitative data with annotation is available as Supplemental Dataset 1.

ACCESSION NUMBER

The read data have been submitted to the National Center for Biotechnology Information Gene Expression Omnibus under accession number GSE70601.

http://www.ncbi.nlm.nih.gov/geo/query/acc.cgi?token=wryvugcifxexnml&acc=GSE70601

SUPPLEMENTAL DATA

Supplemental Dataset S1. Quantitative information and annotation for all reads mapped onto the reference genome of *Arabidopsis thaliana*.

Supplemental Dataset S2. Quantitative information and annotation for all reads mapped onto the *Talinum* contigs.

Supplemental Dataset S3. Levels of all putative CAM genes *ss.* and *sl.*

Supplemental Dataset S4. Enriched Mapman categories for all plants harvested 4, 9, 12 days after water deprivation and 2 days after rewatering (re2) at the middle of the day (MD) or night (MN)

Supplemental Dataset S5. Full list of enriched GO-terms in *k*-means clusters (Figure 5 and Supplemental Figure S7)

Supplemental Dataset S6. Transcription factors differentially expressed on day 9 and/or day 12

Supplemental Figure S1. Changes in leaf transcriptomes and metabolomes under varying levels of water availability in the middle of the night (Analogous to Figure 1. B and C).

Supplemental Figure S2. *T. triangulare* PEPCs show characteristics of both C_3 and C_4 plants.

Supplemental Figure S3. *Talinum* NADP-ME with highest transcript are predicted to be localized in the plastid.

Supplemental Figure S4. Levels of photorespiratory metabolites.

Supplemental Figure S5. Levels of compatible solutes.

Supplemental Figure S6. Mapman overview of metabolism for all drought samples (day 4, day 9, day 12 of water-deprivation and 2 days after re-watering (re2) compared to day 0.

Supplemental Figure S7. *K*-means clustering of relative gene expression at the middle of the night.

Supplemental Figure S8. Overlap of differentially expressed genes during CAM in *T. triangulare* with hormone treated leaves of *A. thaliana* (Goda et al., 2008).

Supplemental Figure S9. Mapman overview of metabolism for ABA-response in *A. thailana.*

Supplemental Figure S10. Experiments to assay activity of NADP-malic enzyme (panels 1-4) or malate dehydrogenase (panel 5) with leaf extracts of *T. triangulare* ("*Talinum* extract") or recombinant NADP-malic enzyme from *Zea mays* (ZmNADP-ME, provided by Anastasiia Bovdilova, group of Veronica G. Maurino). Leave extraction and enzyme assays were performed as described in Ashton et al. (1990). NADP-ME activity is not detectable in *Talinum* leaf extracts (panel 1). Strong activity of recombinant ZmNADP-ME (panel 2) is fully inhibited by addition of *Talinum* leaf extract (panel 3), while only slightly inhibited by boiled leaf extract of the NADP-ME C4 plant *Flaveria bidentis* ("Flaveria extract", panel 4). This indicates the formation of an inhibitor of unknown kind during the leaf extraction of *T. triangulare* leaves, which affects NADP-ME activity, but not MDH activity (panel 5).

Supplemental Figure S11. Levels of additional metabolites.

Supplemental Table S1. mRNA-Seq statistics

Supplemental Table S2. Metabolite profiling statistics

Supplemental Table S3. Expression levels of *T. triangulare* contigs encoding PEPC

Supplemental Table S4. Expression levels of all *T. triangulare* contigs encoding for subunits of vacuolar ATP synthases

Supplemental Table S5. Expression levels of *T. triangulare* contigs encoding NADP-ME

Supplemental Table S6. Expression levels of two *T. triangulare* contigs encoding PPDK

Supplemental Table S7. Expression levels of genes encoding for photorespiratory enzymes

Supplemental Table S8. Estimated partitioning of carbon in organic acids and starch on day 12

ACKNOWLEDGEMENTS

We acknowledge the excellent technical assistance of M. Graf, K. Weber and E. Klemp for GC-MS measurements, S. Kurz for help with Illumina library preparation and A. Virgo for titration of organic acids.

LIST OF AUTHOR CONTRIBUTIONS

D.B., A.B., T.M.-A., K.W. and A.P.M.W. designed the research. D.B., K.W. and T.M.-A. performed the research. D.B., A.B. and T.M.-A. analyzed data. D.B., A.B., T.M.-A., K.W. and A.P.M.W. wrote the article.

885 **Table I.** *50 most highly upregulated genes on day 12 after drought. RPM, reads per million (n =*
886 *3). MD, middle of the night, MN middle of the day. log_2-FC, log_2-fold change in expression*
887 *at given time point on day 12 compared to day 0. ns, not significantly DEG.*

Locus	Annotation (TAIR10)	Day 0 MD [rpm]	Day 0 MN [rpm]	Day 12 MD [rpm]	Day 12 MN [rpm]	log_2-fold change (MD; MN)
AT2G42600	phospho*enol*pyruvate carboxylase 2	208.67	374.33	4803.67	9910.67	4.05 ; 4.7
AT1G53310	phospho*enol*pyruvate carboxylase 1	312.00	613.33	6656.33	15510.33	3.91 ; 4.61
AT4G17030	expansin-like B1	0.00	0.00	4.67	1.67	4.91 ; 2.55
AT4G26260	myo-inositol oxygenase 4	1.00	0.00	373.33	29.00	7.36 ; 5.02
AT1G14520	myo-inositol oxygenase 1	3.33	1.33	1290.00	112.67	7.25 ; 5.42
AT2G19800	myo-inositol oxygenase 2	1.67	0.67	451.00	37.00	6.6 ; 4.83
AT1G55740	seed imbibition 1	9.33	46.67	605.33	2236.33	5.41 ; 5.38
AT3G08860	PYRIMIDINE 4	3.33	44.33	139.67	23.33	4.68 ; ns
AT2G38400	alanine:glyoxylate aminotransferase 3	2.67	30.00	103.67	17.67	4.54 ; ns
AT3G50980	dehydrin xero 1	0.00	0.00	7.67	0.00	4.9 ; ns
AT3G22840	Chlorophyll A-B binding family protein	17.67	15.00	4029.67	17.33	6.74 ; ns
AT5G15250	FTSH protease 6	6.67	2.67	764.33	3.00	6.18 ; ns
AT5G20110	Dynein light chain type 1 family protein	3.67	23.67	368.67	12.33	6.05 ; ns
AT4G27360	Dynein light chain type 1 family protein	19.67	32.33	654.33	54.33	4.62 ; 0.83
AT3G29410	Terpenoid cyclases/Protein prenyltransferases superfamily protein	0.00	0.00	4.67	17.67	4.86 ; 5.96
AT5G16020	gamete-expressed 3	0.33	1.33	41.00	3.67	5.75 ; 1.59
AT1G80920	Chaperone DnaJ-domain superfamily protein	0.33	12.33	23.33	578.33	4.6 ; 5.46
AT3G22740	homocysteine S-methyltransferase 3	2.33	23.33	118.33	145.33	5.08 ; 2.68
AT1G10060	branched-chain amino acid transaminase 1	1.00	4.67	31.33	11.00	4.63 ; ns
AT1G29900	carbamoyl phosphate synthetase B	69.67	80.67	309.67	1955.67	1.75 ; 4.56
AT1G12740	cytochrome P450, family 87, subfamily A, polypeptide 2	4.00	86.33	290.67	10.67	4.47 ; -2.13
AT1G52240	RHO guanyl-nucleotide exchange factor 11	6.67	113.33	1652.00	31.00	7.23 ; -1.69
AT1G28480	Thioredoxin superfamily protein	1.00	0.67	2.00	37.00	ns ; 5.76
AT1G18100	PEBP (phosphatidylethanolamine-binding protein) family protein	1.00	1.00	34.67	59.00	4.52 ; 5.57
AT1G03790	SOMNUS	0.00	0.67	19.67	4.33	5.15 ; 2.38
AT1G54070	Dormancy/auxin associated family protein	0.00	1.67	2.33	75.33	2.5 ; 5.01
AT1G80390	indole-3-acetic acid inducible 15	0.00	0.00	5.67	5.33	4.73 ; 5
AT5G12840	nuclear factor Y, subunit A1	0.67	2.67	25.67	31.00	4.75 ; 3.56
AT1G15330	Cystathionine beta-synthase (CBS) protein	0.00	0.00	1.33	5.00	3.54 ; 4.74
AT3G21700	Ras-related small GTP-binding family protein	0.67	3.00	17.33	82.33	3.56 ; 4.61
AT1G21000	PLATZ transcription factor family protein	0.33	25.33	18.33	135.00	4.48 ; 2.45
AT3G63060	EID1-like 3	0.00	0.00	22.00	13.33	5.88 ; 5.32
AT3G48530	SNF1-related protein kinase regulatory subunit gamma 1	0.67	31.00	39.67	275.00	5.05 ; 3.1
AT5G56550	oxidative stress 3	1.33	4.33	18.33	310.33	3.03 ; 5.71
AT5G47560	tonoplast dicarboxylate transporter	0.00	0.00	5.33	10.67	4.99 ; 5.93
AT1G32450	nitrate transporter 1.5	4.33	68.00	233.67	34.33	5.04 ; ns
AT4G21680	NITRATE TRANSPORTER 1.8	2.00	20.33	101.33	16.67	5.02 ; ns
AT3G27250	unknown	0.00	1.00	85.67	58.33	7.08 ; 5.63
AT1G52720	unknown	0.67	26.67	156.33	80.33	6.72 ; 1.63
AT4G19390	Uncharacterised protein family (UPF0114)	6.33	49.33	1234.33	276.00	6.58 ; 2.35
AT3G03170	unknown	0.00	0.67	4.33	66.00	3.56 ; 6.21
AT3G48510	unknown	2.67	1.33	78.33	106.00	4.16 ; 6.08
AT4G26288	unknown	0.00	0.33	2.00	32.67	3.02 ; 5.99
AT5G40790	unknown	1.67	0.33	38.33	48.00	3.96 ; 5.85
AT1G15380	Lactoylglutathione lyase / glyoxalase I family protein	4.67	9.67	337.00	109.33	5.65 ; 3.42
AT5G50360	unknown	1.00	0.00	3.67	11.67	ns ; 5.3
AT2G44670	Protein of unknown function (DUF581)	0.33	2.33	3.33	65.67	1.92 ; 4.81
AT5G02020	unknown	1.67	3.33	7.33	96.67	1.74 ; 4.57
AT1G27461	unknown	0.00	0.00	0.00	3.67	ns ; 4.51
AT2G28780	unknown	0.33	0.00	16.00	0.00	4.49 ; ns

888

889 **Table II.** *50 most highly downregulated genes on day 12 after drought. RPM, reads per million (n*
890 *= 3). MD, middle of the night, MN middle of the day. log_2-FC, log_2-fold change in expression*
891 *at given time point on day 12 compared to day 0. ns, not significantly DEG.*

Locus	Annotation (TAIR10)	Day 0 MD [rpm]	Day 0 MN [rpm]	Day 12 MD [rpm]	Day 12 MN [rpm]	log_2-fold change (MD; MN)
AT5G20630	germin 3	2449.67	648.33	2.00	1.67	-9.13 ; -7.24
AT1G72610	germin-like protein 1	932.67	274.67	1.00	1.00	-8.55 ; -6.45
AT1G64390	glycosyl hydrolase 9C2	177.00	80.00	0.67	1.67	-7.45 ; -5.27
AT4G21960	Peroxidase superfamily protein	1529.33	8040.00	10.67	349.67	-7.09 ; -4.22
AT4G11050	glycosyl hydrolase 9C3	70.67	31.67	0.00	0.33	-7.06 ; -5.32
AT5G22740	cellulose synthase-like A02	272.67	207.00	3.33	4.67	-6.42 ; -5.27
AT2G32990	glycosyl hydrolase 9B8	42.00	34.33	0.33	0.00	-6.36 ; -6.19
AT2G04780	FASCICLIN-like arabinoogalactan 7	15.00	24.33	0.00	0.00	-6.12 ; -6.27
AT4G37450	arabinogalactan protein 18	10.33	22.67	0.00	0.00	-5.64 ; -6.24
AT2G35860	FASCICLIN-like arabinogalactan protein 16 precursor	94.33	125.67	2.67	1.33	-5.11 ; -6.12
AT5G03760	Nucleotide-diphospho-sugar transferases superfamily protein	61.00	64.33	1.00	0.67	-5.75 ; -6.11
AT2G37130	Peroxidase superfamily protein	21.00	7.67	0.00	0.00	-6.03 ; -4.26
AT3G11700	FASCICLIN-like arabinogalactan protein 18 precursor	129.33	195.67	4.67	2.67	-5.04 ; -5.92
AT1G02335	germin-like protein subfamily 2 member 2 precursor	9.33	16.33	0.00	0.00	-5.47 ; -5.91
AT1G67750	Pectate lyase family protein	15.00	53.33	0.00	0.67	-5.82 ; -5.5
AT4G13410	Nucleotide-diphospho-sugar transferases superfamily protein	27.67	23.00	0.67	0.00	-5.65 ; -5.81
AT3G28150	TRICHOME BIREFRINGENCE-LIKE 22	35.67	12.00	0.33	0.00	-5.79 ; -5.33
AT3G53190	Pectin lyase-like superfamily protein	14.67	23.33	0.00	1.00	-5.79 ; -4.07
AT3G62020	germin-like protein 10	8.33	14.33	0.00	0.00	-5.66 ; -5.65
AT1G12090	extensin-like protein	151.33	29.33	3.33	1.33	-5.65 ; -4.22
AT1G41830	SKU5-similar 6	19.00	47.33	0.33	0.33	-5.03 ; -5.65
AT5G46890	Bifunctional inhibitor/lipid-transfer protein/seed storage 2S albumin superfamily protein	28.67	5.67	0.00	0.00	-6.42 ; -3.84
AT3G04290	Li-tolerant lipase 1	235.00	817.67	1.00	13.00	-6.39 ; -4.91
AT1G76160	SKU5 similar 5	37.33	89.33	0.33	1.00	-6.13 ; -6.34
AT5G33370	GDSL-like Lipase/Acylhydrolase superfamily protein	162.00	675.00	1.00	6.33	-6.17 ; -5.57
AT5G23940	HXXXD-type acyl-transferase family protein	95.00	148.33	1.33	11.67	-6.13 ; -3.47
AT3G16370	GDSL-like Lipase/Acylhydrolase superfamily protein	298.00	307.67	5.33	4.67	-5.98 ; -5.78
AT3G15850	fatty acid desaturase 5	20.00	9.00	0.00	2.00	-5.91 ; -1.93
AT1G21850	SKU5 similar 8	17.33	35.33	0.33	0.67	-5.17 ; -5.73
AT4G28780	GDSL-like Lipase/Acylhydrolase superfamily protein	111.00	569.33	0.33	4.33	-5.63 ; -5.47
AT1G63710	cytochrome P450, family 86, subfamily A, polypeptide 7	45.00	193.33	1.00	1.00	-5.27 ; -6.59
AT3G10185	Gibberellin-regulated family protein	177.33	292.33	1.00	4.33	-6.46 ; -4.94
AT1G12570	Glucose-methanol-choline (GMC) oxidoreductase family protein	88.67	59.33	1.00	2.67	-6.09 ; -4.2
AT2G45970	cytochrome P450, family 86, subfamily A, polypeptide 8	34.33	140.33	1.00	1.33	-5.3 ; -6.07
AT1G74670	Gibberellin-regulated family protein	19.67	28.00	0.00	0.33	-6.03 ; -5.03
AT1G61720	NAD(P)-binding Rossmann-fold superfamily protein	6.00	89.67	0.00	0.67	-3.32 ; -5.82
AT3G52500	Eukaryotic aspartyl protease family protein	43.33	35.67	1.33	0.33	-5.01 ; -5.75
AT5G44635	minichromosome maintenance (MCM2/3/5) family protein	37.67	6.67	0.00	0.00	-6.6 ; -4.12
AT5G67100	DNA-directed DNA polymerases	21.67	9.67	0.33	1.00	-5.93 ; -3.47
AT5G46280	Minichromosome maintenance (MCM2/3/5) family protein	26.67	5.33	0.00	0.00	-5.91 ; -3.97
AT1G44900	minichromosome maintenance (MCM2/3/5) family protein	66.00	12.00	0.67	0.33	-5.87 ; -3.62
AT2G07690	Minichromosome maintenance (MCM2/3/5) family protein	73.67	22.67	1.33	5.67	-5.74 ; -1.74
AT4G02060	Minichromosome maintenance (MCM2/3/5) family protein	38.00	6.33	0.67	0.00	-5.73 ; -3.52
AT1G27040	Major facilitator superfamily protein	44.33	2.67	0.00	2.00	-6.87 ; ns
AT5G62730	Major facilitator superfamily protein	40.00	3.00	0.00	3.00	-6.49 ; ns
AT3G02500		28.33	4.00	0.33	0.00	-5.89 ; -3.27
AT1G27930	Protein of unknown function (DUF579)	8.67	19.00	0.00	0.00	-4.65 ; -5.79
AT2G21100	Disease resistance-responsive (dirigent-like protein) family protein	16.33	49.67	0.67	0.33	-4.04 ; -5.66
AT4G17340	tonoplast intrinsic protein 2;2	321.33	125.00	3.67	31.00	-5.74 ; ns
AT1G13260	related to ABI3/VP1 1	18.33	5.33	0.00	0.33	-5.86 ; -3.45

892

893 **Table III.** Transcription factors of *k*-means cluster midday 4. TF Family, transcription factor
894 family based on Pérez-Rodríguez et al. (2010)

Locus	Annotation (TAIR10)	TF Family
AT1G12610	Integrase-type DNA-binding superfamily protein	AP2-EREBP
AT1G19210	Integrase-type DNA-binding superfamily protein	AP2-EREBP
AT1G33760	Integrase-type DNA-binding superfamily protein	AP2-EREBP
AT1G53170	ethylene response factor 8	AP2-EREBP
AT4G25470	C-repeat/DRE binding factor 2	AP2-EREBP
AT4G25480	dehydration response element B1A	AP2-EREBP
AT4G34410	redox responsive transcription factor 1	AP2-EREBP
AT5G21960	Integrase-type DNA-binding superfamily protein	AP2-EREBP
AT3G47640	basic helix-loop-helix (bHLH) DNA-binding superfamily protein	bHLH
AT2G21230	Basic-leucine zipper (bZIP) transcription factor family protein	bZIP
AT1G27730	salt tolerance zinc finger	C2H2
AT2G40140	SALT-INDUCIBLE ZINC FINGER 2	C3H
AT4G17230	SCARECROW-like 13	GRAS
AT1G18710	myb domain protein 47	MYB
AT3G13540	myb domain protein 5	MYB
AT1G01380	Homeodomain-like superfamily protein	MYB-related
AT1G33060	NAC 014	NAC
AT3G49530	NAC domain containing protein 62	NAC
AT4G35580	NAC transcription factor-like 9	NAC

895

896

Table IV. *25 most highly upregulated transcription factors on day 12 after drought.* TF Family, transcription factor family based on Pérez-Rodríguez et al. (2010). *RPM, reads per million (n = 3). MD, middle of the night, MN middle of the day. log_2-FC, log_2-fold change in expression at given time point on day 12 compared to day 0. ns, not significantly DEG.*

Locus	Annotation (TAIR10)	TF Family	Day 0 MD [rpm]	Day 0 MN [rpm]	Day 12 MD [rpm]	Day 12 MN [rpm]	log_2-fold change (MD; MN)
AT1G03790	SOMNUS	C3H	0.00	0.67	19.67	4.33	5.15 ; 2.38
AT5G12840	nuclear factor Y, subunit A1	CCAAT	0.67	2.67	25.67	31.00	4.75 ; 3.56
AT1G21000	PLATZ transcription factor family protein	PLATZ	0.33	25.33	18.33	135.00	4.48 ; 2.45
AT3G54320	Integrase-type DNA-binding superfamily protein	AP2-EREBP	1.00	1.33	3.33	27.00	1.4 ; 4.41
AT5G67480	BTB and TAZ domain protein 4	TAZ	19.67	71.00	461.33	129.00	4.15 ; 0.95
AT2G46680	homeobox 7	HB	7.67	38.00	165.33	445.00	3.92 ; 3.56
AT1G69490	NAC-like, activated by AP3/PI	NAC	8.67	76.00	206.33	366.00	3.73 ; 2.09
AT1G52880	NAC (No Apical Meristem) domain transcriptional regulator superfamily protein	NAC	0.00	2.67	5.00	10.67	3.51 ; 1.8
AT3G02550	LOB domain-containing protein 41	LOB	0.00	0.00	0.00	1.33	ns ; 3.3
AT1G17590	nuclear factor Y, subunit A8	CCAAT	3.67	9.33	41.67	63.00	3.19 ; 2.75
AT3G23150	ETHYLENE RESPONSE 2	Orphans	12.33	10.67	86.00	94.00	2.47 ; 3.13
AT3G04580	ETHYLENE INSENSITIVE 4	Orphans	14.33	9.67	94.00	82.33	2.38 ; 3.13
AT2G26150	heat shock transcription factor A2	HSF	4.67	6.00	9.00	47.00	ns ; 3.06
AT1G80840	WRKY DNA-binding protein 40	WRKY	2.33	0.67	0.33	6.67	-2.38 ; 3.04
AT4G17900	PLATZ transcription factor family protein	PLATZ	8.33	38.67	91.67	55.33	3.01 ; ns
AT3G11580	AP2/B3-like transcriptional factor family protein	ABI3VP1	0.33	1.33	4.33	1.67	3 ; ns
AT4G13980	winged-helix DNA-binding transcription factor family protein	HSF	2.67	9.00	4.33	68.67	ns ; 2.98
AT3G24520	heat shock transcription factor C1	HSF	2.67	11.33	5.00	88.00	ns ; 2.96
AT3G20910	nuclear factor Y, subunit A9	CCAAT	11.00	25.67	72.67	181.00	2.32 ; 2.87
AT4G02640	bZIP transcription factor family protein	bZIP	1.67	6.67	0.67	48.33	ns ; 2.83
AT2G25900	Zinc finger C-x8-C-x5-C-x3-H type family protein	C3H	12.67	12.67	119.00	45.33	2.83 ; 1.91
AT3G15500	NAC domain containing protein 3	NAC	0.67	8.00	8.33	21.00	2.82 ; 1.39
AT1G32700	PLATZ transcription factor family protein	PLATZ	16.00	56.00	141.33	75.67	2.78 ; ns
AT4G39070	B-box zinc finger family protein	Orphans	1.00	3.00	1.67	22.00	ns ; 2.77
AT5G28770	bZIP transcription factor family protein	bZIP	2.67	11.00	2.00	74.00	ns ; 2.77

FIGURE LEGENDS

Figure 1. Time course in response to 0 (darkgreen), 4 (light green), 9 (orange) and 12 (red) days of drought and 2 days after re-watering (re2, blue) in *Talinum triangulare*. A, Fresh weight to dry weight ratio (Mean ± SE of leaves harvested at the middle of the day and the middle of the night, n = 14-16). B, Levels of titratable acidity of leaves (Mean ± SE, n = 8-16). C, Representative pictures of plants during the course of the experiment. Asterisks indicate Student's *t* test significance in comparison to day 0 at ***$P < 0.001$, **$P < 0.01$, *$P < 0.05$.

Figure 2. Changes in leaf transcriptomes and metabolomes under varying levels of water availability. A, Histograms of $\log_2$-fold changes in gene expression compared to day 0 ($\log_{10}$-scaled). Colored bars indicate significant changes (DESeq2, $q < 0.01$). B, C, Venn diagrams representing overlapping changes (↑: increased, ↓: depleted) in gene expression (B, DESeq2 $q < 0.01$, n = 3, 16,766 genes analyzed in total), or metabolite levels (C, Student's *t* test, $p < 0.05$, n = 3-4, 39 metabolites measured in total) at the middle of the day between water-limited stages compared to day 0. See supplemental Figure S1. for analogous Venn diagrams of changes at the middle of the night.

Figure 3. Abundances of CAM genes *sensu stricto* and *sensu lato.* Scheme of carbon assimilation via CAM and gene expression of central enzymes and transporters. Metabolites are represented in grey. Transcript levels were measured at the middle of the day and the middle of the night in leaves of *T. triangulare* plants under five different stages of water availability. Scaled to largest expression by gene; Mean ± SD, n = 3. Asterisks indicate differential gene expression in comparison to day 0 as determined by DESeq2, * $q < 0.05$:, ** $q < 0.01$:, *** $q < 0.001$. Blue and yellow arrows represent reactions occurring at night and day, respectively. Abbreviations are explained in the text and in Supplemental Dataset S3. Question mark and dotted arrows indicate putative activity of plastidial NADP-ME, mitochondrial NAD-ME and cytosolic PPDK as discussed in the text. Separation into phosphorolytic and hydrolytic starch degradation is based on the models presented by Weise et al. (2011) and Streb and Zeeman (2012). 1,3-BPG, 1,3-Bisphosphoglycerate; 2-PGA, 2-Phosphoglycerate; 3-PGA, 3-Phosphoglycerate; ADP-Glc, ADP-glucose;

DHAP, Dihydroxyacetone phosphate; F1,6BP, Fructose 1,6-bisphosphate; F6P, Fructose 6-phosphate; G1P, Glucose 1-phosphate; G6P, Glucose 6-phosphate; GAP, Glyceraldehyde 3-phosphate; Mito, Mitochondrion; OAA, Oxaloacetate; PEP, Phospho*enol*pyruvate. re2, 2 days after re-watering.

Figure 4. Levels of organic acids, soluble sugars and starch in *T. triangulare* in response to varying levels of water availability. Except for starch, all metabolites were measured by GC-MS and normalized to dry weight (DW) and internal ribitol standard (Mean ± SE, n = 3-4, asterisks indicate Student's *t* test significance in comparison to day 0 at ***$P < 0.001$, **$P < 0.01$, *$P < 0.05$). Starch was normalized to DW (Mean ± SE, n = 2-4). re2, 2 days after re-watering.

Figure 5. *K*-means clustering of relative gene expression and selected enriched gene ontology (GO) terms. Genes that were found to be differentially expressed in the middle of the day between one of the water-limited stages and day 0 (DESeq2, q < 0.01) were used for the *k*-means approach (6800 genes in total). For the full list of enriched GO Terms see Supplemental Dataset S4. Grey line, expression of single genes; black line, average of all genes in cluster; re2, two days after re-watering.

Figure 6. Proposed regulation of the coordinated drought response in *T. triangulare*. Shown are genes discussed in the text. A general stress signal was mediated by transcription factors, which were transiently upregulated on day 9 (*CBF2, C-repeat/DRE binding factor 2; CBF3, C-repeat/DRE binding factor 3; ERF8, ethylene response factor 8; RRTF1, redox responsive transcription factor 1; STZ, salt tolerance zinc finger*) and triggered a yet unclear response. The sustained response to persistent drought was primarily mediated via ABA, the activity of which was maintained through a feed-forward loop (*KING1, SNF1-related protein kinase regulatory subunit gamma 1; EDL3, EID1-like 3*), through ABA-responsive transcription factors (*SOM*, *SOMNUS*; *HB-7, homeobox 7; NAP, NAC-like, activated by AP3/PI; NF-YA1*, *nuclear factor Y, subunit A1 and NF-YA9*) and besides the induction of CAM (see Fig. 3 for details: *PPC1, phosphoenolpyruvate carboxylase 1; PPDK, Pyruvate phosphate dikinase, PEP/pyruvate binding domain; NADP-ME1, NADP-malic enzyme 1*) included a classical drought response, i.e. synthesis of compatible solutes (*RS1,*

968 *Raffinose synthase 1; MIOX1, myo-inositol oxygenase 1; OXS3, oxidative stress*
969 *3*) and light protection (*ELIP1, early light inducible protein 1; FTSH6, FTSH*
970 *protease 6*). At the same time, growth was repressed through downregulation of
971 the replication cassette (*MCMs, minichromosome maintenance; ICU2, incurvata*
972 *2*)) and processes related to photosynthesis, amino acid synthesis and cell wall
973 synthesis (see Fig. 5 and Supplemental Fig. S4) allowing *T. triangulare* to
974 engage in a state of quiescence during drought. Log_2-FC, absolute maximum
975 log_2-fold changes in gene expression compared to day 0 at midday or midnight.
976
977
978
979
980
981
982
983
984
985
986

Parsed Citations

Alexa A, Rahnenführer J, Lengauer T (2006) Improved scoring of functional groups from gene expression data by decorrelating GO graph structure. Bioinformatics 22: 1600-1607
Pubmed: Author and Title
CrossRef: Author and Title
Google Scholar: Author Only Title Only Author and Title

Ashton AR, Burnell JN, Furbank RT, Jenkins CLD, Hatch MD (1990) 3 Enzymes of C4 Photosynthesis. Enzymes of Primary Metabolism 3: 39
Pubmed: Author and Title
CrossRef: Author and Title
Google Scholar: Author Only Title Only Author and Title

Baena-Gonzalez E, Rolland F, Thevelein JM, Sheen J (2007) A central integrator of transcription networks in plant stress and energy signalling. Nature 448: 938-942
Pubmed: Author and Title
CrossRef: Author and Title
Google Scholar: Author Only Title Only Author and Title

Bartels D, Sunkar R (2005) Drought and salt tolerance in plants. Critical Reviews in Plant Sciences 24: 23-58
Pubmed: Author and Title
CrossRef: Author and Title
Google Scholar: Author Only Title Only Author and Title

Benjamini Y, Hochberg Y (1995) Controlling the False Discovery Rate - a Practical and Powerful Approach to Multiple Testing. Journal of the Royal Statistical Society Series B-Methodological 57: 289-300
Pubmed: Author and Title
CrossRef: Author and Title
Google Scholar: Author Only Title Only Author and Title

Bläsing OE, Westhoff P, Svensson P (2000) Evolution of C4 phosphoenolpyruvate carboxylase in Flaveria, a conserved serine residue in the carboxyl-terminal part of the enzyme is a major determinant for C4-specific characteristics. J Biol Chem 275: 27917-27923
Pubmed: Author and Title
CrossRef: Author and Title
Google Scholar: Author Only Title Only Author and Title

Bohnert HJ (1995) Adaptations to Environmental Stresses. Plant Cell 7: 1099-1111
Pubmed: Author and Title
CrossRef: Author and Title
Google Scholar: Author Only Title Only Author and Title

Borland AM, Barrera Zambrano VA, Ceusters J, Shorrock K (2011) The photosynthetic plasticity of Crassulacean acid metabolism: an evolutionary innovation for sustainable productivity in a changing world. New Phytol 191: 619-633
Pubmed: Author and Title
CrossRef: Author and Title
Google Scholar: Author Only Title Only Author and Title

Borland AM, Hartwell J, Jenkins GI, Wilkins MB, Nimmo HG (1999) Metabolite control overrides circadian regulation of phosphoenolpyruvate carboxylase kinase and CO2 fixation in Crassulacean acid metabolism. Plant Physiol 121: 889-896
Pubmed: Author and Title
CrossRef: Author and Title
Google Scholar: Author Only Title Only Author and Title

Bray EA (1997) Plant responses to water deficit. Trends in Plant Science 2: 48-54
Pubmed: Author and Title
CrossRef: Author and Title
Google Scholar: Author Only Title Only Author and Title

Bräutigam A, Hoffmann-Benning S, Hofmann-Benning S, Weber APM (2008) Comparative proteomics of chloroplast envelopes from C3 and C4 plants reveals specific adaptations of the plastid envelope to C4 photosynthesis and candidate proteins required for maintaining C4 metabolite fluxes. Plant Physiol 148: 568-579
Pubmed: Author and Title
CrossRef: Author and Title
Google Scholar: Author Only Title Only Author and Title

Bräutigam A, Kajala K, Wullenweber J, Sommer M, Gagneul D, Weber KL, Carr KM, Gowik U, Maß J, Lercher MJ, et al (2011) An mRNA blueprint for C4 photosynthesis derived from comparative transcriptomics of closely related C3 and C4 species. Plant Physiol 155: 142-156
Pubmed: Author and Title
CrossRef: Author and Title
Google Scholar: Author Only Title Only Author and Title

Bräutigam A, Schliesky S, Külahoglu C, Osborne CP, Weber APM (2014) Towards an integrative model of C4 photosynthetic subtypes: insights from comparative transcriptome analysis of NAD-ME, NADP-ME, and PEP-CK C4 species. J Exp Bot 65: 3579-3593
Pubmed: Author and Title
CrossRef: Author and Title

Google Scholar: Author Only Title Only Author and Title

Camacho C, Coulouris G, Avagyan V, Ma N, Papadopoulos J, Bealer K, Madden TL (2009) BLAST+: architecture and applications. BMC Bioinformatics 10: 421
Pubmed: Author and Title
CrossRef: Author and Title
Google Scholar: Author Only Title Only Author and Title

Carter PJ, Nimmo HG, Fewson CA, Wilkins MB (1991) Circadian rhythms in the activity of a plant protein kinase. EMBO J 10: 2063-2068
Pubmed: Author and Title
CrossRef: Author and Title
Google Scholar: Author Only Title Only Author and Title

Chaves MM, Maroco J, Pereira JS (2003) Understanding plant responses to drought - from genes to the whole plant. Functional Plant Biol 30: 239-264
Pubmed: Author and Title
CrossRef: Author and Title
Google Scholar: Author Only Title Only Author and Title

Cheffings CM, Pantoja O, Ashcroft FM, Smith JA (1997) Malate transport and vacuolar ion channels in CAM plants. J Exp Bot 48 Spec No: 623-631
Pubmed: Author and Title
CrossRef: Author and Title
Google Scholar: Author Only Title Only Author and Title

Chia T, Thorneycroft D, Chapple A, Messerli G, Chen J, Zeeman SC, Smith SM, Smith AM (2004) A cytosolic glucosyltransferase is required for conversion of starch to sucrose in Arabidopsis leaves at night. Plant J 37: 853-863
Pubmed: Author and Title
CrossRef: Author and Title
Google Scholar: Author Only Title Only Author and Title

Christin P-A, Arakaki M, Osborne CP, Braeutigam A, Sage RF, Hibberd JM, Kelly S, Covshoff S, Wong GK-S, Hancock L, et al (2014) Shared origins of a key enzyme during the evolution of C-4 and CAM metabolism. J Exp Bot 65: 3609-3621
Pubmed: Author and Title
CrossRef: Author and Title
Google Scholar: Author Only Title Only Author and Title

Cushman JC, Agarie S, Albion RL, Elliot SM, Taybi T, Borland AM (2008a) Isolation and characterization of mutants of common ice plant deficient in Crassulacean acid metabolism. Plant Physiol 147: 228-238
Pubmed: Author and Title
CrossRef: Author and Title
Google Scholar: Author Only Title Only Author and Title

Cushman JC, Tillett RL, Wood JA, Branco JM, Schlauch KA (2008b) Large-scale mRNA expression profiling in the common ice plant, Mesembryanthemum crystallinum, performing C3 photosynthesis and Crassulacean acid metabolism (CAM). J Exp Bot 59: 1875-1894
Pubmed: Author and Title
CrossRef: Author and Title
Google Scholar: Author Only Title Only Author and Title

Cutler SR, Rodriguez PL, Finkelstein RR, Abrams SR (2010) Abscisic acid: emergence of a core signaling network. Annu Rev Plant Biol 61: 651-679
Pubmed: Author and Title
CrossRef: Author and Title
Google Scholar: Author Only Title Only Author and Title

Dever LV, Boxall SF, Knerová J, Hartwell J (2015) Transgenic perturbation of the decarboxylation phase of Crassulacean acid metabolism alters physiology and metabolism but has only a small effect on growth. Plant Physiol 167: 44-59
Pubmed: Author and Title
CrossRef: Author and Title
Google Scholar: Author Only Title Only Author and Title

Dittrich P (1976) Nicotinamide Adenine Dinucleotide-specific "Malic" Enzyme in Kalanchoë daigremontiana and Other Plants Exhibiting Crassulacean Acid Metabolism. Plant Physiol 57: 310-314
Pubmed: Author and Title
CrossRef: Author and Title
Google Scholar: Author Only Title Only Author and Title

Dohm JC, Minoche AE, Holtgräwe D, Capella-Gutiérrez S, Zakrzewski F, Tafer H, Rupp O, Sörensen TR, Stracke R, Reinhardt R, et al (2013) The genome of the recently domesticated crop plant sugar beet (Beta vulgaris). Nature 505: 546-549
Pubmed: Author and Title
CrossRef: Author and Title
Google Scholar: Author Only Title Only Author and Title

Elbein AD, Pan YT, Pastuszak I, Carroll D (2003) New insights on trehalose: a multifunctional molecule. Glycobiology 13: 17R-27R
Pubmed: Author and Title
CrossRef: Author and Title
Google Scholar: Author Only Title Only Author and Title

Emanuelsson O, Nielsen H, Brunak S, Heijne von G (2000) Predicting subcellular localization of proteins based on their N-terminal

amino acid sequence. J Mol Biol 300: 1005-1016
Pubmed: Author and Title
CrossRef: Author and Title
Google Scholar: Author Only Title Only Author and Title

Fiehn O, Kopka J, Dörmann P, Altmann T, Trethewey RN, Willmitzer L (2000) Metabolite profiling for plant functional genomics. Nat Biotechnol 18: 1157-1161
Pubmed: Author and Title
CrossRef: Author and Title
Google Scholar: Author Only Title Only Author and Title

Findling S, Zanger K, Krueger S, Lohaus G (2014) Subcellular distribution of raffinose oligosaccharides and other metabolites in summer and winter leaves of Ajuga reptans (Lamiaceae). Planta 241: 229-241
Pubmed: Author and Title
CrossRef: Author and Title
Google Scholar: Author Only Title Only Author and Title

Flexas J, Bota J, Galmés J, Medrano H, Ribas-Carbó M (2006) Keeping a positive carbon balance under adverse conditions: responses of photosynthesis and respiration to water stress. Physiol Plant 127: 343-352
Pubmed: Author and Title
CrossRef: Author and Title
Google Scholar: Author Only Title Only Author and Title

Franssen SU, Shrestha RP, Bräutigam A, Bornberg-Bauer E, Weber APM (2011) Comprehensive transcriptome analysis of the highly complex Pisum sativum genome using next generation sequencing. BMC Genomics 12: 227
Pubmed: Author and Title
CrossRef: Author and Title
Google Scholar: Author Only Title Only Author and Title

Furumoto T, Yamaguchi T, Ohshima-Ichie Y, Nakamura M, Tsuchida-Iwata Y, Shimamura M, Ohnishi J, Hata S, Gowik U, Westhoff P, et al (2011) A plastidial sodium-dependent pyruvate transporter. Nature 476: 472-475
Pubmed: Author and Title
CrossRef: Author and Title
Google Scholar: Author Only Title Only Author and Title

Goda H, Sasaki E, Akiyama K, Maruyama-Nakashita A, Nakabayashi K, Li W, Ogawa M, Yamauchi Y, Preston J, Aoki K, et al (2008) The AtGenExpress hormone and chemical treatment data set: experimental design, data evaluation, model data analysis and data access. Plant J 55: 526-542
Pubmed: Author and Title
CrossRef: Author and Title
Google Scholar: Author Only Title Only Author and Title

Gouy M, Guindon S, Gascuel O (2010) SeaView version 4: A multiplatform graphical user interface for sequence alignment and phylogenetic tree building. Molecular Biology and Evolution 27: 221-224
Pubmed: Author and Title
CrossRef: Author and Title
Google Scholar: Author Only Title Only Author and Title

Gowik U, Bräutigam A, Weber KL, Weber APM, Westhoff P (2011) Evolution of C4 photosynthesis in the genus Flaveria: how many and which genes does it take to make C4? Plant Cell 23: 2087-2105
Pubmed: Author and Title
CrossRef: Author and Title
Google Scholar: Author Only Title Only Author and Title

Gowik U, Engelmann S, Bläsing OE, Raghavendra AS, Westhoff P (2006) Evolution of C(4) phosphoenolpyruvate carboxylase in the genus Alternanthera: gene families and the enzymatic characteristics of the C(4) isozyme and its orthologues in C(3) and C(3)/C(4) Alternantheras. Planta 223: 359-368
Pubmed: Author and Title
CrossRef: Author and Title
Google Scholar: Author Only Title Only Author and Title

Grabherr MG, Haas BJ, Yassour M, Levin JZ, Thompson DA, Amit I, Adiconis X, Fan L, Raychowdhury R, Zeng Q, et al (2011) Full-length transcriptome assembly from RNA-Seq data without a reference genome. Nat Biotechnol 29: 644-U130
Pubmed: Author and Title
CrossRef: Author and Title
Google Scholar: Author Only Title Only Author and Title

Guindon S, Dufayard J-F, Lefort V, Anisimova M, Hordijk W, Gascuel O (2010) New Algorithms and Methods to Estimate Maximum-Likelihood Phylogenies: Assessing the Performance of PhyML 3.0. Syst Biol 59: 307-321
Pubmed: Author and Title
CrossRef: Author and Title
Google Scholar: Author Only Title Only Author and Title

Haider MS, Barnes JD, Cushman JC, Borland AM (2012) A CAM- and starch-deficient mutant of the facultative CAM species Mesembryanthemum crystallinum reconciles sink demands by repartitioning carbon during acclimation to salinity. J Exp Bot 63: 1985-1996
Pubmed: Author and Title
CrossRef: Author and Title
Google Scholar: Author Only Title Only Author and Title

Hare PD, Cress WA, Van Staden J (1998) Dissecting the roles of osmolyte accumulation during stress. Plant Cell Environ 21: 535-553
Pubmed: Author and Title
CrossRef: Author and Title
Google Scholar: Author Only Title Only Author and Title

Harris D, Martin C (1991) Plasticity in the Degree of Cam-Cycling and Its Relationship to Drought Stress in 5 Species of Talinum (Portulacaceae). Oecologia 86: 575-584
Pubmed: Author and Title
CrossRef: Author and Title
Google Scholar: Author Only Title Only Author and Title

Hartwell J, Gill A, Nimmo GA, Wilkins MB, Jenkins GL, Nimmo HG (1999) Phosphoenolpyruvate carboxylase kinase is a novel protein kinase regulated at the level of expression. Plant J 20: 333-342
Pubmed: Author and Title
CrossRef: Author and Title
Google Scholar: Author Only Title Only Author and Title

Hartwell J, Smith LH, Wilkins MB, Jenkins GI, Nimmo HG (1996) Higher plant phosphoenolpyruvate carboxylase kinase is regulated at the level of translatable mRNA in response to light or a circadian rhythm. Plant J 10: 1071-1078
Pubmed: Author and Title
CrossRef: Author and Title
Google Scholar: Author Only Title Only Author and Title

Häusler RE, Baur B, Scharte J, Teichmann T, Eicks M, Fischer KL, Flügge U-I, Schubert S, Weber APM, Fischer K (2000) Plastidic metabolite transporters and their physiological functions in the inducible Crassulacean acid metabolism plant Mesembryanthemum crystallinum. Plant J 24: 285-296
Pubmed: Author and Title
CrossRef: Author and Title
Google Scholar: Author Only Title Only Author and Title

Heddad M, Adamska I (2000) Light stress-regulated two-helix proteins in Arabidopsis thaliana related to the chlorophyll a/b-binding gene family. Proc Natl Acad Sci USA 97: 3741-3746
Pubmed: Author and Title
CrossRef: Author and Title
Google Scholar: Author Only Title Only Author and Title

Herrera A (1999) Effects of photoperiod and drought on the induction of Crassulacean acid metabolism and the reproduction of plants of Talinum triangulare. Can J Bot 77: 404-409
Pubmed: Author and Title
CrossRef: Author and Title
Google Scholar: Author Only Title Only Author and Title

Herrera A (2009) Crassulacean acid metabolism and fitness under water deficit stress: if not for carbon gain, what is facultative CAM good for? Annals of Botany 103: 645-653
Pubmed: Author and Title
CrossRef: Author and Title
Google Scholar: Author Only Title Only Author and Title

Herrera A, Ballestrini C, Montes E (2015) What is the potential for dark CO2 fixation in the facultative Crassulacean acid metabolism species Talinum triangulare? Journal of Plant Physiology 174: 55-61
Pubmed: Author and Title
CrossRef: Author and Title
Google Scholar: Author Only Title Only Author and Title

Herrera A, Delgado J, Paraguatey I (1991) Occurrence of Inducible Crassulacean Acid Metabolism in Leaves of Talinum triangulare (Portulacaceae). J Exp Bot 42: 493-499
Pubmed: Author and Title
CrossRef: Author and Title
Google Scholar: Author Only Title Only Author and Title

Holtum JAM, Winter K (1982) Activity of enzymes of carbon metabolism during the induction of Crassulacean acid metabolism in Mesembryanthemum crystallinum L. Planta 155: 8-16
Pubmed: Author and Title
CrossRef: Author and Title
Google Scholar: Author Only Title Only Author and Title

Hutin C, Nussaume L, Moise N, Moya I, Kloppstech K, Havaux M (2003) Early light-induced proteins protect Arabidopsis from photooxidative stress. Proc Natl Acad Sci USA 100: 4921-4926
Pubmed: Author and Title
CrossRef: Author and Title
Google Scholar: Author Only Title Only Author and Title

Ingram J, Bartels D (1996) The molecular basis of dehydration tolerance in plants. Annu Rev Plant Physiol Plant Mol Biol 47: 377-403
Pubmed: Author and Title
CrossRef: Author and Title
Google Scholar: Author Only Title Only Author and Title

Kim DH, Yamaguchi S, Lim S, Oh E, Park J, Hanada A, Kamiya Y, Choi G (2008) SOMNUS, a CCCH-type zinc finger protein in

Arabidopsis, negatively regulates light-dependent seed germination downstream of PIL5. Plant Cell 20: 1260-1277
Pubmed: Author and Title
CrossRef: Author and Title
Google Scholar: Author Only Title Only Author and Title

Kluge M, Osmond CB (1971) Pyruvate Pi Dikinase in Crassulacean Acid Metabolism. Naturwissenschaften 58: 414-415
Pubmed: Author and Title
CrossRef: Author and Title
Google Scholar: Author Only Title Only Author and Title

Kollist H, Nuhkat M, Roelfsema MRG (2014) Closing gaps: linking elements that control stomatal movement. New Phytol 203: 44-62
Pubmed: Author and Title
CrossRef: Author and Title
Google Scholar: Author Only Title Only Author and Title

Kore-eda S, Noake C, Ohishi M, Ohnishi J, Cushman JC (2005) Transcriptional profiles of organellar metabolite transporters during induction of Crassulacean acid metabolism in Mesembryanthemum crystallinum. Functional Plant Biol 32: 451-466
Pubmed: Author and Title
CrossRef: Author and Title
Google Scholar: Author Only Title Only Author and Title

Lawlor DW, Cornic G (2002) Photosynthetic carbon assimilation and associated metabolism in relation to water deficits in higher plants. Plant Cell Environ 25: 275-294
Pubmed: Author and Title
CrossRef: Author and Title
Google Scholar: Author Only Title Only Author and Title

Lim S, Park J, Lee N, Jeong J, Toh S, Watanabe A, Kim J, Kang H, Kim DH, Kawakami N, et al (2013) ABA-insensitive3, ABA-insensitive5, and DELLAs Interact to activate the expression of SOMNUS and other high-temperature-inducible genes in imbibed seeds in Arabidopsis. Plant Cell 25: 4863-4878
Pubmed: Author and Title
CrossRef: Author and Title
Google Scholar: Author Only Title Only Author and Title

Liu Q, Kasuga M, Sakuma Y, Abe H, Miura S, Yamaguchi-Shinozaki K, Shinozaki K (1998) Two transcription factors, DREB1 and DREB2, with an EREBP/AP2 DNA binding domain separate two cellular signal transduction pathways in drought- and low-temperature-responsive gene expression, respectively, in Arabidopsis. Plant Cell 10: 1391-1406
Pubmed: Author and Title
CrossRef: Author and Title
Google Scholar: Author Only Title Only Author and Title

Lobell DB, Gourdji SM (2012) The influence of climate change on global crop productivity. Plant Physiol 160: 1686-1697
Pubmed: Author and Title
CrossRef: Author and Title
Google Scholar: Author Only Title Only Author and Title

Love MI, Huber W, Anders S (2014) Moderated estimation of fold change and dispersion for RNA-seq data with DESeq2. Genome Biol 15: 550-570
Pubmed: Author and Title
CrossRef: Author and Title
Google Scholar: Author Only Title Only Author and Title

Lüttge U (2002) CO2-concentrating: consequences in Crassulacean acid metabolism. J Exp Bot 53: 2131-2142
Pubmed: Author and Title
CrossRef: Author and Title
Google Scholar: Author Only Title Only Author and Title

Lüttge U (2011) Photorespiration in phase III of Crassulacean acid metabolism: evolutionary and ecophysiological implications. Progress in Botany 72 2: 371-384
Pubmed: Author and Title
CrossRef: Author and Title
Google Scholar: Author Only Title Only Author and Title

Nägele T, Heyer AG (2013) Approximating subcellular organisation of carbohydrate metabolism during cold acclimation in different natural accessions of Arabidopsis thaliana. New Phytol 198: 777-787
Pubmed: Author and Title
CrossRef: Author and Title
Google Scholar: Author Only Title Only Author and Title

Niewiadomska E, Borland AM (2007) Crassulacean acid metabolism: a cause or consequence of oxidative stress in planta? Progress in Botany 247-266

Niittylä T, Messerli G, Trevisan M, Chen J, Smith AM, Zeeman SC (2004) A previously unknown maltose transporter essential for starch degradation in leaves. Science 303: 87-89
Pubmed: Author and Title
CrossRef: Author and Title
Google Scholar: Author Only Title Only Author and Title

Nishizawa A, Yabuta Y, Shigeoka S (2008) Galactinol and raffinose constitute a novel function to protect plants from oxidative damage. Plant Physiol 147: 1251-1263
Pubmed: Author and Title

CrossRef: Author and Title
Google Scholar: Author Only Title Only Author and Title

Noctor G, Foyer CH (2000) Homeostasis of adenylate status during photosynthesis in a fluctuating environment. J Exp Bot 51: 347-356
Pubmed: Author and Title
CrossRef: Author and Title
Google Scholar: Author Only Title Only Author and Title

Osmond CB (1978) Crassulacean acid metabolism: a curiosity in context. Annu Rev Plant Physiol 29: 379-414
Pubmed: Author and Title
CrossRef: Author and Title
Google Scholar: Author Only Title Only Author and Title

Park S-Y, Fung P, Nishimura N, Jensen DR, Fujii H, Zhao Y, Lumba S, Santiago J, Rodrigues A, Chow T-FF, et al (2009) Abscisic acid inhibits type 2C protein phosphatases via the PYR/PYL family of START proteins. Science 324: 1068-1071
Pubmed: Author and Title
CrossRef: Author and Title
Google Scholar: Author Only Title Only Author and Title

Parsley K, Hibberd JM (2006) The Arabidopsis PPDK gene is transcribed from two promoters to produce differentially expressed transcripts responsible for cytosolic and plastidic proteins. Plant Mol Biol 62: 339-349
Pubmed: Author and Title
CrossRef: Author and Title
Google Scholar: Author Only Title Only Author and Title

Paulus JK, Schlieper D, Groth G (2013) Greater efficiency of photosynthetic carbon fixation due to single amino-acid substitution. Nat Comms 4: 1518-1524
Pubmed: Author and Title
CrossRef: Author and Title
Google Scholar: Author Only Title Only Author and Title

Pérez-Rodríguez P, Riaño-Pachón DM, Corrêa LGG, Rensing SA, Kersten B, Mueller-Roeber B (2010) PlnTFDB: updated content and new features of the plant transcription factor database. Nucleic Acids Research 38: D822-7
Pubmed: Author and Title
CrossRef: Author and Title
Google Scholar: Author Only Title Only Author and Title

Sage RF (2003) The evolution of C4 photosynthesis. New Phytol 161: 341-370
Pubmed: Author and Title
CrossRef: Author and Title
Google Scholar: Author Only Title Only Author and Title

Sakamoto H, Araki T, Meshi T, Iwabuchi M (2000) Expression of a subset of the Arabidopsis Cys2/His2-type zinc-finger protein gene family under water stress. Gene 248: 23-32
Pubmed: Author and Title
CrossRef: Author and Title
Google Scholar: Author Only Title Only Author and Title

Sakamoto H, Maruyama K, Sakuma Y, Meshi T, Iwabuchi M, Shinozaki K, Yamaguchi-Shinozaki K (2004) Arabidopsis Cys2/His2-type zinc-finger proteins function as transcription repressors under drought, cold, and high-salinity stress conditions. Plant Physiol 136: 2734-2746
Pubmed: Author and Title
CrossRef: Author and Title
Google Scholar: Author Only Title Only Author and Title

Sievers F, Wilm A, Dineen D, Gibson TJ, Karplus K, Li W, Lopez R, McWilliam H, Remmert M, Soding J, et al (2011) Fast, scalable generation of high-quality protein multiple sequence alignments using Clustal Omega. Molecular Systems Biology 7: 539-539
Pubmed: Author and Title
CrossRef: Author and Title
Google Scholar: Author Only Title Only Author and Title

Smith SM, Fulton DC, Chia T, Thorneycroft D, Chapple A, Dunstan H, Hylton C, Zeeman SC, Smith AM (2004) Diurnal changes in the transcriptome encoding enzymes of starch metabolism provide evidence for both transcriptional and posttranscriptional regulation of starch metabolism in Arabidopsis leaves. Plant Physiol 136: 2687-2699
Pubmed: Author and Title
CrossRef: Author and Title
Google Scholar: Author Only Title Only Author and Title

Sun J, Jiang H, Xu Y, Li H, Wu X, Xie Q, Li C (2007) The CCCH-type zinc finger proteins AtSZF1 and AtSZF2 regulate salt stress responses in Arabidopsis. Plant Cell Physiol 48: 1148-1158
Pubmed: Author and Title
CrossRef: Author and Title
Google Scholar: Author Only Title Only Author and Title

Svensson P, Bläsing OE, Westhoff P (1997) Evolution of the enzymatic characteristics of C-4 phosphoenolpyruvate carboxylase - A comparison of the orthologous PPCA phosphoenolpyruvate carboxylases of Flaveria trinervia (C4) and Flaveria pringlei (C3). Eur J Biochem 246: 452-460
Pubmed: Author and Title
CrossRef: Author and Title

Google Scholar: Author Only Title Only Author and Title

Svensson P, Bläsing OE, Westhoff P (2003) Evolution of C4 phosphoenolpyruvate carboxylase. Arch Biochem Biophys 414: 180-188
Pubmed: Author and Title
CrossRef: Author and Title
Google Scholar: Author Only Title Only Author and Title

Taisma MA, Herrera A (1998) A relationship between fecundity, survival, and the operation of Crassulacean acid metabolism in Talinum triangulare. Can J Bot 76: 1908-1915
Pubmed: Author and Title
CrossRef: Author and Title
Google Scholar: Author Only Title Only Author and Title

Taisma MA, Herrera A (2003) Drought under natural conditions affects leaf properties, induces CAM and promotes reproduction in plants of Talinum triangulare. Interciencia 28: 292-297
Pubmed: Author and Title
CrossRef: Author and Title
Google Scholar: Author Only Title Only Author and Title

Taybi T, Cushman JC (2002) Abscisic acid signaling and protein synthesis requirements for phosphoenolpyruvate carboxylase transcript induction in the common ice plant. Journal of Plant Physiology 159: 1235-1243
Pubmed: Author and Title
CrossRef: Author and Title
Google Scholar: Author Only Title Only Author and Title

Taybi T, Nimmo HG, Borland AM (2004) Expression of phosphoenolpyruvate carboxylase and phosphoenolpyruvate carboxylase kinase genes. Implications for genotypic capacity and phenotypic plasticity in the expression of Crassulacean acid metabolism. Plant Physiol 135: 587-598
Pubmed: Author and Title
CrossRef: Author and Title
Google Scholar: Author Only Title Only Author and Title

Taybi T, Patil S, Chollet R, Cushman JC (2000) A minimal serine/threonine protein kinase circadianly regulates phosphoenolpyruvate carboxylase activity in Crassulacean acid metabolism-induced leaves of the common ice plant. Plant Physiol 123: 1471-1482
Pubmed: Author and Title
CrossRef: Author and Title
Google Scholar: Author Only Title Only Author and Title

Taybi T, Sotta B, Gehrig H, Guclu S, Kluge M, Brulfert J (1995) Differential Effects of Abscisic Acid on Phosphoenolpyruvate Carboxylase and Cam Operation in Kalanchoë Blossfeldiana. Botanica Acta 108: 240-246
Pubmed: Author and Title
CrossRef: Author and Title
Google Scholar: Author Only Title Only Author and Title

Thimm O, Bläsing OE, Gibon Y, Nagel A, Meyer S, Krüger P, Selbig J, Müller LA, Rhee SY, Stitt M (2004) MAPMAN: a user-driven tool to display genomics data sets onto diagrams of metabolic pathways and other biological processes. Plant J 37: 914-939
Pubmed: Author and Title
CrossRef: Author and Title
Google Scholar: Author Only Title Only Author and Title

Tsuzuki M, Miyachi S, Winter K, Edwards GE (1982) Localization of carbonic anhydrase in Crassulacean acid metabolism plants. Plant Science Letters 211-218
Pubmed: Author and Title
CrossRef: Author and Title
Google Scholar: Author Only Title Only Author and Title

Umezawa T, Sugiyama N, Mizoguchi M, Hayashi S, Myouga F, Yamaguchi-Shinozaki K, Ishihama Y, Hirayama T, Shinozaki K (2009) Type 2C protein phosphatases directly regulate abscisic acid-activated protein kinases in Arabidopsis. Proc Natl Acad Sci USA 106: 17588-17593
Pubmed: Author and Title
CrossRef: Author and Title
Google Scholar: Author Only Title Only Author and Title

Weber APM, Servaites JC, Geiger DR, Kofler H, Hille D, Gröner F, Hebbeker U, Flügge U-I (2000) Identification, Purification, and Molecular Cloning of a Putative Plastidic Glucose Translocator. Plant Cell 787-801
Pubmed: Author and Title
CrossRef: Author and Title
Google Scholar: Author Only Title Only Author and Title

Weise SE, van Wijk KJ, Sharkey TD (2011) The role of transitory starch in C3, CAM, and C4 metabolism and opportunities for engineering leaf starch accumulation. J Exp Bot 62: 3109-3118
Pubmed: Author and Title
CrossRef: Author and Title
Google Scholar: Author Only Title Only Author and Title

Wheeler MCG, Arias CL, Tronconi MA, Maurino VG, Andreo CS, Drincovich MF (2008) Arabidopsis thaliana NADP-malic enzyme isoforms: high degree of identity but clearly distinct properties. Plant Mol Biol 67: 231-242
Pubmed: Author and Title

CrossRef: Author and Title
Google Scholar: Author Only Title Only Author and Title

White PJ, Smith JA (1989) Proton and anion transport at the tonoplast in Crassulacean-acid-metabolism plants: specificity of the malate-influx system in Kalanchoë daigremontiana. Planta 179: 265-274
Pubmed: Author and Title
CrossRef: Author and Title
Google Scholar: Author Only Title Only Author and Title

Wilson RL, Kim H, Bakshi A, Binder BM (2014) The Ethylene Receptors ETHYLENE RESPONSE1 and ETHYLENE RESPONSE2 Have Contrasting Roles in Seed Germination of Arabidopsis during Salt Stress. Plant Physiol 165: 1353-1366
Pubmed: Author and Title
CrossRef: Author and Title
Google Scholar: Author Only Title Only Author and Title

Winter K, Foster JG, Edwards GE, Holtum JAM (1982) Intracellular localization of enzymes of carbon metabolism in Mesembryanthemum crystallinum exhibiting C3 photosynthesic characteristics or performing Crassulacean acid metabolism. Plant Physiology 69: 300-307
Pubmed: Author and Title
CrossRef: Author and Title
Google Scholar: Author Only Title Only Author and Title

Winter K, Garcia M, Holtum JAM (2008) On the nature of facultative and constitutive CAM: environmental and developmental control of CAM expression during early growth of Clusia, Kalanchöe, and Opuntia. J Exp Bot 59: 1829-1840
Pubmed: Author and Title
CrossRef: Author and Title
Google Scholar: Author Only Title Only Author and Title

Winter K, Holtum JAM (2007) Environment or development? Lifetime net CO2 exchange and control of the expression of Crassulacean acid metabolism in Mesembryanthemum crystallinum. Plant Physiology 143: 98-107
Pubmed: Author and Title
CrossRef: Author and Title
Google Scholar: Author Only Title Only Author and Title

Winter K, Holtum JAM (2014) Facultative Crassulacean acid metabolism (CAM) plants: powerful tools for unravelling the functional elements of CAM photosynthesis. J Exp Bot 65: 3425-3441
Pubmed: Author and Title
CrossRef: Author and Title
Google Scholar: Author Only Title Only Author and Title

Winter K, Willert von DJ (1972) NaCl-induzierter Crassulaceensäurestoffwechsel bei Mesembryanthemum crystallinum. Zeitschrift für Pflanzenphysiologie 67: 166-170
Pubmed: Author and Title
CrossRef: Author and Title
Google Scholar: Author Only Title Only Author and Title

Yang J, Worley E, Udvardi M (2014) A NAP-AAO3 regulatory module promotes chlorophyll degradation via ABA biosynthesis in Arabidopsis leaves. Plant Cell 26: 4862-4874
Pubmed: Author and Title
CrossRef: Author and Title
Google Scholar: Author Only Title Only Author and Title

Yang X, Cushman JC, Borland AM, Edwards EJ, Wullschleger SD, Tuskan GA, Owen NA, Griffiths H, Smith JAC, De Paoli HC, et al (2015) A roadmap for research on Crassulacean acid metabolism (CAM) to enhance sustainable food and bioenergy production in a hotter, drier world. New Phytol 207: 491-504
Pubmed: Author and Title
CrossRef: Author and Title
Google Scholar: Author Only Title Only Author and Title

Zelisko A, Garcia-Lorenzo M, Jackowski G, Jansson S, Funk C (2005) AtFtsH6 is involved in the degradation of the light-harvesting complex II during high-light acclimation and senescence. Proc Natl Acad Sci USA 102: 13699-13704
Pubmed: Author and Title
CrossRef: Author and Title
Google Scholar: Author Only Title Only Author and Title

Zhu J-K (2002) Salt and drought stress signal transduction in plants. Annu Rev Plant Biol 53: 247-273
Pubmed: Author and Title
CrossRef: Author and Title
Google Scholar: Author Only Title Only Author and Title

Zou C, Sun K, Mackaluso JD, Seddon AE, Jin R, Thomashow MF, Shiu S-H (2011) Cis-regulatory code of stress-responsive transcription in Arabidopsis thaliana. Proc Natl Acad Sci USA 108: 14992-14997
Pubmed: Author and Title
CrossRef: Author and Title
Google Scholar: Author Only Title Only Author and Title

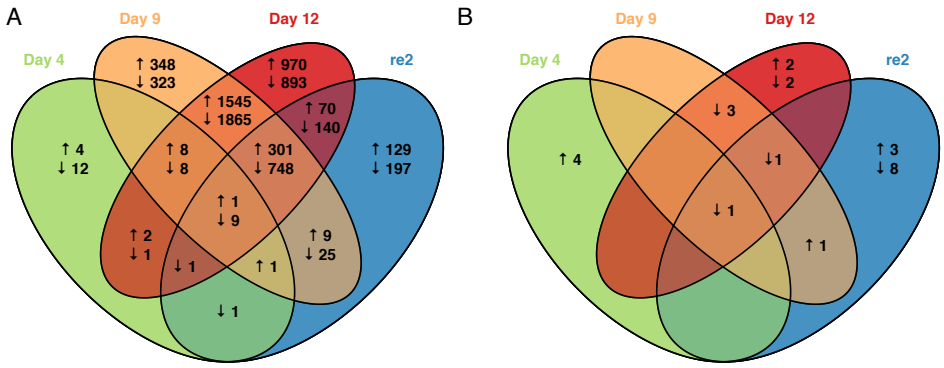

Supplemental Figure S1. Changes in leaf transcriptomes and metabolomes under varying levels of water availability in the middle of the night (Analogous to Figure 1. B and C). Venn diagrams representing overlapping changes (↑: increased, ↓: depleted) in gene expression (A, DESeq2 $q < 0.01$, $n = 3$, 16,766 genes analyzed in total), or metabolite levels (B, Student's *t* test, $p < 0.05$, $n = 3$-4, 39 metabolites measured in total) at the middle of the night between water-limited stages compared to day 0.

A

```
Zea mays (C4)                              779 FSWTQTRFHLPV(…)ILEGDPFLKQGLVLRNPY     897
Flaveria trinervia (C4)                    773 FSWTQTRFHLPV(…)LLEGDPYLKQGIRLRDPY     891
Sorghum bicolor (C4)                       770 FSWTQTRFHLPV(…)ILEGDPYLKQGLRLRNPY     888
Flaveria pringlei (C3)                     774 FAWTQTRFHLPV(…)LLEGDPYLKQRIRLRDSY     892
Arabidopsis thaliana (C3)                  775 FAWTQTRFHLPV(…)LLEGDPYLKQRLRLRDSY     893
Mesembryanthemum crystallinum (CAM)        774 FAWTQTRFHLPV(…)LLEGDPYLKQRLRLRDPY     892
Portulaca fulgens ppc-1E1b (C4)            341 FAWTQTRFHLPV(…)VLEGDPYLKQRLRLRDPY     459
Portulaca grandiflora ppc-1E1b (C4-CAM)    341 FAWTQTRFHLPV(…)VLEGDPYLKQRLRLRDPY     459
Portulaca oleracea ppc-1E1a' (C4-CAM)      334 FAWTQTRFHLPV(…)VLEGDPYLKQRLRLRDPY     452
Portulaca oleracea ppc-1E1b (C4-CAM)       673 FSWTQTRFHLPV(…)LLERNPSLKQRLHLRGPY     791
Portulaca oleracea ppc-1E1c (C4-CAM)       762 FSWTQTRLHLPV(…)LLENDPYLKQMLRLRDPY     881
T. triangulare ppc1E1c                      19 FSWTQTRFHLPV(…)LLEGNPSLKQRLHLRGPY     137
Tt63271                                    192 FAWTQTRFHLPV(…)LLERDPYLKHRLHLRDPY     310
Tt9871_4                                   750 FSWTQTRFHLPV(…)LLEGNPSLKQRLHLRGPY     868
Tt9871_6                                   750 FSWTQTRFHLPV(…)LLEGNPSLKQRLHLRGPY     868
Tt9871_8                                   246 FAWTQTRFHLPV(…)LLEGDPYLKQRLRLRDPY     364
```

B

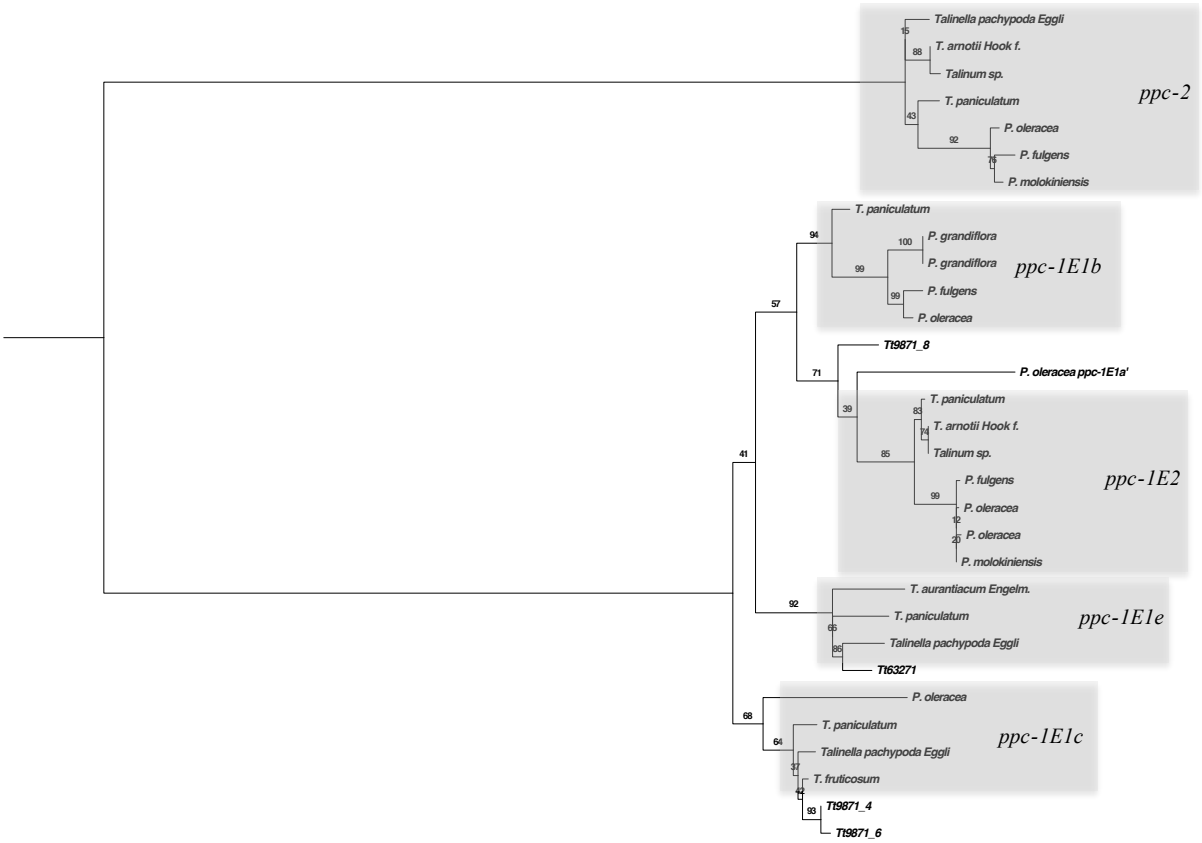

Supplemental Figure S2. *T. triangulare* PEPCs show characteristics of both C_3 and C_4 plants. A, Alignment of translated *T. triangulare* contigs encoding PEPC with protein sequences of C_4 plants (*Zea mays* PPC1, UniProt No.: CAA33317; *Flaveria trinervia* PPCA, UniProt No.: P30694; *Sorghum bicolor* PEPC3, UniProt No.: P15804; *Portulaca fulgens* ppc-1E1b, UniProt No.: KJ161577), C_3 plants (*Flaveria pringlei* PPCA1, UniProt No.: Q01647; *Arabidopsis thaliana* PEPC1, UniProt No.: Q9MAH0), facultative CAM plants (*Mesembryanthemum crystallinum* PEPC1, UniProt No.: P10490; *T. triangulare* ppc1E1c, UniProt No.: A0A075J1W2) and C_4-CAM plants (*Portulaca grandiflora* ppc-1E1b, UniProt No.: KJ161578; *Portulaca oleracea* ppc-1E1b, UniProt No.: KJ161580; *P. oleracea* ppc1E1a' and ppc1E1c are translated contigs from Christin et al. (2014)). Sequences of *M. crystallinum*, *Portulaceae* and *T. triangulare* ppc1E1c were retrieved from Christin et al. (2014). Shaded areas highlight the amino residues determining PEP saturation kinetics (Ser780, counting based on *Zea mays*, Bläsing et al. (2000)) and sensitivity towards malate inhibition (Gly890, Paulus et al. (2013)). B, Maximum likelihood estimate of phylogenetic relationships of *T. triangulare* contigs encoding PEPC and protein sequences of the *ppc* gene families of *Portulacaceae* and *Talinaceae, ppc-1E1b* (*T. paniculatum*, UniProt No.: KJ161572; *P. fulgens*, UniProt No.: KJ161577; *P. grandiflora*, UniProt No.: KJ161578; *P. grandiflora*, UniProt No.: KJ161579; *P. oleracea*, UniProt No.: KJ161580), *ppc-1E1c* (*T. paniculatum*, UniProt No.: KJ161605; *T. fruticosum*, UniProt No.: KJ161606; *Talinella pachypoda* Eggli, UniProt No.: KJ161607), *ppc-1E1e* (*T. aurantiacum* Engelm., UniProt No.: KJ161647; *T. paniculatum*, UniProt No.: KJ161648; *Talinella pachypoda* Eggli, UniProt No.: KJ161649), *ppc-1E2* (*T. arnotii* Hook f, UniProt No.: KJ161736; *T. paniculatum*, UniProt No.: KJ161737; *Talinum* sp., UniProt No.: KJ161738; *P. fulgens*, UniProt No.: KJ161742; *P. molokiniensis*, UniProt No.: KJ161743; *P. oleracea*, UniProt No.: KJ161744; *P. oleracea*, UniProt No.: KJ161745), *ppc-2* (*P. fulgens*, UniProt No.: KJ161807; *P. molokiniensis*, UniProt No.: KJ161808; *P. oleracea*, UniProt No.: KJ161809; *T. arnotii* Hook, UniProt No.: KJ161799; *T. paniculatum*, UniProt No.: KJ161800; *Talinum sp.*, UniProt No.: KJ161802; *Talinella pachypoda* Eggli, UniProt No.: KJ161801) extracted from Christin et al. (2014). Numbers above nodes represent maximum likelihood bootstrap values (n = 100). For details see Material and Methods. See Supplemental Table S3 for quantification of the *T. triangulare* contigs. Only contigs with an average expression of over 100 reads per million across all 30 samples were included.

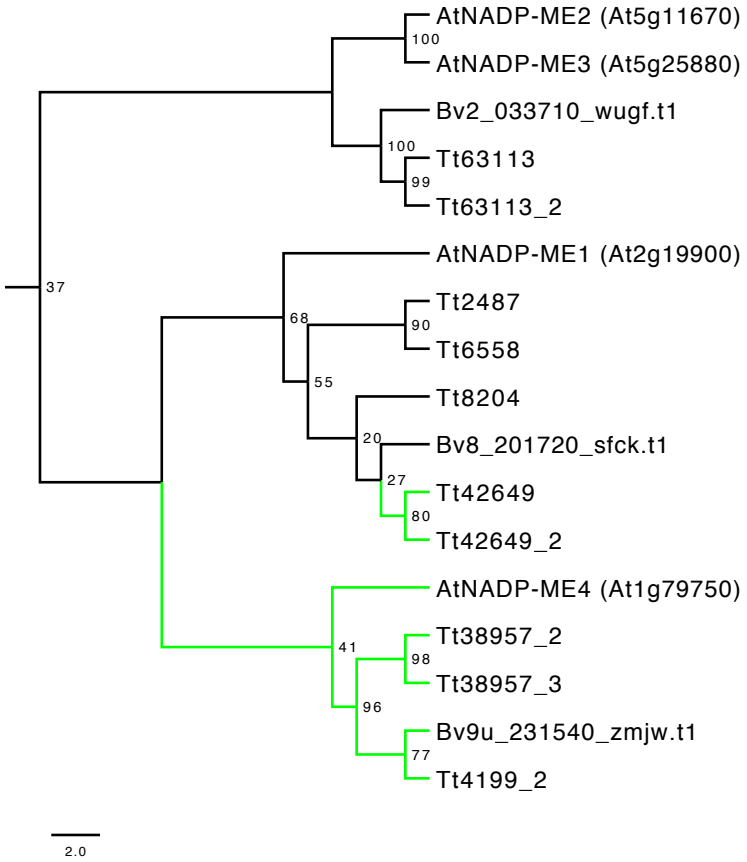

Supplemental Figure S3. *Talinum* NADP-ME with highest transcript are predicted to be localized in the plastid. Maximum likelihood estimate of phylogenetic relationships of *T. triangulare* contigs and *B. vulgaris* and *A. thaliana* genes encoding isoforms of NADP-ME. PhyML analysis was performed on protein level. Numbers above nodes represent maximum likelihood bootstrap values (n = 100). Green nodes indicate predicted chloroplast targeting based on TargetP (Emanuelsson et al., 2000). For details see Material and Methods. See Supplemental Table S4 for quantification of the *T. triangulare* contigs.

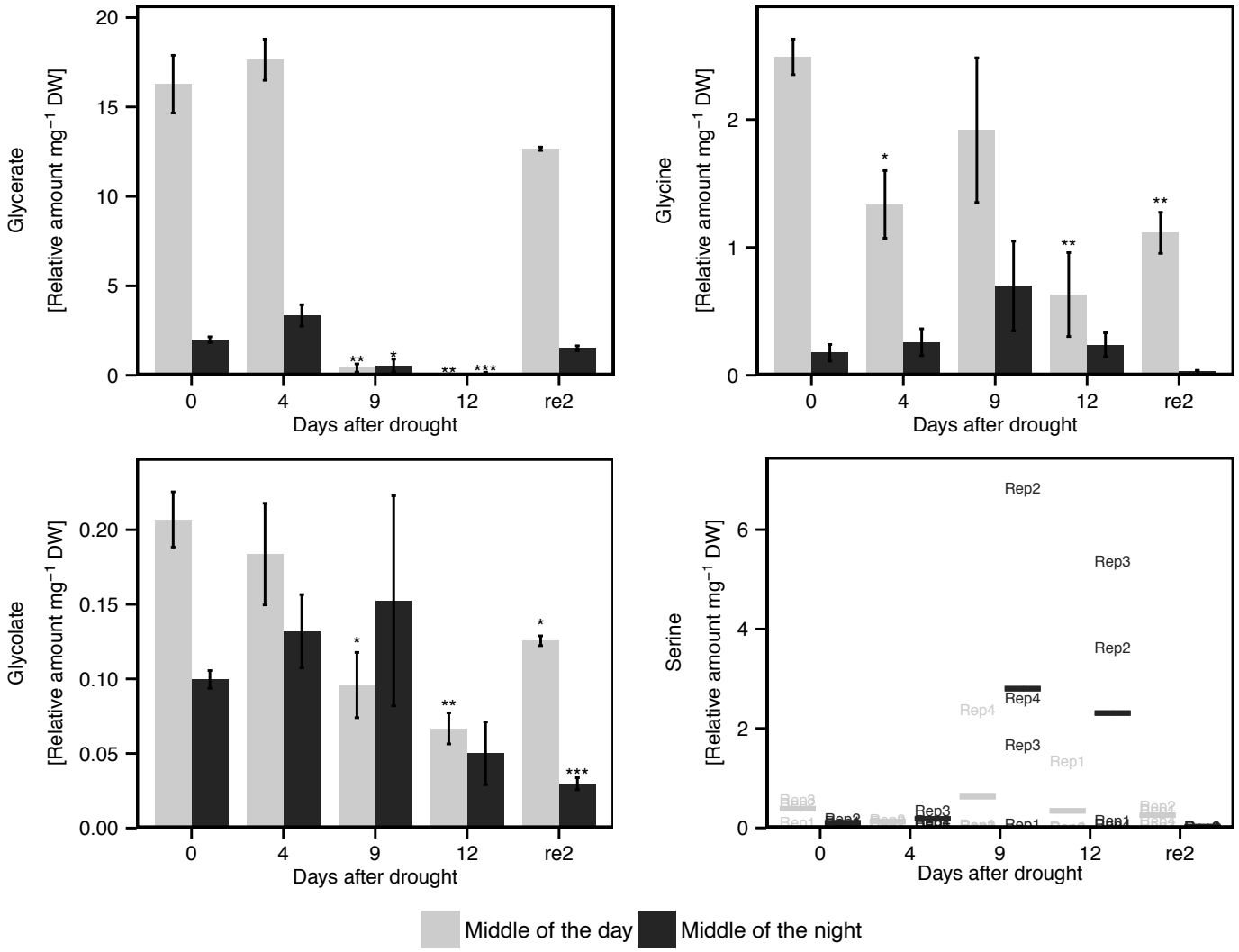

Supplemental Figure S4. Levels of photorespiratory metabolites. Metabolites were measured by GC-MS and normalized to dry weight (DW) and internal ribitol standard (Mean ± SE, n = 3-4, Asterisks indicate Student's *t* test significance in comparison to day 0 at ***$P < 0.001$, **$P < 0.01$, *$P < 0.05$). re2, two days after re-watering. Bar in serine plot represents the mean of biological replicates (Rep).

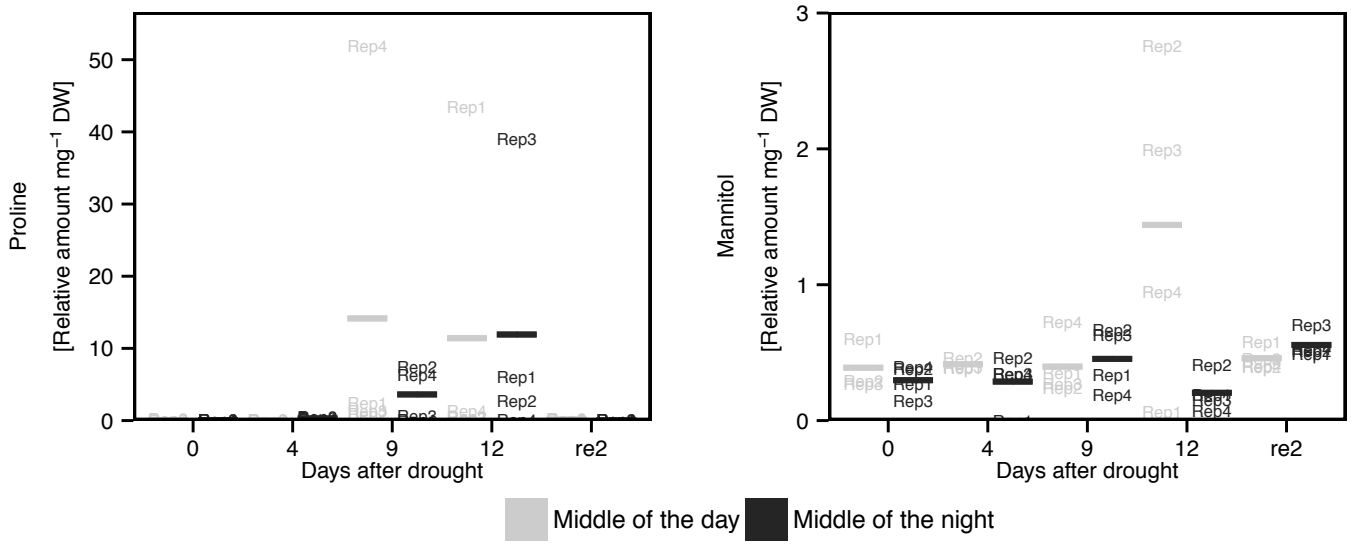

Supplemental Figure S5. Levels of compatible solutes. Metabolites were measured by GC-MS and normalized to dry weight (DW) and internal ribitol standard. Bar represents the mean of biological replicates (Rep).

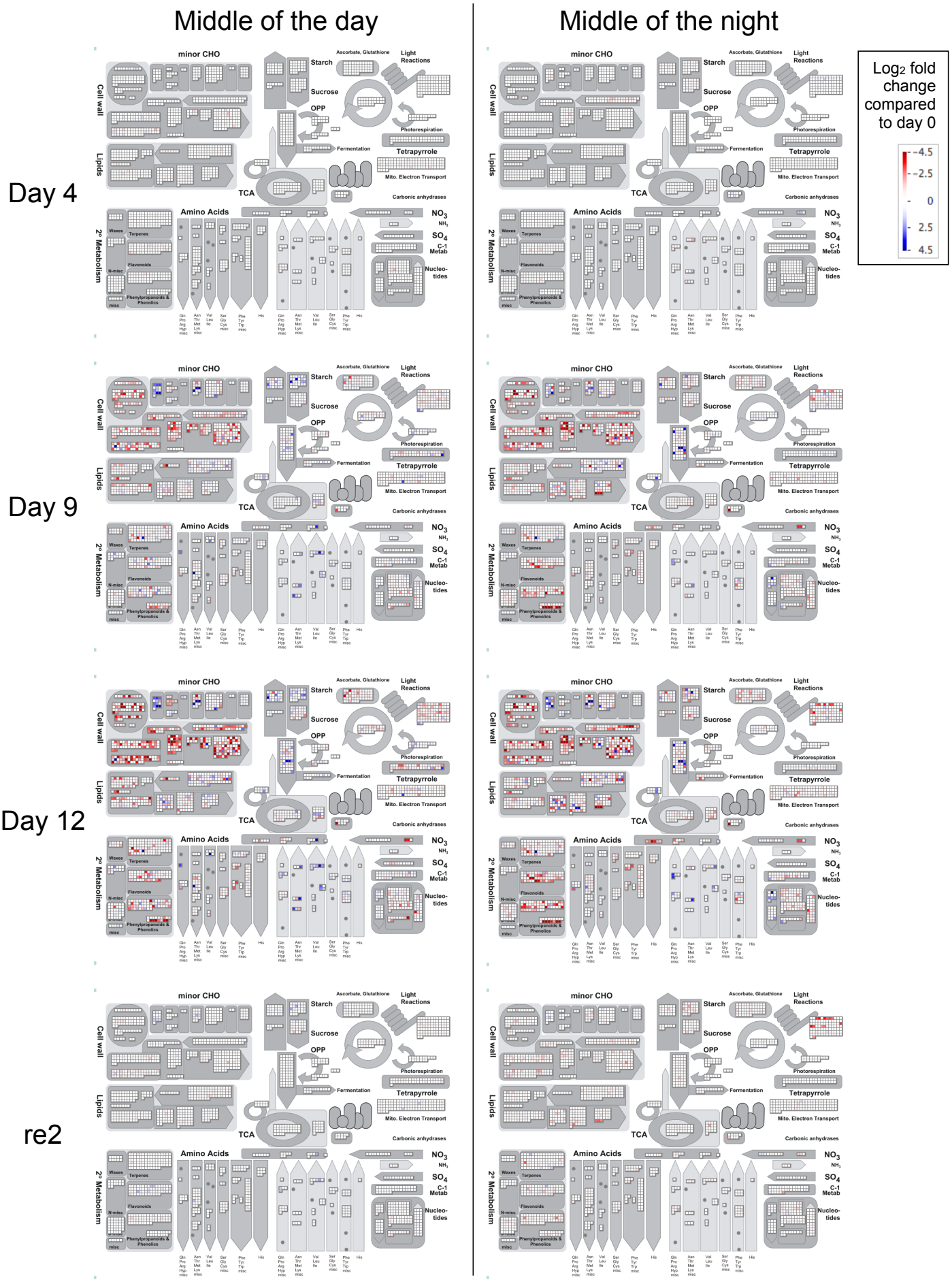

Supplemental Figure S6. Mapman overview of metabolism for all drought samples (day 4, day 9, day 12 of water-deprivation and 2 days after re-watering (re2) compared to day 0. Details see Materials and Methods.

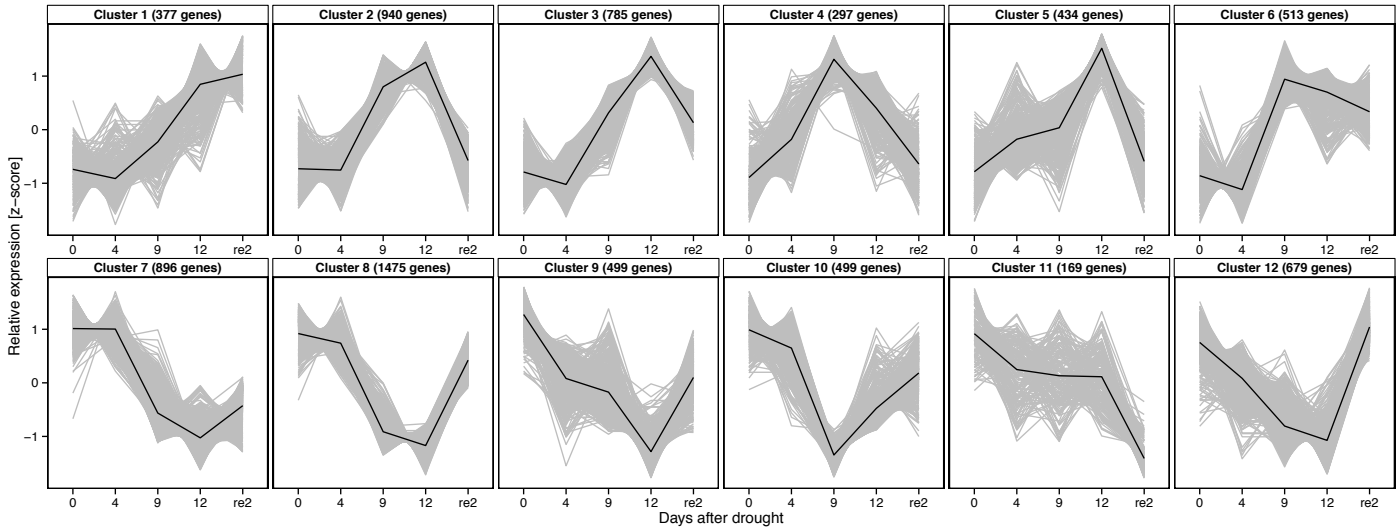

Supplemental Figure S7. *K*-means clustering of relative gene expression at the middle of the night. Genes that were found to be differentially expressed in the middle of the night between one of the water-limited stages and day 0 (DESeq2, $q < 0.01$) were used for the *k*-means approach (7563 genes in total). For a list of enriched GO Terms see Supplemental Dataset S4. Grey line, expression of single genes; black line, average of all genes in cluster; re2, two days after re-watering.

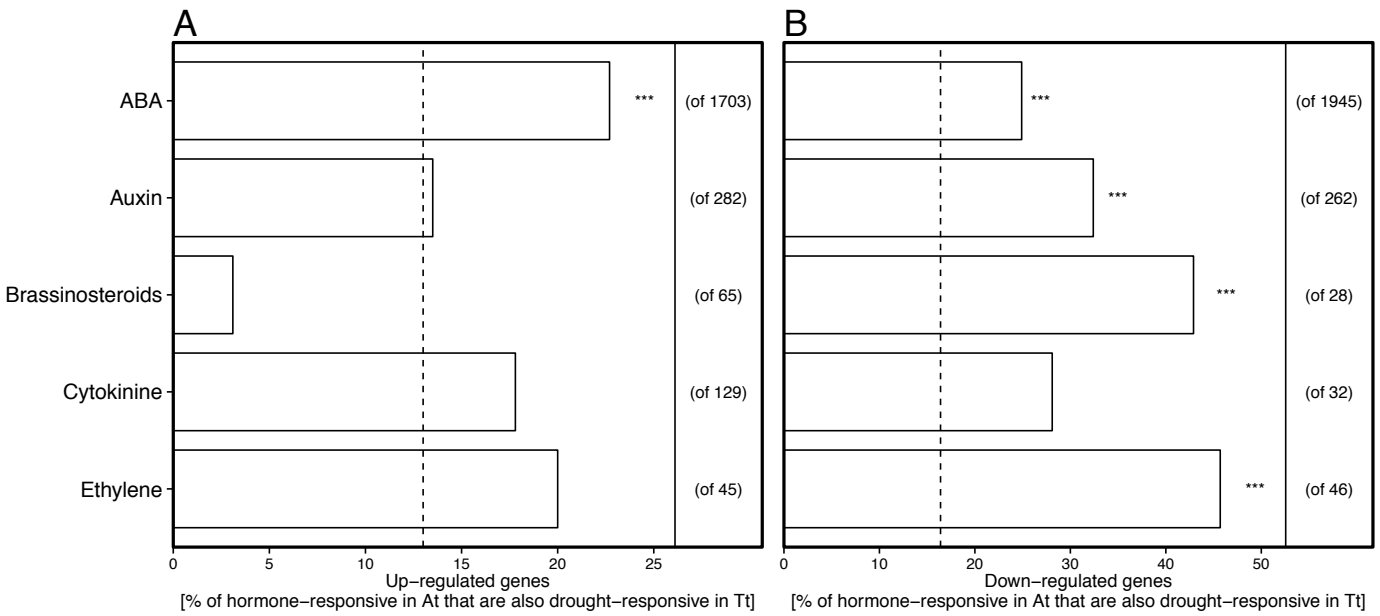

Supplemental Figure S8. Overlap of differentially expressed genes during CAM in *T. triangulare* with hormone treated leaves of *A. thaliana* (Goda et al., 2008). Bars represent the percentage of *T. triangulare* genes that are upregulated (A) or downregulated (B) on day 12 compared to day 0 (DESeq2, $q < 0.01$) in response to the respective hormone treatment in *A. thaliana*. Dashed line indicates the expected value (i.e. average of upregulated and downregulated genes on day 12, respectively). Asterisks indicate significant enrichment compared to the average response (Fisher's exact test, $***P < 0.001$). Numbers to the right represent the total number of responsive genes in *A. thaliana*. Details see Materials and Methods and Supplemental Dataset S1.

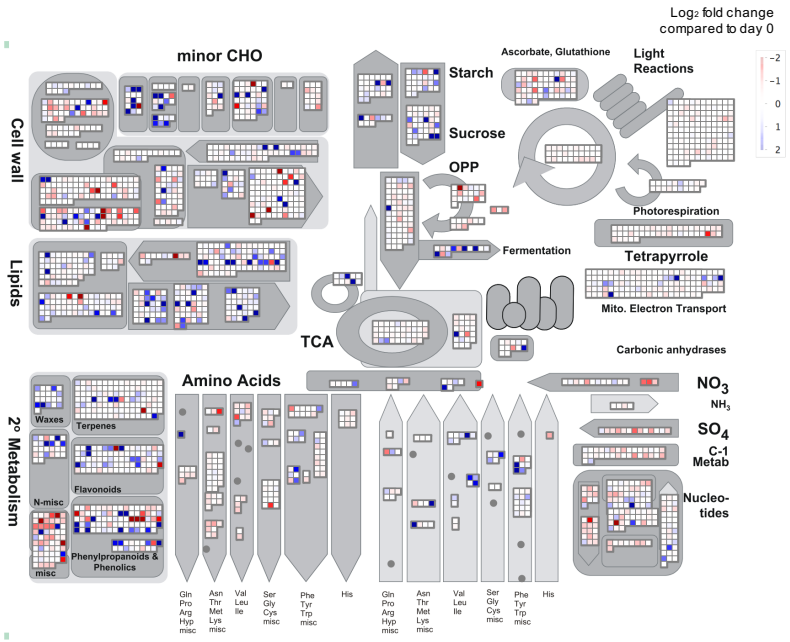

Supplemental Figure S9. Mapman overview of metabolism for ABA-response in *A. thailana.* Details see Materials and Methods.

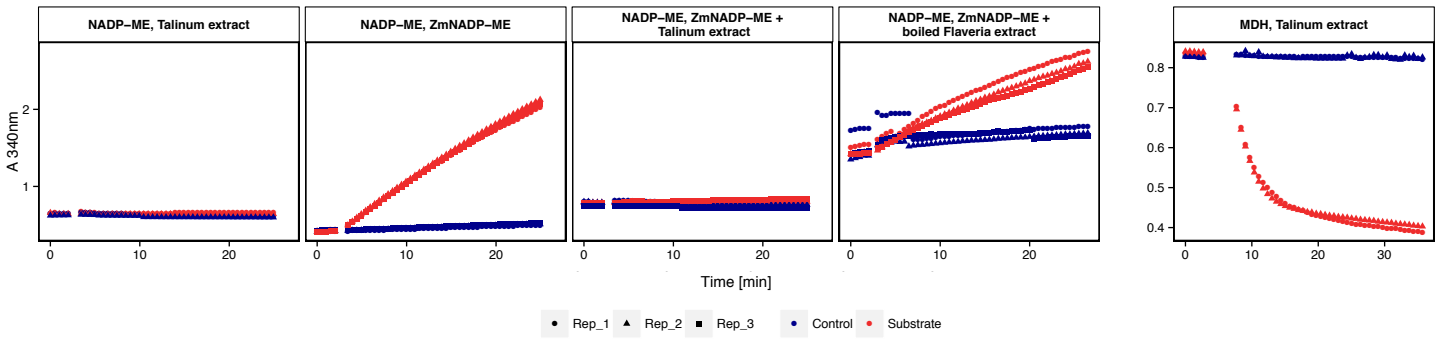

Supplemental Figure S10. Experiments to assay activity of NADP-malic enzyme (panels 1-4) or malate dehydrogenase (panel 5) with leaf extracts of *T. triangulare* ("*Talinum* extract") or recombinant NADP-malic enzyme from *Zea mays* (ZmNADP-ME, provided by Anastasiia Bovdilova, group of Veronica G. Maurino). Leave extraction and enzyme assays were performed as described in Ashton et al. (1990). NADP-ME activity is not detectable in *Talinum* leaf extracts (panel 1). Strong activity of recombinant ZmNADP-ME (panel 2) is fully inhibited by addition of *Talinum* leaf extract (panel 3), while only slightly inhibited by boiled leaf extract of the NADP-ME C4 plant *Flaveria bidentis* ("Flaveria extract", panel 4). This indicates the formation of an inhibitor of unknown kind during the leaf extraction of *T. triangulare* leaves, which affects NADP-ME activity, but not MDH activity (panel 5).

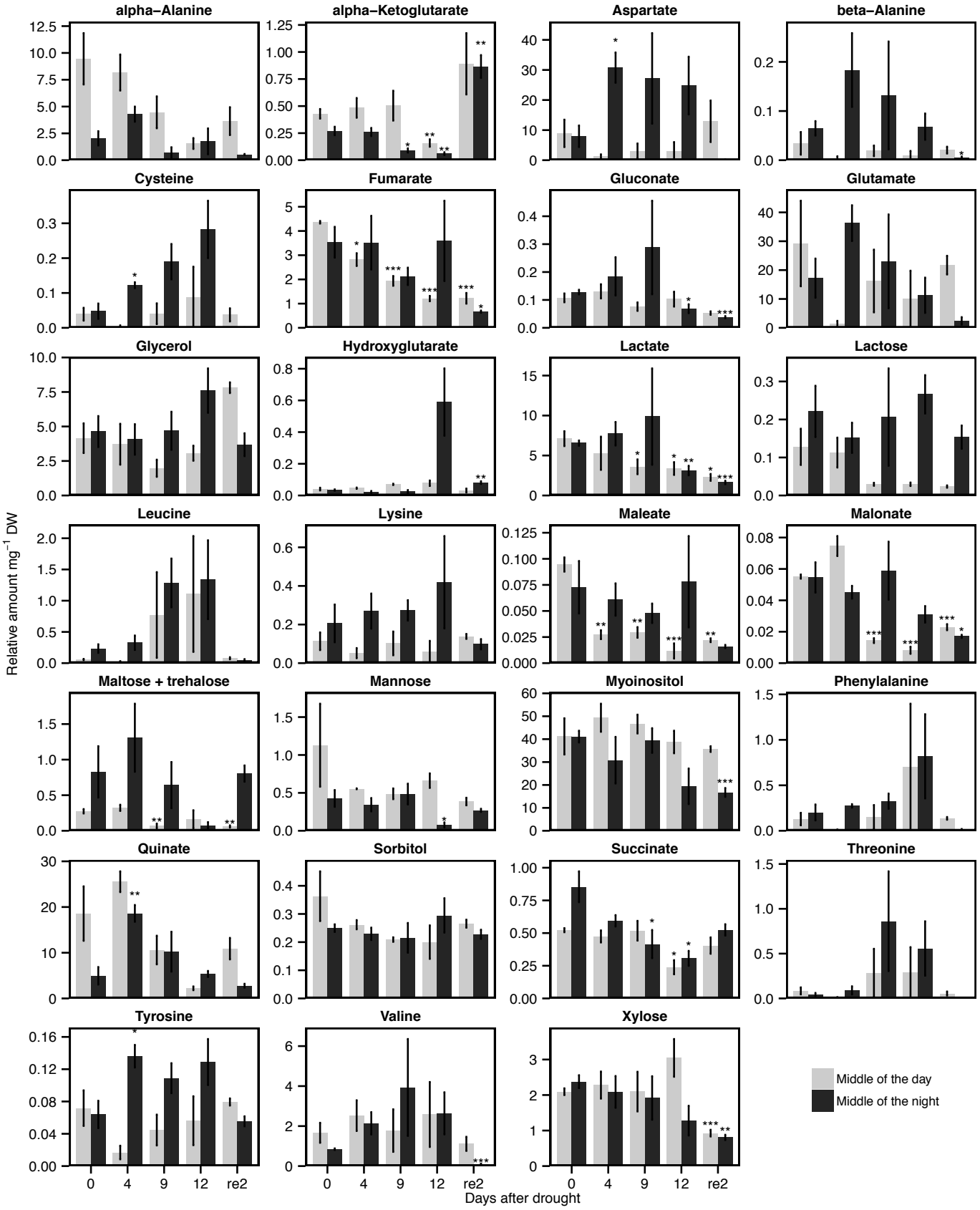

Supplemental Figure S11. Levels of additional metabolites. Metabolites were measured by GC-MS and normalized to dry weight (DW) and internal ribitol standard (Mean ± SE, n = 3-4, Asterisks indicate Student's *t* test significance in comparison to day 0 at ***$P < 0.001$, **$P < 0.01$, *$P < 0.05$). re2, two days after re-watering.

Supplemental Table S1. mRNA-Seq statistics

[a]Leaves were harvested from mature *T. triangulare* plants (n= 3) after 0 (Day 0), 4 (Day 4), 9 (Day 9) and 12 days (Day 12) of drought as well as after 2 d of re-watering (re2). [b]Total reads are the total number of 150 bp Illumina reads of three biological replicates per sample. [c]Mapped reads are the number of reads that could be matched to the TAIR10 reference genome of *A. thaliana*. [d]Mapping efficiency is the percentage of c/b. [e]Indicates how many genes (out of 21,869 genes of the minimal reference genome) matched at least one read. [f]Representation of TAIR10 gives the percentage of 21,869 genes of the minimal reference genome, that were hit by at least one read.

Sample[a]	Time of sampling	Replicate	Total reads[b]	Sum total reads of triplicate group	Mapped reads[c]	Sum mapped reads of triplicate group	Mapping efficiency against TAIR10[d]	Average mapping efficiency of triplicate group	Genes with at least one read[e]	Genes with at least one read by triplicate group	Represantation of TAIR10[f]
Day 0	MD	Replicate 1	15,213,727	41,908,047	8,756,533	23,688,643	58%	57%	15,192	15,746	72%
		Replicate 2	13,142,342		7,160,926		54%		15,178		
		Replicate 3	13,551,978		7,771,184		57%		15,111		
	MN	Replicate 1	14,666,449	40,863,248	6,731,139	20,025,434	46%	49%	15,423	15,903	73%
		Replicate 2	11,862,902		5,829,721		49%		15,306		
		Replicate 3	14,333,897		7,464,574		52%		15,397		
Day 4	MD	Replicate 1	13,276,380	38,821,817	7,140,769	21,441,452	54%	55%	15,219	15,728	72%
		Replicate 2	13,120,679		7,373,641		56%		15,106		
		Replicate 3	12,424,758		6,927,042		56%		15,145		
	MN	Replicate 1	9,661,691	30,562,513	4,266,915	14,318,644	44%	47%	15,049	15,660	72%
		Replicate 2	10,922,104		5,177,651		47%		15,189		
		Replicate 3	9,978,718		4,874,078		49%		15,123		
Day 9	MD	Replicate 1	14,467,089	45,931,558	6,418,919	21,819,528	44%	48%	15,004	15,645	72%
		Replicate 2	16,888,163		8,110,932		48%		15,183		
		Replicate 3	14,576,306		7,289,677		50%		14,965		
	MN	Replicate 1	14,280,800	44,283,472	7,382,494	22,471,234	52%	51%	15,111	15,677	72%
		Replicate 2	13,930,814		7,247,181		52%		15,017		
		Replicate 3	16,071,858		7,841,559		49%		15,199		
Day 12	MD	Replicate 1	11,060,708	38,449,744	5,712,636	20,015,280	52%	52%	14,620	15,431	71%
		Replicate 2	14,318,061		7,579,969		53%		14,783		
		Replicate 3	13,070,975		6,722,675		51%		14,849		
	MN	Replicate 1	14,541,469	46,449,946	6,962,404	23,231,393	48%	50%	14,951	15,638	72%
		Replicate 2	14,440,636		7,690,020		53%		14,989		
		Replicate 3	17,467,841		8,578,969		49%		15,143		
re2	MD	Replicate 1	12,772,394	40,739,535	7,433,710	22,686,620	58%	56%	15,111	15,719	72%
		Replicate 2	14,298,024		8,137,123		57%		15,151		
		Replicate 3	13,669,117		7,115,787		52%		15,202		
	MN	Replicate 1	12,994,986	38,667,014	6,714,748	20,015,370	52%	52%	15,175	15,757	72%
		Replicate 2	12,849,492		6,673,096		52%		15,185		
		Replicate 3	12,822,536		6,627,526		52%		15,246		

Supplemental Table S2. Metabolite profiling statistics

[a]Leaves were harvested from mature *T. triangulare* plants (n= 3-4) after 0 (Day 0), 4 (Day 4), 9 (Day 9) and 12 days (Day 12) of drought as well as after 2 d of re-watering (re2). Numbers indicate the fold change of metabolites with significantly different accumulation (negative values indicate decrease) compared to day 0 (Student's *t* test, $p < 0.05$). ns, not significant.

	Middle of the day				Middle of the night			
	Day 4	**Day 9**	**Day 12**	**re2**	**Day 4**	**Day 9**	**Day 12**	**re2**
Aspartate	ns	ns	ns	ns	3.9	ns	ns	ns
Citrate	1.3	3.6	ns	3.1	ns	ns	3.7	ns
Cysteine	ns	ns	ns	ns	2.6	ns	ns	ns
Fructose	ns	-12.4	-35.0	-1.9	-2.8	-4.5	-40.2	-5.4
Fumarate	-1.5	-2.2	-3.6	-3.6	ns	ns	ns	-5.3
Gluconate	ns	ns	ns	ns	ns	ns	-1.9	-3.4
Glucose	ns	-42.5	-119.5	ns	ns	ns	-16.0	ns
Glutamate	ns	ns	ns	ns	ns	ns	ns	ns
Glycerate	ns	-40.2	-238.9	ns	ns	-3.6	-16.7	ns
Glycerol	ns	ns	ns	ns	ns	ns	ns	ns
Glycine	-1.9	ns	-3.9	-2.2	ns	ns	ns	ns
Glycolate	ns	-2.2	-3.1	-1.6	ns	ns	ns	-3.3
Hydroxyglutarate	ns	ns	ns	ns	ns	ns	ns	2.4
Lactate	ns	-2.0	-2.1	-3.1	ns	ns	-2.1	-4.0
Lactose	ns	ns	ns	ns	ns	ns	ns	ns
Leucine	ns	ns	ns	ns	ns	ns	ns	ns
Lysine	ns	ns	ns	ns	ns	ns	ns	ns
Maleate	-3.5	-3.2	-8.1	-4.3	ns	ns	ns	ns
Malate	ns	-1.9	-4.0	ns	ns	ns	2.8	ns
Malonate	ns	-3.8	-6.7	-2.4	ns	ns	ns	-3.2
Maltose	ns	-4.1	ns	-4.5	ns	ns	ns	ns
Mannitol	ns	ns	ns	ns	ns	ns	ns	1.9
Mannose	ns	ns	ns	ns	ns	ns	-5.5	ns
Myoinositol	ns	ns	ns	ns	ns	ns	ns	-2.5
Phenylalanine	ns	ns	ns	ns	ns	ns	ns	ns
Proline	ns	ns	ns	ns	ns	ns	ns	-2.6
Quinate	ns	ns	ns	ns	3.8	ns	ns	ns
Raffinose	ns	14.4	12.3	ns	ns	9.2	ns	4.7
Serine	ns	ns	ns	ns	ns	ns	ns	ns
Sorbitol	ns	ns	ns	ns	ns	ns	ns	ns
Succinate	ns	ns	-2.2	ns	ns	-2.1	-2.8	ns
Sucrose	ns	-1.9	-2.9	ns	ns	-1.7	-3.6	-3.6
Threonine	ns	ns	ns	ns	ns	ns	ns	ns
Tyrosine	ns	ns	ns	ns	2.1	ns	ns	ns
Valine	ns	ns	ns	ns	ns	ns	ns	-8.4
Xylose	ns	ns	ns	-2.3	ns	ns	ns	-2.9
α-Alanine	ns	ns	ns	ns	ns	ns	ns	ns
α-Ketoglutarate	ns	ns	-2.7	ns	ns	-3.0	-4.5	3.2
β-Alanine	ns	ns	ns	ns	ns	ns	ns	-12.2

Supplemental Table S3. Expression levels of *T. triangulare* contigs encoding PEPC

Contigs of *T. triangulare* plants were assembled from Illumina paired-end reads (100 bp length) as described in Materials and Methods and matched to the reference genome RefBeet-1.1 of *Beta vulgaris* (Dohm et al., 2014) and the minimal reference genome of *Arabidopsis thaliana* (TAIR10) via BlastX for annotation. The single-end Illumina reads (150 bp) were mapped to the assembled contigs. Numbers indicate mean expression (rpm, reads per million) of all contigs orthologous to *Beta vulgaris* or *Arabidopsis thaliana* PEPC isoforms at five different stages of water-availability (n = 3) in the middle of the day (MD) and the middle of the night (MN) in *T. triangulare* (bold numbers indicate significantly DEG compared to day 0, q < 0.01, DESeq2). re2, 2 days after re-watering.

Talinum triangulare Contig ID	Arabidopsis thaliana gene ID	Annotation (TAIR10)	Beta vulgaris gene ID	Annotation (RefBeet-1.1)	Day 0 MD [rpm]	Day 0 MN [rpm]	Day 4 MD [rpm]	Day 4 MN [rpm]	Day 9 MD [rpm]	Day 9 MN [rpm]	Day 12 MD [rpm]	Day 12 MN [rpm]	re2 MD [rpm]	re2 MN [rpm]
Tt14682	AT1G53310	phosphoenolpyruvate carboxylase 1	Bv9_215080_xeaz.t1	Phosphoenolpyruvate carboxylase 1 Short=PEPCase 1; Short=PEPC 1; EC=4.1.1.31;	0.00	1.33	0.00	1.33	0.00	**11.67**	**1.00**	**54.33**	0.00	2.67
Tt14682_2	AT1G53310	phosphoenolpyruvate carboxylase 1	Bv4_084890_ihek.t1	Phosphoenolpyruvate carboxylase 2 Short=PEPCase 2; Short=PEPC 2; EC=4.1.1.31;	27.00	20.67	22.67	19.67	**13.33**	**6.33**	**19.00**	**6.33**	35.00	**7.00**
Tt16423	AT1G53310	phosphoenolpyruvate carboxylase 1	Bv4_084890_ihek.t1	Phosphoenolpyruvate carboxylase 2 Short=PEPCase 2; Short=PEPC 2; EC=4.1.1.31;	12.00	12.67	15.67	10.33	9.67	**3.33**	13.00	**4.33**	20.33	**5.67**
Tt22933	AT3G42628	phosphoenolpyruvate carboxylase-related / PEP carboxylase-related	Bv_55700_psaz.t1	Phosphoenolpyruvate carboxylase 1 Short=PEPCase 1; Short=PEPC 1; EC=4.1.1.31;	1.00	1.67	0.67	1.33	2.00	**7.00**	2.67	**9.33**	1.00	1.67
Tt32711	AT2G42600	phosphoenolpyruvate carboxylase 2	Bv9_215080_xeaz.t1	Phosphoenolpyruvate carboxylase 1 Short=PEPCase 1; Short=PEPC 1; EC=4.1.1.31;	0.00	1.00	0.00	0.67	0.00	**10.00**	0.33	**37.00**	0.00	1.67
Tt32711_2	AT2G42600	phosphoenolpyruvate carboxylase 2	Bv9_215080_xeaz.t1	Phosphoenolpyruvate carboxylase 1 Short=PEPCase 1; Short=PEPC 1; EC=4.1.1.31;	0.00	0.00	0.00	0.00	0.00	0.00	0.00	0.00	0.00	0.00
Tt33875	AT2G42600	phosphoenolpyruvate carboxylase 2	Bv9_215080_xeaz.t1	Phosphoenolpyruvate carboxylase 1 Short=PEPCase 1; Short=PEPC 1; EC=4.1.1.31;	0.67	6.33	0.33	3.33	2.00	**36.33**	**4.33**	**23.67**	3.00	16.00
Tt37959	AT1G53310	phosphoenolpyruvate carboxylase 1	Bv9_215080_xeaz.t1	Phosphoenolpyruvate carboxylase 1 Short=PEPCase 1; Short=PEPC 1; EC=4.1.1.31;	0.00	1.33	0.00	1.33	0.00	**14.33**	**1.00**	**62.33**	0.00	3.00
Tt37959_2	AT1G53310	phosphoenolpyruvate carboxylase 1	Bv9_215080_xeaz.t1	Phosphoenolpyruvate carboxylase 1 Short=PEPCase 1; Short=PEPC 1; EC=4.1.1.31;	0.00	0.00	0.00	0.00	0.00	0.33	0.00	1.00	0.00	0.00
Tt41156	AT1G68750	phosphoenolpyruvate carboxylase 4	Bv6_138910_yout.t1	Phosphoenolpyruvate carboxylase 4 Short=PEPCase 4; Short=PEPC 4; Short=AtPPC4; EC=4.1.1.31;	1.67	3.00	1.67	2.00	1.00	**0.00**	**0.67**	**0.33**	1.33	1.00
Tt43681	AT2G42600	phosphoenolpyruvate carboxylase 2	Bv9_215080_xeaz.t1	Phosphoenolpyruvate carboxylase 1 Short=PEPCase 1; Short=PEPC 1; EC=4.1.1.31;	0.00	1.00	0.00	0.33	0.00	**9.67**	**1.00**	**39.00**	0.00	1.67
Tt47449	AT1G53310	phosphoenolpyruvate carboxylase 1	Bv9_215080_xeaz.t1	Phosphoenolpyruvate carboxylase 1 Short=PEPCase 1; Short=PEPC 1; EC=4.1.1.31;	0.33	12.33	0.67	5.33	**4.67**	**64.00**	**8.00**	**47.00**	**5.33**	31.67
Tt53912	AT1G53310	phosphoenolpyruvate carboxylase 1	Bv9_215080_xeaz.t1	Phosphoenolpyruvate carboxylase 1 Short=PEPCase 1; Short=PEPC 1; EC=4.1.1.31;	0.00	1.00	0.00	0.33	0.00	**9.67**	0.33	**41.00**	0.00	2.00
Tt55601	AT1G68750	phosphoenolpyruvate carboxylase 4	Bv6_138910_yout.t1	Phosphoenolpyruvate carboxylase 4 Short=PEPCase 4; Short=PEPC 4; Short=AtPPC4; EC=4.1.1.31;	1.67	2.00	1.33	2.67	1.00	**0.33**	**0.67**	**0.33**	1.00	1.00
Tt63271	AT1G53310	phosphoenolpyruvate carboxylase 1	Bv9_215080_xeaz.t1	Phosphoenolpyruvate carboxylase 1 Short=PEPCase 1; Short=PEPC 1; EC=4.1.1.31;	4.00	66.33	1.00	**8.67**	**65.67**	**7638.00**	**63.33**	**6462.33**	2.33	168.00
Tt9871	AT1G53310	phosphoenolpyruvate carboxylase 1	Bv9_215080_xeaz.t1	Phosphoenolpyruvate carboxylase 1 Short=PEPCase 1; Short=PEPC 1; EC=4.1.1.31;	0.00	0.67	0.00	0.00	0.67	**5.67**	**1.33**	**5.00**	0.33	2.33
Tt9871_2	AT1G53310	phosphoenolpyruvate carboxylase 1	Bv9_215080_xeaz.t1	Phosphoenolpyruvate carboxylase 1 Short=PEPCase 1; Short=PEPC 1; EC=4.1.1.31;	0.00	0.33	0.00	0.00	0.00	1.00	**1.00**	1.00	0.00	1.00
Tt9871_3	AT1G53310	phosphoenolpyruvate carboxylase 1	Bv9_215080_xeaz.t1	Phosphoenolpyruvate carboxylase 1 Short=PEPCase 1; Short=PEPC 1; EC=4.1.1.31;	0.00	0.00	0.00	0.00	0.00	0.00	0.00	0.00	0.00	0.00
Tt9871_4	AT1G53310	phosphoenolpyruvate carboxylase 1	Bv9_215080_xeaz.t1	Phosphoenolpyruvate carboxylase 1 Short=PEPCase 1; Short=PEPC 1; EC=4.1.1.31;	0.33	10.67	0.33	**1.33**	**10.00**	**1408.67**	**12.00**	**1196.33**	0.33	**39.67**
Tt9871_5	AT1G53310	phosphoenolpyruvate carboxylase 1	Bv9_215080_xeaz.t1	Phosphoenolpyruvate carboxylase 1 Short=PEPCase 1; Short=PEPC 1; EC=4.1.1.31;	0.33	5.33	0.00	**0.33**	**4.33**	**476.67**	**4.33**	**481.33**	0.00	**15.33**
Tt9871_6	AT1G53310	phosphoenolpyruvate carboxylase 1	Bv9_215080_xeaz.t1	Phosphoenolpyruvate carboxylase 1 Short=PEPCase 1; Short=PEPC 1; EC=4.1.1.31;	0.33	4.33	0.33	2.33	**47.33**	**325.00**	**334.67**	**399.00**	0.33	4.33
Tt9871_7	AT1G53310	phosphoenolpyruvate carboxylase 1	Bv9_215080_xeaz.t1	Phosphoenolpyruvate carboxylase 1 Short=PEPCase 1; Short=PEPC 1; EC=4.1.1.31;	16.00	18.67	19.67	30.00	27.33	**44.33**	**50.00**	**72.67**	18.33	19.67
Tt9871_8	AT2G42600	phosphoenolpyruvate carboxylase 2	Bv9_215080_xeaz.t1	Phosphoenolpyruvate carboxylase 1 Short=PEPCase 1; Short=PEPC 1; EC=4.1.1.31;	300.33	357.67	356.33	591.33	491.67	641.00	**856.33**	**1198.33**	350.00	281.00

Supplemental Table S4. Expression levels of all *T. triangulare* contigs encoding for subunits of vacuolar ATP synthases

Contigs of *T. triangulare* plants were assembled from Illumina paired-end reads (100 bp length) as described in Materials and Methods. Contigs encoding V-ATPases were extracted via BlastP in protein space using protein sequences of *A. thaliana* V-ATPases identified with SUBA3 (http://suba3.plantenergy.uwa.edu.au) and retrieved from TAIR (http://arabidopsis.org). The single-end Illumina reads (150 bp) were mapped to the assembled contigs. Numbers indicate mean expression (rpm, reads per million) at five different stages of water-availability (n = 3) in the middle of the day (MD) and the middle of the night (MN) in *T. triangulare* (bold numbers indicate significantly DEG compared to day 0, q < 0.01, DESeq2). re2, 2 days after re-watering.

AGI	Description (SUBA)	**Talinum triangulare Contig ID**	**Day 0 MD [rpm]**	**Day 0 MN [rpm]**	**Day 4 MD [rpm]**	**Day 4 MN [rpm]**	**Day 9 MD [rpm]**	**Day 9 MN [rpm]**	**Day 12 MD [rpm]**	**Day 12 MN [rpm]**	**re2 MD [rpm]**	**re2 MN [rpm]**
AT1G20260.1	ATPase, V1 complex, subunit B protein;	Tt13863	81.67	151.67	87.67	142.67	67.67	139.67	73.33	155.00	87.67	139.00
AT1G76030.1	ATPase, V1 complex, subunit B protein;Encodes the vacuolar ATP synthase subunit B1. This subunit was shown to interact with the gene product of hexokinase1 (ATHXK1). This interaction, however, is solely restricted to the nucleus.	Tt13863	81.67	151.67	87.67	142.67	67.67	139.67	73.33	155.00	87.67	139.00
AT4G38510.1	ATPase, V1 complex, subunit B protein;	Tt13863	81.67	151.67	87.67	142.67	67.67	139.67	73.33	155.00	87.67	139.00
AT4G11150.1	vacuolar ATP synthase subunit E1;Encodes a vacuolar H+-ATPase subunit E isoform 1 which is required for Golgi organization and vacuole function in embryogenesis.	Tt14339	277.67	361.67	308.33	406.33	279.33	295.33	261.00	**270.67**	299.67	**257.67**
AT1G16820.1	vacuolar ATP synthase catalytic subunit-related / V-ATPase-related / vacuolar proton pump-related;	Tt23235	43.67	65.33	47.67	71.33	**29.33**	**40.00**	**30.67**	**34.00**	48.67	54.00
AT1G12840.1	vacuolar ATP synthase subunit C (VATC) / V-ATPase C subunit / vacuolar proton pump C subunit (DET3);Encodes subunit C of the vacuolar H(+)-ATPase (V-ATPase). Bound and phosphorylated by AtWNK8.	Tt33042	21.00	25.33	19.67	31.00	24.00	25.33	26.33	22.67	20.00	22.67
AT3G58730.1	vacuolar ATP synthase subunit D (VATD) / V-ATPase D subunit / vacuolar proton pump D subunit (VATPD);	Tt41117	114.00	160.33	110.00	155.33	**92.33**	**106.33**	**97.67**	**80.00**	108.33	**89.67**
AT3G42050.1	vacuolar ATP synthase subunit H family protein;	Tt43428_4	47.67	60.67	53.00	74.33	**28.67**	**30.00**	**28.67**	**30.67**	46.33	41.67
AT1G78900.1	vacuolar ATP synthase subunit A;Encodes catalytic subunit A of the vacuolar ATP synthase. Mutants are devoid of vacuolar ATPase activity as subunit A is encoded only by this gene and show strong defects in male gametophyte development and in Golgi stack morphology.	Tt49354	110.00	205.00	131.33	188.67	**81.33**	**126.00**	101.00	**127.00**	139.67	191.67
AT4G02620.1	vacuolar ATPase subunit F family protein;	Tt56663	63.67	71.00	59.67	67.00	53.33	51.00	**50.33**	**34.67**	73.33	**45.00**
AT4G23710.1	vacuolar ATP synthase subunit G2;	Tt8658	122.67	169.67	109.00	152.67	134.00	126.33	115.33	**74.67**	117.00	**95.67**
AT4G25950.1	vacuolar ATP synthase G3;V-ATPase G-subunit like protein	Tt8658	122.67	169.67	109.00	152.67	134.00	126.33	115.33	**74.67**	117.00	**95.67**

Supplemental Table S5. Expression levels of *T. triangulare* contigs encoding NADP-ME

Contigs of *T. triangulare* plants were assembled from Illumina paired-end reads (100 bp length) as described in Materials and Methods and matched to the reference genome RefBeet-1.1 of *Beta vulgaris* (Dohm et al., 2014) and the minimal reference genome of *Arabidopsis thaliana* (TAIR10) via BlastX for annotation. The single-end Illumina reads (150 bp) were mapped to the assembled contigs. Numbers indicate mean expression (rpm, reads per million) of all contigs orthologous to *Beta vulgaris* or *Arabidopsis thaliana* NADP-ME isoforms at five different stages of water-availability (n = 3) in the middle of the day (MD) and the middle of the night (MN) in *T. triangulare* (bold numbers indicate significantly DEG compared to day 0, q < 0.01, DESeq2). re2, 2 days after re-watering.

Talinum triangulare Contig ID	Arabidopsis thaliana gene ID	Annotation (TAIR10)	Beta vulgaris gene ID	Annotation (RefBeet-1.1)	Day 0 MD [rpm]	Day 0 MN [rpm]	Day 4 MD [rpm]	Day 4 MN [rpm]	Day 9 MD [rpm]	Day 9 MN [rpm]	Day 12 MD [rpm]	Day 12 MN [rpm]	re2 MD [rpm]	re2 MN [rpm]
Tt2487	AT2G19900	NADP-malic enzyme 1	Bv8_201720_sfck.t1	NADP-dependent malic enzyme Short=NADP-ME; EC=1.1.1.40;	1.00	6.00	1.67	4.00	2.67	6.33	**7.67**	3.67	4.33	7.33
Tt38957_2	AT1G79750	NADP-malic enzyme 4	Bv9u_231540_zmjw.t1	NADP-dependent malic enzyme Short=NADP-ME; EC=1.1.1.40;	107.33	115.33	100.33	50.33	**302.00**	86.33	**369.33**	**52.67**	231.33	**53.67**
Tt38957_3	AT1G79750	NADP-malic enzyme 4	Bv9u_231540_zmjw.t1	NADP-dependent malic enzyme Short=NADP-ME; EC=1.1.1.40;	105.00	313.00	110.67	271.33	**460.00**	**611.33**	**727.33**	**580.67**	149.33	417.67
Tt4199_2	AT1G79750	NADP-malic enzyme 4	Bv9u_231540_zmjw.t1	NADP-dependent malic enzyme Short=NADP-ME; EC=1.1.1.40;	30.00	40.33	36.00	17.00	**101.00**	30.33	**138.67**	**20.33**	**78.33**	21.67
Tt42649	AT2G19900	NADP-malic enzyme 1	Bv8_201720_sfck.t1	NADP-dependent malic enzyme Short=NADP-ME; EC=1.1.1.40;	1.67	5.00	1.67	3.67	**20.00**	8.33	**36.67**	7.33	**21.33**	**12.00**
Tt42649_2	AT2G19900	NADP-malic enzyme 1	Bv8_201720_sfck.t1	NADP-dependent malic enzyme Short=NADP-ME; EC=1.1.1.40;	1.00	4.67	1.67	3.67	**21.33**	7.33	**36.33**	6.67	**21.00**	**10.67**
Tt63113	AT1G79750	NADP-malic enzyme 4	Bv8_201720_sfck.t1	NADP-dependent malic enzyme Short=NADP-ME; EC=1.1.1.40;	0.00	0.00	0.00	0.00	0.00	0.00	0.00	0.00	0.00	0.00
Tt63113_2	AT1G79750	NADP-malic enzyme 4	Bv8_201720_sfck.t1	NADP-dependent malic enzyme Short=NADP-ME; EC=1.1.1.40;	1.67	2.33	2.00	1.33	1.00	1.00	**0.00**	1.33	1.33	1.00
Tt6558	AT2G19900	NADP-malic enzyme 1	Bv8_201720_sfck.t1	NADP-dependent malic enzyme Short=NADP-ME; EC=1.1.1.40;	0.67	3.33	1.00	2.67	**1.67**	2.67	**3.33**	2.00	**2.33**	3.33
Tt8204	AT5G11670	NADP-malic enzyme 2	Bv8_201720_sfck.t1	NADP-dependent malic enzyme Short=NADP-ME; EC=1.1.1.40;	0.33	1.00	0.00	1.67	0.33	2.00	**1.67**	1.00	1.33	2.33

Supplemental Table S6. Expression levels of two *T. triangulare* contigs encoding PPDK

Contigs of *T. triangulare* plants were assembled from Illumina paired-end reads (100 bp length) as described in Materials and Methods and matched to the reference genome RefBeet-1.1 of *Beta vulgaris* (Dohm et al., 2014) and the minimal reference genome of *Arabidopsis thaliana* (TAIR10) via BlastX for annotation. The single-end Illumina reads (150 bp) were mapped to the assembled contigs. Numbers indicate mean expression (rpm, reads per million) of all contigs orthologous to *Beta vulgaris* or *Arabidopsis thaliana* PPDK isoforms at five different stages of water-availability (n = 3) in the middle of the day (MD) and the middle of the night (MN) in *T. triangulare* (bold numbers indicate significantly DEG compared to day 0, q < 0.01, DESeq2). re2, 2 days after re-watering.

Talinum triangulare Contig ID	Length of encoded peptide (aa)	Arabidopsis thaliana gene ID	Annotation (TAIR10)	Beta vulgaris gene ID	Annotation (RefBeet-1.1)	Day 0 MD [rpm]	Day 0 MN [rpm]	Day 4 MD [rpm]	Day 4 MN [rpm]	Day 9 MD [rpm]	Day 9 MN [rpm]	Day 12 MD [rpm]	Day 12 MN [rpm]	re2 MD [rpm]	re2 MN [rpm]
Tt24575	964	AT4G15530	pyruvate orthophosphate dikinase	Bv1_015500_fjqs.t1	Pyruvate, phosphate dikinase, chloroplastic EC=2.7.9.1; AltName: Full=Pyruvate, orthophosphate dikinase; Flags: Precursor;	399.00	358.00	328.33	198.67	498.67	267.00	589.67	220.00	541.67	367.67
Tt26901	887	AT4G15530	pyruvate orthophosphate dikinase	Bv1_015500_fjqs.t1	Pyruvate, phosphate dikinase, chloroplastic EC=2.7.9.1; AltName: Full=Pyruvate, orthophosphate dikinase; Flags: Precursor;	160.33	1558.33	195.33	1117.67	**1759.33**	**17488.33**	**3285.33**	**12924.33**	262.33	2049.67

Supplemental Table S7. Expression levels of genes encoding for photorespiratory enzymes

Expression levels were extracted from the cross-species mapping (Supplemental Dataset S1). Numbers indicate mean expression (rpm, reads per million) at five different stages of water-availability (n = 3) in the middle of the day (MD) and the middle of the night (MN) in *T. triangulare* (bold numbers indicate significantly DEG compared to day 0, q < 0.01, DESeq2). re2, 2 days after re-watering.

Locus[a]	Annotation (TAIR10)	Day 0 MD [rpm]	Day 0 MN [rpm]	Day 4 MD [rpm]	Day 4 MN [rpm]	Day 9 MD [rpm]	Day 9 MN [rpm]	Day 12 MD [rpm]	Day 12 MN [rpm]	re2 MD [rpm]	re2 MN [rpm]
AT4G32520	serine hydroxymethyltransferase 3	34.0	43.0	38.3	34.3	**170.3**	48.3	**202.7**	**23.3**	41.7	45.3
AT3G14130	Aldolase-type TIM barrel family protein	3.3	7.0	4.7	6.7	**12.0**	**11.0**	**17.3**	**14.7**	6.0	11.0
AT2G26080	glycine decarboxylase P-protein 2	2331.3	5268.0	2261.7	4127.7	**7350.7**	4898.0	**6474.0**	3832.7	3548.3	7660.0
AT2G13360	alanine:glyoxylate aminotransferase	2080.7	3847.0	2037.3	3514.3	3563.7	**6019.3**	3226.3	**6226.7**	2304.7	5590.0
AT1G68010	hydroxypyruvate reductase	1115.3	2214.0	1146.0	2229.7	**2262.3**	**3560.3**	1772.7	**3317.3**	1070.7	2810.0
AT1G12550	D-isomer specific 2-hydroxyacid dehydrogenase family protein	27.0	78.7	25.7	91.7	**44.7**	**106.0**	**50.7**	**109.0**	35.7	105.0
AT1G11860	Glycine cleavage T-protein family	1956.7	3114.7	1903.3	3233.0	1872.0	3304.3	**1362.0**	2605.7	1711.3	3027.3
AT1G32470	Single hybrid motif superfamily protein	1755.0	2474.3	1721.3	2773.7	2480.0	2054.7	1681.0	**1386.7**	1520.3	1710.7
AT1G79870	D-isomer specific 2-hydroxyacid dehydrogenase family protein	51.3	102.7	53.7	107.7	58.0	82.3	51.7	**63.0**	65.0	81.0
AT1G80380	P-loop containing nucleoside triphosphate hydrolases superfamily protein	262.3	179.3	244.7	186.7	276.7	178.0	326.3	167.7	241.0	140.3
AT2G35120	Single hybrid motif superfamily protein	107.3	146.3	98.7	178.7	135.7	96.3	97.7	**73.3**	92.0	101.0
AT2G45630	D-isomer specific 2-hydroxyacid dehydrogenase family protein	29.3	55.0	30.0	67.3	29.7	54.3	31.0	60.0	31.7	59.3
AT3G14415	Glycolate oxidase 2	1186.7	1608.0	1292.0	1806.3	1735.3	1946.3	1385.3	1824.0	1236.0	1899.0
AT3G14420	Glycolate oxidase 1	2684.3	3855.7	2877.0	4180.3	3995.0	4692.7	3329.3	4365.3	2900.3	4609.3
AT4G17360	Formyl transferase	33.7	56.3	32.0	55.0	44.7	53.0	40.0	44.3	30.7	44.7
AT4G18360	Glycolate oxidase 3	212.0	321.3	243.7	378.0	349.0	397.7	279.7	364.7	236.0	395.0
AT5G36700	2-phosphoglycolate phosphatase 1	1340.3	366.7	1245.3	355.7	**821.0**	427.3	**624.3**	440.7	1006.7	391.0

Supplemental Table S8. Estimated partitioning of carbon in organic acids and starch on day 12

Concentrations of starch and organic acids were measured from the same plants (n = 4) but independent mature leaves at the end of the night and the end of the day, respectively. Starch was measured with an assay. Organic acids were measured via acid titration (See Fig. 1). Amount of carbon in starch was estimated as six multiplied with the concentration of glucose (accounting for six C atoms). For approximation of carbon in organic acids, acid concentrations were multiplied with three under the assumption that malate (C4) accounts for the major day-night fluctuations during CAM (Fig. 4) and subtracting one molecule of CO_2 which is released to the Calvin-Benson cycle after decarboxylation during the day (Fig. 3).

Time	Compound	Concentration	Carbon
End of the day	Starch	20.8 µmol Glc / g FW	125
	Acid	0 µmol H+/ g FW	0
End of the night	Starch	6.4 µmol Glc / g FW	38
	Acid	31.5 µmol H+/ g FW	95